THE ROLE OF PGC-1α IN MEDIATING EXERCISE-INDUCED TFEB EXPRESSION AND ACTIVITY IN SKELETAL MUSCLE

AVIGAIL T. ERLICH

A THESIS SUBMITTED TO THE FACULTY OF GRADUATE STUDIES IN PARTIAL FULFILLMENT OF THE REQUIREMENTS FOR THE DEGREE OF

MASTER OF SCIENCE

GRADUATE PROGRAM IN KINESIOLOGY AND HEALTH SCIENCE

YORK UNIVERSITY
TORONTO, ONTARIO

DECEMBER 2016

ABSTRACT

A healthy mitochondrial pool in skeletal muscle is maintained by the coordinated processes of biogenesis and mitophagy. PGC-1α is a key transcriptional co-activator necessary for mitochondrial synthesis, whereas transcription factor EB (TFEB) regulates the degradation of dysfunctional organelles via activation of genes associated with autophagy. Despite TFEB's known role as a key regulator of autophagy and lysosomal genes, its response to exercise and the mechanisms behind its transcription and activation have yet to be elucidated. To identify TFEB's role and its dependence on PGC-1α, we subjected WT and PGC-1α KO mice to an acute bout of exercise and analyzed factors regulating TFEB transcription and nuclear translocation. We found a PGC-1α-dependent induction of TFEB transcription and activation with exercise, proving a strong correlation between the two processes involved in mitochondrial quality control.

ACKNOWLEDGMENTS

I am not the person I was before this amazing experience, and I would like to convey my deepest appreciation to those who have supported me along the way.

First and foremost, I would like to express my sincere gratitude to my thesis advisor and mentor, Dr. David Hood. Thank you for always believing in me, and introducing me to the wonderful world of research. Over the past three years, your door was always open whenever I had even the silliest of questions. You always provided me with guidance, encouragement, support, and an immense amount of knowledge. I consider myself extremely lucky to have been a part of this lab, and to have had you as my thesis supervisor. I can honestly say that it is thanks to you that I have been able to develop this passion and love for science.

A loving thank you to my fellow lab mates, without whom I wouldn't have survived the ups and downs of the science world. I loved being a part of this "lab family" and want to thank you for all the fun and support that made this lab an amazing environment to work in. The friends and memories that I have made here truly mean so much to me.
A very special thanks goes to Josh, the only person I ever trusted with my valuable samples! You really earned that trust. From day one you were eager, responsible, hard working, and most of all, dependable. I am so grateful for all of your help and support while I was finishing up. We were a great team and I loved having a partner in crime that knew what I was going to say before I said it. Thanks for everything!!
To Anna, Matt, and Jon, you were my mentors and you really took me under your wing. If it weren't for you, I never would have known as much as I do about " the powerhouse of the cell". I want to thank you for the guidance, patience, and assistance you provided me when I first started as a deer in the headlights. As time went on you became not only my mentors, but also my confidants, and made my time in the lab an extremely enjoyable experience.
Ashley and Kaitlyn (my science squad, my backbone, my sounding board): You really were my "lab survival pack", and I couldn't have done this without you. It's hard to think that I've only known you for two years. You have supported me through this process more than words could describe. From science help, to keeping me sane, thank you for the love and understanding you have provided me every step of the way.

Lastly, I am so deeply thankful and appreciative of my family. Imma and Abba, I love you so much, and your support throughout my Master's has meant so much to me. You have always told me to do what I love, and for that I am forever grateful. I wouldn't have been able to survive the past few years without your encouragement, patience, and understanding. Even when my thesis got the best of me, you were always there to provide me with the strength and courage I needed to reach this goal. Thank you for putting up with me and always believing in me. I appreciate it more than you know. I love you.
Izzy, you are my role model. Ever since we were little, you have always been full of knowledge and insight, and I am so proud to call you my brother. Thank you for always being there for me and offering your help, wisdom, and love.

My time in the lab has been a part of my life that I will never forget, and will cherish forever.

TABLE OF CONTENTS

Abstract ii
Acknowledgements iii
Table of Contents iv
List of Tables vii
List of Figures vii
List of Abbreviations viii

REVIEW OF LITERATURE 1
1.1.0. SKELETAL MUSCLE MITOCHONDRIA 1
1.1.1. Skeletal muscle 1
1.1.2. Mitochondrial Structure and Function 2
1.1.2.1. ETC 4
1.1.3. ROS and Antioxidants 6
1.2.0. MITOCHONDRIAL TURNOVER 7
1.2.1. Mitochondrial Biogenesis 8
1.2.1.1. PGC-1α 9
1.2.1.2. Regulation of Mitochondrial Biogenesis 10
1.2.1.3. Mitochondrial Biogenesis and Exercise 11
1.2.2. Mitochondrial Degradation 12
1.2.2.1. Mitophagy 13
1.2.2.2. Signaling 13
1.2.2.3. Mitophagy Pathways 16
1.2.2.4. Mitophagy and Exercise 19
1.3.0. TFEB 20
1.3.1.1. The Role of TFEB 20
1.3.1.2. Targets of TFEB 21
1.3.1.3. Activation of TFEB 24
1.3.1.2. TFEB and exercise 26
RESEARCH OBJECTIVES 28
HYPOTHESES 28

REFERENCES 29

MANUSCRIPT 46

The Role of PGC-1α in Mediating Exercise-induced TFEB Expression and Activity in Skeletal Muscle 46

Summary 46

Introduction 47

Methods 50

Results 57

Discussion 71

References 77

Future Work 84

APPENDIX A: DATA AND STATISTICAL ANALYSES 85

APPENDIX B: ADDITIONAL DATA 106

APPENDIX C: LABORATORY METHODS AND PROTOCOLS 109

E-coli transformation with plasmid DNA 109

DNA injection and electroporation into muscle hindlimb muscles 110

Mouse Muscle Tissue Preparation for Luciferase Assay 113

RNA isolation 115

Reverse transcription: first strand cDNA synthesis 116

Oligonucleotide primer design 117

Real-time polymerase chain reaction (qPCR) 118

Gel Electrophoresis 129

Western blotting and immunodetection 122

APPENDIX D: OTHER CONTRIBUTIONS TO THE LITERATURE 124

Peer-reviewed publications 124

Published abstracts and conference proceedings 124

Oral Presentations 124

LIST OF TABLES

MANUSCRIPT

Table 1 – List of primer antibodies used 53

Table 2 – List of primer sequences used in qPCR analysis 56

APPENDIX A: DATA AND STATISTICAL ANALYSIS

Table 1 – Animal characteristics and response to exercise

A- Body Mass 85

B- Lactate 86

C- Distance to Exhaustion 87

Table 2 – Gene expression of early response genes and mitochondrial markers

A- PGC-1α 88

B- Egr1 89

C- COXI 90

D- Tfam 91

Table 3 – TFEB localization and activation

A- TFEB nuclear content 92

B- mTOR activation 93

Table 4 – TFEB Transcription with exercise

A- Promoter activity 94

B- YY1 nuclear content 95

C- p65 nuclear content 96

D- PGC-1α nuclear content 97

Table 5 – Protein expression of TFEB and downstream targets

A- TFEB 98

B- Tfe3 98

C- Beclin1 99

D- Lamp1 99

Table 6 – Gene expression of TFEB and downstream targets

A- Lamp1 100

B- Cathepsin D 101

C- Beclin1 102

D- TFEB 103
E- p62 104
F- Lamp2 105

LIST OF FIGURES

REVIEW OF LITERATURE

Fig. 1 – Schematic of the electron transport chain 5
Fig. 2 – The regulation of mTORC1 and ULK1 complex 15
Fig. 3 – General scheme of the degradation of dysfunctional mitochondria through the process of mitophagy 18

MANUSCRIPT

Fig. 1 – Animal characteristics and response to exercise 58
Fig. 2 – Gene expression of early response genes and mitochondrial markers 59
Fig. 3 – TFEB localization and activation 61
Fig. 4 – TFEB Transcription with exercise 63
Fig. 5 – Protein expression of TFEB and downstream targets 65
Fig. 6 Gene expression of TFEB and downstream targets 67
Fig. 7 – Effect of TFEB overexpression on downstream targets 70

APPENDIX B: ADDITIONAL DATA

Fig. S1 – Nrf2-Keap1 antioxidant pathway in WT and PGC-1α KO mice 106
Fig. S2 – Inflammation, apoptotic, and autophagy markers in response to aging 107
Fig. S3 – Inflammation, apoptotic, and autophagy markers in. WT and PGC-1α KO mice 108

APPENDIX C: LABORATORY METHODS AND PROTOCOLS

Fig. 1 – Illustration for in vivo muscle transfection 112
Fig. 2 – Illustration for luciferase assay protocol 114

LIST OF ABBREVIATIONS:

ADP	Adenosine diphosphate
Akt	Serine/threonine protein kinase Akt
AMP	Adenosine monophosphate
AMPK	AMP-activated protein kinase
ANOVA	Analysis of variance1
ATG	Autophagy-related protein
ATP	Adenosine triphosphate
Bak	Bcl-2 homologous antagonist killer
Bax	Bcl-2 associated X protein
Bcl-2	B-cell lymphoma 2
BH3	Bcl-2 homology domain 3
Ca^{2+}	Calcium ion
CaMK	Ca^{2+}/calmodulin-dependent protein kinase
cAMP	Cyclic AMP
CCA	Chronic contractile activity
cDNA	Complimentary DNA
CLEAR	Coordinated Lysosomal Expression and Regulation
COX	Cytochrome c oxidase
CREB	cAMP response element-binding protein
DNA	Deoxyribonucleic acid
EDL	Extensor digitorum longus
ERRα	Estrogen-related receptor alpha
ERK	Extracellular-signal-regulated kinases 1 and 2
ETC	Electron transport chain
FA	Fatty acids
FTR	Fast-twitch red
FTW	Fast-twitch white
GCN5L1	General Control of amino synthesis 5-like 1
GTPase	Guanosine triphosphate
HSP	Heat shock protein
IMF	Intermyofibrillar
IMM	Inner mitochondrial membrane
IMS	Intermembrane space
LAMP 1/2	Lysosomal associated membrane proteins 1 and 2
LC3	Microtubule-associated proteins 1A/1B light chain 3A
LIR	LC3-interacting region
MAPK	Mitogen-activated protein kinase
MCOLN1	Mucolipin
Mfn 1/2	Mitofusin-1/2
MHC	Myosin heavy chain

Mit/TFE	Microthalmia-transcription factor E
mRNA	Messenger RNA
mtDNA	Mitochondrial DNA
mtHSP70	75 kDA mitochondrial heat shock protein
mTORC1	Mammalian/mechanistic target of rapamycin complex 1
mtPTP	Mitochondrial permeability transition pore
NAD	Nicotinamide adenine dinucleotide
NF-κB	Nuclear factor kappa-light-chain-enhancer of activated B cells
NIX	Bcl2/E1B 19 kDa-interacting protein 3-like protein
NLS	Nuclear localization sequence
NRF-1/-2	Nuclear respiratory factor-1 and -2
Nrf2	Nuclear factor (erythroid-derived 2)-like 2
NUGEMP	Nuclear gene-encoded mitochondrial protein
OMM	Outer mitochondrial membrane
p38 MAPK	p38 mitogen-activated protein kinase
PCR	Polymerase chain reaction
PGC-1α	Peroxisome proliferator activator receptor (PPAR) γ coactivator 1 alpha
PIM	Protein import machinery
PINK1	PTEN-induced putative kinase 1
RNA	Ribonucleic acid
RNase	Endoribonuclease
ROS	Reactive oxygen species
rRNA	Ribosomal RNA
SDS-PAGE	Sodium dodecyl sulfate polyacrylamide gel electrophoresis
SR	Sarcoplasmic reticulum
SS	Subsarcolemmal
STR	Slow-twitch red
TA	Tibialis anterior
Tfam	Mitochondrial transcription factor A
TFEB	Transcription factor EB
TIM	Translocase of the inner mitochondrial membrane
TNF	Tumor necrosis factor
TOM	Translocase of the outer mitochondrial membrane
tRNA	Transfer RNA
ULK1	Serine/threonine protein kinase ULK1
UVRAG	UV radiation resistance-associated gene protein
VDAC	Voltage Dependent anion channels
Δψm	Mitochondrial membrane potential

REVIEW OF LITERATURE

1.1. SKELETAL MUSCLE MITOCHONDRIA

1.1.1 SKELETAL MUSCLE

Skeletal muscle is one of three major muscle types, the other two being cardiac and smooth muscle. It the largest organ in the human body as it comprises 40-50% of a healthy individual's body mass. Muscle cells retain many of the organelles found within other cell types, but are unique in their long cylindrical shape and multinucleated composition. The structure of skeletal muscle is characterized by a very particular arrangement of muscle fibres, each comprised of specialized contractile elements known as myofibrils. Myofibrils consist of myosin and actin proteins repeated in units referred to as sarcomeres.

Skeletal muscle contains several different types of fibers, which can be classified based on their biochemical, mechanical, and metabolic phenotypes. The three fiber types are: 1) slow-twitch red (STR) fibers, which are considered the most slow, oxidative and fatigue resistant and are comprised predominantly of myosin heavy chain (MHC) type I, 2) Fast-twitch red (FTR) fibers comprised of mostly MHC type IIa, and are fast, oxidative, and contain intermediate metabolic properties, and 3) fast-twitch white (FTW) containing an abundant amount of MHC type IIx, causing them to be the most glycolytic, and easily fatigable (78, 88, 99). The oxidative capacity is determined by the number of mitochondria and capillaries, as well as the amount of myoglobin in the fibre. The categorization of muscle groups as being fast or slow depends on the type of myosin heavy chain (MHC) ATPase the muscle possesses (99).

The primary function of skeletal muscle is to convert chemical energy, in the form of adenosine triphosphate (ATP), into mechanical energy to generate force, maintain posture, and produce movement. This type of muscle is a highly malleable tissue, and it exhibits remarkable capabilities in its ability to adapt to a number of physiological and pathological conditions. It is extremely sensitive to its environments and is able to adjust its internal phenotype to match the energy demands and needs depending on the stimuli imposed. From a metabolic perspective, skeletal muscle is essential for energy storage, maintenance of blood glucose homeostasis, fatty acid oxidation and temperature regulation.

1.2 Mitochondrial Structure and Function

Cellular ATP is required for the function and maintenance of the cell and is paramount for skeletal muscle performance. The primary energy sourcse for skeletal muscle are mitochondria, as these organelles produce ATP through the process of mitochondrial respiration. In contrast to other organelles, mitochondria are not formed *de novo*, as they originate only through the division of existing organelles (15). These organelles are also unique in that they contain their own DNA (mtDNA) in a circular configuration, encoding 13 proteins, 22 tRNAs and two rRNAs (34). However, mitochondria require much more than their own DNA to exist, as they are made up of ~1200 proteins, most of which are nuclear-encoded. Once these genes are transcribed in the nucleus and translated in the cytosol, they are imported into mitochondria via the protein import machinery (PIM) and are organized and sent to their destined location. Mitochondria are dynamic organelles and are structurally unique as they maintain two intra-organelle subdivisions separated by phospholipid bilayers (44). The first is the

inner mitochondrial matrix, which is bound by the inner membrane, and the second is termed the intermembrane space and is located between outer membrane, and the second inner membrane (34, 46). Mitochondria exist as interconnected networks known as the mitochondrial reticulum, which is maintained and regulated by fission and fusion events. These processes add new mitochondria or remove dysfunctional organelles segments in an attempt to maintain metabolic homeostasis in the cell (38, 87).

Within skeletal muscle, mitochondria exist in two subcellular localizations with related, yet distinct functional and biochemical characteristics. Subsarcolemmal mitochondria (SS) are located along the inside surface of the muscle fiber below the sarcolemmal membrane, and lie in proximity to the myonuclei. Due to their strategic location, it has been proposed that these mitochondria play a role in supplying ATP for nuclear and membrane functions (76). The second population of mitochondria is interspersed amongst the myofibrils, and they are therefore termed intermyofibrillar (IMF) mitochondria. This fraction of organelles is primarily responsible for the provision of ATP that enables the interaction between actin and myosin, thereby facilitating muscle contraction. IMF mitochondria make up approximately 80-85% of the total mitochondrial volume and exhibit higher rates of respiration, protein import into the matrix, and protein synthesis. Conversely, SS mitochondria exhibit a higher membrane potential and reactive oxygen species (ROS) production. Due to their distinctive localizations and biochemical, functional, and compositional properties, the subfractions react differently to environmental stimuli, and the SS are found to be are more adaptive to muscle use and disuse (2, 19, 76, 108).

1.2.1 ELECTRON TRANSPORT CHAIN

Located within the cristae of the mitochondria is the electron transport chain (ETC) (**Fig. 1)**. The by-products of carbohydrate and lipid metabolism are reduced coenzymes, such as NADH and $FADH_2$. These coenzymes carry electrons, which are donated to the ETC when they are oxidized. The movement of electrons throughout the complexes of the ETC is coupled to the pumping of protons into intermembrane space (IMS), the space between the inner and outer mitochondrial membranes, creating an electrochemical gradient which is utilized as the energy source in the formation of ATP. This process is known as oxidative phosphorylation. The first step of this process involves the oxidation of NADH by NADH dehydrogenase, or complex I, thereby reducing the complex. Alternatively, in complex II, $FADH_2$ is oxidized into FAD and its electrons are sequestered by the complex. The electrons are then passed on to the electron carrier ubiquinone, also known as Coenzyme Q, which is dissolved in the hydrophobic region of the mitochondrial inner membrane and can move freely within it. When ubiquinone is in its oxidized form and comes into contact with Complex1, it accepts an electron and is reduced. The free energy released by the spontaneous reaction is used to pump protons (H^+ ions) out of the matrix. Once reduced, ubiquinone continues to move through the hydrophobic region of the membrane until it comes into contact with cytochrome b-c1 complex, or complex III, where the electron is accepted. Subunits of this complex simultaneously act as electron carriers and proton pumps, allowing the free energy to pump H^+ into the intermembrane space, further increasing the proton gradient. The electron is then passed from complex III to an oxidized cytochrome C through a random collision. Cytochrome C then collides with cytochrome c oxidase (cox), donating

its electron. This complex passes the electron to O_2, the final electron acceptor. This reaction pumps additional H^+ into the intermembrane space (17).

The electrochemical concentration gradient of protons that is formed is then harnessed to create energy in the form of ATP. ATP synthase passes H^+ from the intermembrane space back into the matrix and uses this energy to turn ADP into ATP by phosphorylation. This theory is known as the chemiosmotic theory and was proposed by Peter Mitchell in 1961 (68). The generation of ATP through this process of oxidative phosphorylation occurring in the ETC is largest supply of energy for muscle, reinforcing the importance of mitochondria for muscle performance and health.

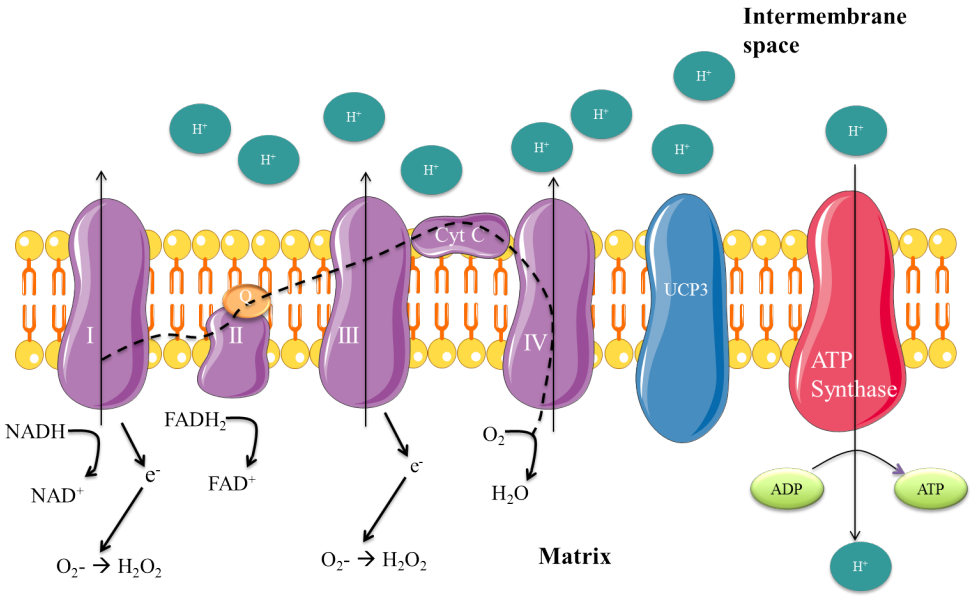

Fig. 1. Schematic of the electron transport chain. Substrates such as NADH and $FADH_2$, generated from Krebs' cycle are oxidized by complexes I and II respectively. These donated electrons are then passed through the subsequent complexes and the energy generated from their movement helps pump protons into the intermembrane space. The transfer of electrons through the ETC culminates in the reduction of O_2 thereby producing water while also contributing to the buildup of H^+ in the IMS. The accumulation of protons in the IMS generates a proton gradient which is utilized by ATP synthase to convert ADP to ATP. In some instances, electrons can escape through complex I or III, prematurely reducing oxygen and subsequently generating reactive oxygen species (ROS). Uncoupling protein 3 (UCP3) can dissipate the proton gradient by allowing the passsage of H^+ into the matrix thereby producing heat without the generation of ATP.

1.3. ROS AND ANTIOXIDANTS

With any dysfunctions in the ETC during respiration, electrons are prone to prematurely escaping and partially reducing O_2, thus forming reactive oxygen species (ROS). Therefore, mitochondria have been regarded as the primary sites of ROS production within skeletal muscle (6, 10, 69, 85). Studies have demonstrated that NADH dehydrogenase (complex I) and cytochrome bc1 (complex III) are the major sites of superoxide production (69, 85). The produced superoxide may be ultimately transformed into highly reactive radicals and causes an accumulation of damaged DNA, oxidized proteins, and peroxidized lipids.

Currently, there is no consensus on whether or not mitochondria-derived ROS are beneficial or detrimental to the cell. At a certain threshold, ROS can exert beneficial effects and act as signaling molecules in processes such mitochondrial biogenesis (10, 33, 39). Within the confines of this range, cellular stress can promote adaptations that contribute to organismal fitness. However, beyond this range, increasing amounts of ROS that cannot be scavenged, are associated with pathologies, senescence or cell death.

Muscle cells contain both enzymatic and non-enzymatic antioxidants making up systems that work together in an attempt to regulate ROS and maintain oxidative balance. Some antioxidant enzymes convert ROS to less active molecules, while others scavenge ROS species. The primary antioxidant enzymes in the cell include superoxide dismutase, glutathione peroxidase, and catalase. Non enzymatic antioxidants found in the cell include glutathione (GSH), uric acid, and bilirubin (67, 82, 83). In addition to endogenous antioxidants, there are several dietary antioxidants that can contribute to the protection against ROS, including vitamin E, vitamin C, and carotenoids (6).

The activation of transcriptional pathways of endogenous antioxidant enzymes, such as the Nrf2/Keap1 pathway are essential in protecting the cell from endogenous and exogenous insults that can alter its redox balance. Nuclear erythroid 2 p45-related factor 2 (Nrf2) is a transcription factor regarded as the master regulator of antioxidant and detoxifying enzyme expression. Under basal conditions, Nrf2 resides in the cytosol where it is bound to Keap1(18, 50, 51) . However, with an increase in oxidative stress, Nrf2 is dissociated from Keap1, translocates to the nucleus and binds to antioxidant response elements (ARE) found on the promoter region of its target genes. Among these target genes are those coding for NADPH quinone oxidoreductase 1 (NQO1) and heme oxygenase 1 (HO1) (51, 79). Nrf2-null mice exhibit a marked reduction in several antioxidant and phase II detoxification enzyme genes that are required to protect the cell against increases in oxidative stress (41), indicating the importance of this pathway in mediating the stress response in the cell.

2.0. MITOCHONDRIAL TURNOVER

Mitochondria are essential organelles for the provision of ATP through oxidative phosphorylation (32, 89). These organelles play a central role in muscle cell metabolism, the regulation of energy-sensitive signaling pathways, reactive oxygen species production/signaling, calcium homeostasis and the regulation of apoptosis (115). Mitochondrial dysfunction has been implicated in a large number of adverse events/conditions affecting skeletal muscle health. In order to provide sufficient energy for muscle, it is vital to maintain a healthy pool of mitochondria. This maintenance is governed through two antagonistic processes: mitochondrial biogenesis and mitochondrial-specific autophagy (mitophagy). These processes work together to

maintain a balance of mitochondria in the cell. General Control of Amino Acid Synthesis 5-like 1 (GCN5L1) is a mitochondrial protein that has been shown to regulate mitochondrial clearance through mitophagy. Cells lacking this protein experience up-regulation in both autophagy and mitochondrial biogenesis through an increase Peroxisome proliferator—activated receptor (PPAR)-γ coactivator (PGC-1α), which is the master regulator of mitochondrial biogenesis, and transcription factor EB (TFEB), the master regulator of lysosomal biogenesis(100). Furthermore, TFEB and PGC-1α have been shown to regulate the expression of one another in a variety of cell types (104, 113). This indicates a correlation and coordinated regulation of mitochondrial synthesis and degradation.

2.1. Mitochondrial Biogenesis

Mitochondrial biogenesis refers to the synthesis of new mitochondria and the subsequent expansion of the mitochondrial network (3, 36). Mitochondria have their own DNA (mtDNA), and thus this process is controlled by the coordinated transcription of nuclear and mitochondrial genes, regulated by the coactivator PGC-1α (3) . Various stimuli are capable of acting as signaling events to initiate biogenesis (34) and induce the transcription of nuclear genes encoding mitochondrial proteins (NUGEMPs) such as mitochondrial transcription factor A (TFAM) and Nuclear Respiratory Factor 1 (NRF1) and 2 (NRF2) (97). Once transcribed, TFAM and other mitochondrial destined proteins are translated in the cytosol and subsequently imported into the mitochondria (123).

Over 1000 nuclear-encoded mitochondrial proteins are synthesized in the cytosol and require proper transport in order to end up in their proper compartment within mitochondria(12). The machinery regulating this process is known as the protein import

machinery (PIM), and include the translocase of outer membrane (TOM) and translocases of inner membrane (TIM) complexes (75). Once a mitochondrial protein is translated in the cytosol, it is recognized and unfolded and linearized by chaperones, exposing a presequence which targets their movement into the mitochondria (44, 107). Once in the mitochondria, and in their respective compartments, the presequence is cleaved off and the proteins are refolded and assembled (37, 75).

2.1.1 PGC-1α

Peroxisome proliferator—activated receptor (PPAR)-γ coactivator (PGC-1α) is a transcriptional coactivator and is known as the master regulator of mitochondrial biogenesis (3, 20, 114). It is involved in many metabolic processes including liver gluconeogenesis, thermogenesis, fiber type specialization in skeletal muscle, and possesses the ability to mediate exercise-induced adaptations (3). PGC-1α lacks the ability to bind to DNA directly, and thus acts by enhancing the activity of transcription factors such as nuclear respiratory factors 1(NRF-1) and 2 (NRF-2), and coactivates the transcription of nuclear-encoded gene products involved in mitochondrial biogenesis (22, 36). These include subunits of protein complexes in the electron transport chain (ETC) and the factors involved in their assembly, mtDNA transcription and replication machinery, and mitochondrial protein import machinery complexes. Furthermore, PGC-1 activates NRF-1 on the promoter of mitochondrial transcription factor A (Tfam), a protein essential for the increased mtDNA expression (20, 112). In addition to coactivating the transcription of NUGEMPS, the expression of several antioxidants such as superoxide dismutases 1 and 2 (SOD1 and SOD2), and catalase are also regulated by PGC-1α (106) . Overexpression of PGC-1α is sufficient to increase mitochondrial

content, the proportion of type 1 muscle fibers, and resistance to fatigue (11). In contrast, mice lacking the PGC-1α gene display reduced mitochondrial content and function resulting in impaired endurance performance (3, 36). Despite the impairments seen in PGC-1α KO mice, there is controversy regarding the requirement of the protein for training-induced adaptations (58). Muscle specific PGC-1α KO mice showed similar exercise capacities and increased mitochondrial biogenesis after training as their WT counterparts indicating that other factors play a role in mitochondrial biogenesis with exercise (58).

2.1.2. Regulation of Mitochondrial Biogenesis

PGC-1α can be regulated both transcriptionally and post-translationally to allow for both short- and long-term regulation of mitochondrial biogenesis and cellular energy management (29). These aspects of modulation are highly sensitive to energy status, temperature, nutrient availability, and more (60). The PGC-1α promoter, via numerous transcription factors is influenced by alterations in ROS, NAD+, AMP and Ca^{2+} levels which occur in response to physiological conditions (24).

Indeed, several transcription factors are implicated in the process of mitochondrial biogenesis by binding and activating the PGC-1α promoter. These include cAMP responsive element binding protein (CREB), calcium-regulated transcription factor 2 (ATF2), p38 mitogen activated protein kinase (MAPK), Forkhead transcription factor, and many others (4, 39, 98). It has been shown that the activation of Ca^{2+}/Calmodulin, as well as calcineurin can induce the transcription of PGC-1α by binding to the CREB and MEF2 binding sites on its promoter (125). p38 MAPK is also able to induce transcription by phosphorylating MEF2 and ATF2 and thus increasing binding. p38 is also known to

not only increase PGC-1α transcription, but also increase the activation of the protein by phosphorylation (40, 84, 125) Many of these metabolically-sensitive signaling pathways are activated during exercise, causing the well-known adaptation of skeletal muscle and the essential increase in mitochondrial structure and function.

2.1.3. MITOCHONDRIAL BIOGENESIS AND EXERCISE:

Exercise has been shown to cause adaptations within skeletal muscle, characterized by a prominent increase in mitochondrial content. Depending on the exercise regimen, mitochondrial content can increase by 50-100% in order to supply the muscle with energy for contractions (1, 35). In response to a single bout of exercise, PGC-1α and Tfam mRNA are significantly increased. PGC-1α and Tfam proteins levels are shown to increase progressively over long-term training protocols (5, 60, 93). This produces an increase in mtDNA copy number, allowing for the mitochondrial reticulum to grow and to increase the oxidative capacity of the exercise trained muscle.

Interestingly, chronic exercise has been shown to increase mitochondrial protein import in order to match the needs of an expanding mitochondrial reticulum (35, 47, 107). This occurs as a result of contractile activity-induced increases in PIM component expression, as well as changes within the cytosolic fraction of the cell. The identity of these cytosolic factors remains largely to be determined (28, 107). The expression of several key protein import machinery components is increased in response to chronic contractile activity. These include the outer membrane receptor TOM20, cytosolic chaperones, as well as mitochondrial heat shock protein 70 (mtHSP70). These increases allow for greater import of precursor mitochondrial destined proteins (107).

Another protein that plays a role in exercise-induced mitochondrial biogenesis, is p53. Various models of chronic endurance exercise training have been shown to increase protein levels of p53 in muscle (7, 8, 92). Contractile activity in cell culture and human models have shown serine 15 phosphorylation of p53 which stabilizes the protein and activates it (7). However, while p53 KO mice show reduced mitochondrial content, exercise training of these mice is sufficient to increase mitochondrial content, indicating a p53-independent pathway to promote mitochondrial biogenesis with exercise (92).

Exercise is associated with the turnover of ATP within muscle causing a decreased ATP-to-ADP ratio, thereby resulting in the accumulation of AMP levels in the cytosol. Consequentially, AMP activates AMP-activated protein kinase (AMPK), leading to enhanced PGC-1α promoter activity (40, 42). Pharmacological activation of AMPK by AICAR increased PGC-1α mRNA as well as protein levels, accompanied by DNA binding of NRF1 (40). In addition, AMPK is able to post-transnationally activate PGC-1α by phosphorylating the protein, allowing it to translocate into the nucleus and coactivate transcription factors involved in mitochondrial biogenesis (39, 40). To further prove the role of AMPK in PGC-1α activation, studies have knocked out AMPK subunits and found reduced mitochondrial content and function in these models, resulting in impaired endurance (74).

2.2. MITOCHONDRIAL DEGRADATION

Organelle degradation is mediated by a process termed autophagy, where double membrane vesicles known as autophagosomes, engulf damaged organelles and fuse with a lysosomal membrane where these organelles are digested (31, 95). This process involves distinct steps including induction, cargo recognition and selection, vesicle formation, autophagosome-vacuole fusion resulting in breakdown of the cargo and the

release of the degradation products back into the cytosol. Mitochondria specifically undergo a selective form of macro-autophagy known as mitophagy (31) .

Mitochondrial content exhibits plasticity in muscle, as it decreases with aging and disuse and can increase with regular physical activity. With increasing amounts of mitochondrial enzymes there is an impact on carbohydrate and lipid metabolism, as well as endurance capacity (13). Due to their vital roles in muscle function, the removal of damaged or dysfunctional mitochondria is extremely necessary for the maintenance of a healthy mitochondrial network and for ensuring quality control. Impairments in this process are characterized by the presence of abnormal mitochondria, oxidative stress, accumulation of polyubiquitinated proteins and structural defects within the sarcomere (63). This could lead to apoptosis, cancer, and numerous muscular and neurodegenerative disorders (16).

2.2.1 MITOPHAGY

The competing processes of mitochondrial biogenesis and mitophagy may be influenced by the same environmental stimuli in an attempt to maintain the cell in a state of homeostasis. Mitochondria are flagged and tagged for degradation by specialized proteins when they exhibit a decreased membrane potential and an increase in ROS (45, 64, 72). This can be induced by a variety of different stimuli such as hypoxia, ischemia, mtDNA damage, caloric restriction, and exercise (25, 105, 115).

2.2.2 SIGNALING

Many cellular stressors are able to activate the pathways involved in the clearance of dysfunctional mitochondria. Oxidative stress is strongly linked to mitochondrial dysfunction as mitochondria are both generators of, and targets of ROS. With an increase

in ATP turnover during exercise, or with dysfunction in mitochondrial ETC respiration, electrons may prematurely escape the ETC and partially reduce oxygen, thus producing reactive oxygen species (ROS) (69, 70). ROS are often viewed as toxic byproducts of the ETC, however under a certain threshold they act as signaling molecules and are important for mitochondrial biogenesis, as well as the induction of mitophagy. Studies have shown that increases in ROS are able to induce mitophagy (26), through various signaling cascades.

Nutrient signaling has been established as an important factor in the regulation of autophagy and mitophagy. Mammalian target of rapamycin complex 1mTORC1 is activated in the presence of growth factors , and cellular nutrients such as amino acids (48). This protein functions as an inhibitor of the initiation step in autophagy and thus its activity is suggested to down-regulate the process. Therefore, the activity of mTORC1 is inhibited under starvation conditions. Autophagy has been shown to be induced by not only nutrient depravation, but also by reduced growth factor signaling (55).

During periods of increased metabolic demand and energy depletion, mitophagy is required to maintain homeostasis in the cell. Under these conditions, AMP activated protein kinase (AMPK) is able to sense an increase of AMP and is activated by the decrease in ATP/AMP ratio. When activated, AMPK is able to inactivate Rheb, which is an activator of mTORC1, thus suppressing mTORC1 activity. Furthermore, AMPK is able to phosphorylate raptor, which further inhibits mTORC1. AMPK and mTORC1 have demonstrated the ability to regulate mitophagy through the phosphorylation of UNC-51-like kinase 1 (Ulk1) (**Fig. 2)**. Both proteins are able to phosphorylate Ulk1, thus directing its activity. Under starvation conditions, AMPK inhibition of mTORC1 releases

its Ser757 phosphorylation and allows for an AMPK-Ulk1 interaction. AMPK then phosphorylates Ulk1 on other serines, activating the kinase. There is a tight regulation between these three proteins. The phosphorylation of Ulk1 by mTORC1 influences the interaction of Ulk1 with AMPK, while the interaction between ULK1 and mTORC1 is influenced by phosphorylation of ULK1 by AMPK (49, 56, 111). Furthermore, Ulk1 phosphorylation is able to act as a feedback loop by phosphorylating and thus regulating AMPK and mTORC1. Upon activation, the Ulk1 complex is recruited to dysfunctional mitochondria and regulated the autophagic clearance of damaged mitochondria (111, 122). Loss of AMPK and Ulk1 results in an accumulation of autophagy related proteins, as well as defective mitophagy (111).

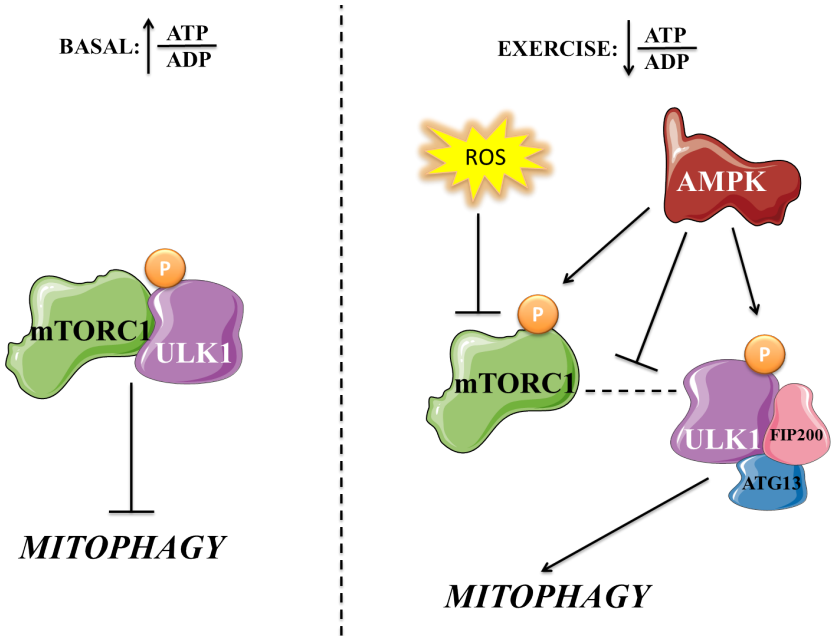

Fig. 2. The regulation of mTORC1 and ULK1 complex. Under basal condition where there is a high ATP to ADP ratio, mTORC1 phosphorylates ULK1 and renders it inactive, inhibiting autophagy. Under exercise conditions, or when the ATP to ADP ratio is low, mTORC1 is inactivated by elevated ROS and by AMPK phosphorylation. Phosphorylation of mTORC1 and ULK1 inhibits the interaction of mTORC1 and ULK1, allowing ULK1 complex to activate autophagy.

2.2.3 MITOPHAGY PATHWAYS

Several pathways are involved in the clearance of dysfunctional mitochondria when all other quality control mechanisms such as the unfolded protein response (UPR) and the ubiquitin proteasome system (52) are unable to restore proper mitochondrial function. The canonical, and most well established pathways involves PTEN-induced putative kinase protein 1 (PINK1) and Parkin (**Fig. 3)**. Under normal conditions when mitochondria are functioning properly, PINK1 is able to be imported into mitochondria and is degraded by proteases (118). However, when there is a reduction in the mitochondrial membrane potential, the import machinery loses its functionality, and PINK1 accumulates and stabilizes on the outer mitochondrial membrane (64, 72, 118). Stabilization of PINK1 facilitates the recruitment of the E3-ubiquitin ligase Parkin to mitochondria. Parkin then mediates the ubiquitination of various outer membrane proteins targeting them for degradation. Among these proteins are ones involved in mitochondrial fusion, such as mitofusion1 (MFN1) and mitofusion 2 (MFN2) (109). Parkin also ubiquitinates other outer mitochondrial membrane proteins such as the voltage dependent anion channels (VDAC), translocase of the outer membrane proteins (TOMs), among many others. Ubiquitination of these proteins recruits the adapter protein p62/SQSTM1. p62 contains both ubiquitin and microtubule-associated protein 1 light chain 3 (LC3) interacting domains (27), serving as an anchor and allowing the facilitation of an autophagic double membrane around the dysfunctional mitochondrion (73, 110). The formation of the autophagic vesicle begins once LC3I is lipidated into LC3II with the aid of other autophagy-related genes such as ATG 7 (73, 110). Once lipidated, LC3II is able to interact with p62 and fully engulf the mitochondria in the autophagosome. The

autophagosome travels on microtubule tracks and fuses with the lysosome with the help of lysosomal associated membrane proteins 1 and 2 (LAMP1 and LAMP2) (23).

Bcl-2/adenovirus E1B 19 kDa protein-interacting protein 3 (BNIP3) and BNIP3-like protein X (NIX) were originally recognized for their role in mitochondrially-induced apoptosis, however recent evident has demonstrated their involvement in the process of mitophagy(119, 124). BNIP3 and NIX localize to the outer membrane of dysfunctional mitochondrion and flag it for degradation. The two proteins possess an LC3 interacting region and are able to act as receptors for LC3 family members and allow the formation of the autophagosome. Furthermore, BNIP3 has demonstrated the ability to recruit dynamin related protein 1 (Drp1) to the mitochondria, thus activating fission and inducing parkin-mediated autophagy (57). This autophagy pathway is often induced by hypoxia when mitochondria can generate excess ROS, further exacerbating oxygen deficits (9).

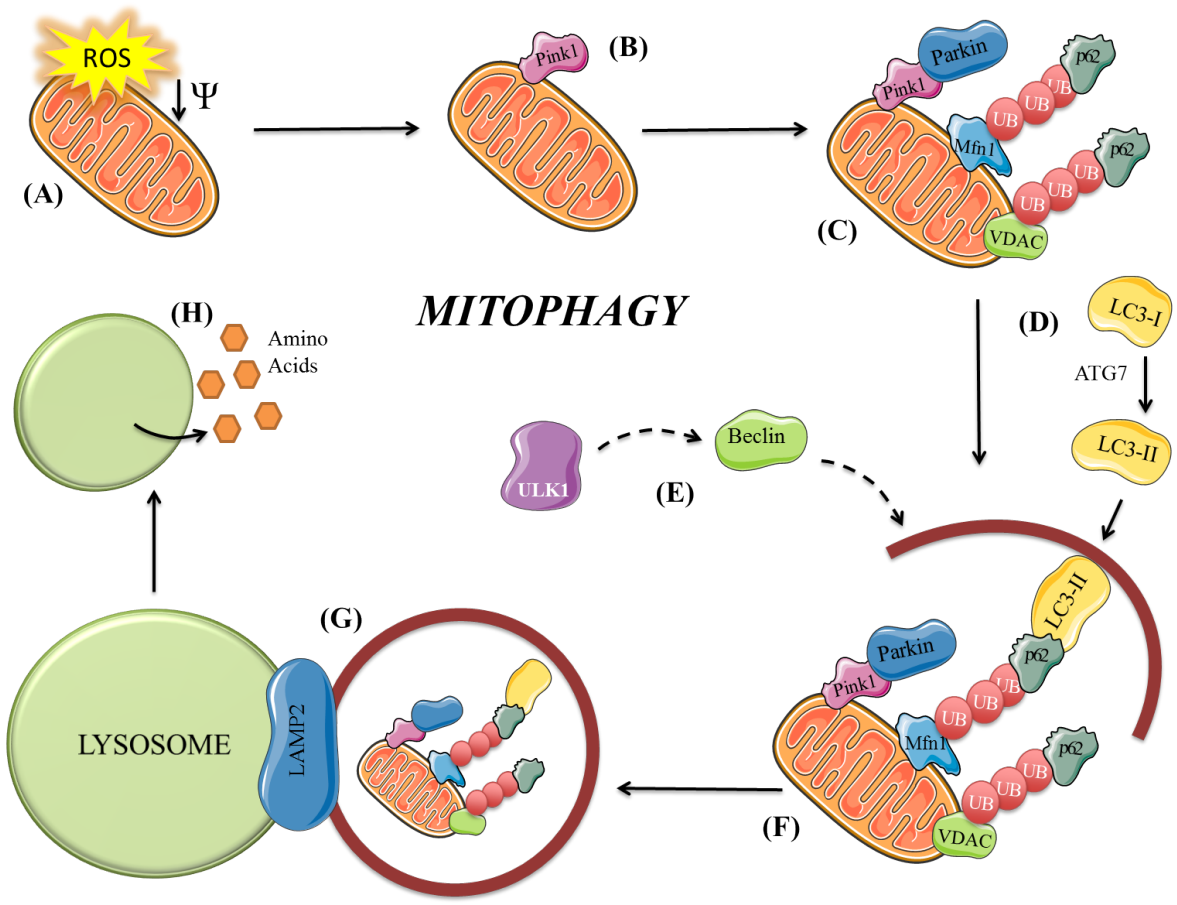

Fig. 3. General scheme of the degradation of dysfunctional mitochondria through the process of mitophagy. (A) A dysfunctional mitochondrion produces higher amounts of ROS and a lowered membrane potential, **(B)** causing an accumulation of Pink1 on the outer mitochondrial membrane. **(C)** Pink1 accumulation recruits the E3 ubiquitin ligase Parkin which in turn ubiquitinates outer mitochondrial proteins such as Mfn1 and VDAC. Ubiquitination of these proteins recruits the adaptor protein p62. **(D)** LC3I lipidation to LC3II by ATG7 and **(E)** Beclin1 activation by ULK1 allow for the initial formation of the autophagosome, **(F)** which is recruited to mitochondria through an interaction of LC3II with p62. **(G)** The autophagosome fully engulfs the mitochondria and fuses with the lysosome with the aid of LAMP1. **(H)** The lysosome then breaks down mitochondria.

2.2.4. MITOPHAGY AND EXERCISE

Chronic exercise training is known to have extremely beneficial health effects. Engaging in regular exercise causes an improvement in glucose homeostasis, muscle mass maintenance, cardiovascular health, and can even help reduce complications that occur with aging (5, 16, 35, 80, 89). On a molecular level, exercise exerts favorable effects on bioenergetics and nutrient delivery and uptake, which largely occur due to the induced adaptations of skeletal muscle in response to exercise (35, 91, 116). As previously mentioned, exercise results in a large increase in mitochondrial content via an induction of organelle biogenesis (35, 89). While it is important to ensure there is a sufficient increase in mitochondrial synthesis, it is also extremely vital to remove any dysfunctional mitochondria that are no longer working to satisfy the newly elevated energy demands to exercise (21, 116).

Recent work has focused on the role of mitophagy as a cellular homeostasis response since protein and organelle degradation and recycling are vital for the cell. This process is ongoing at a basal level, but it is up -regulated as a result of increased oxidative stress, energetic imbalance, or protein misfolding in an attempt to improve and maintain mitochondrial quality (21). In keeping with this, it has been documented that both acute exercise, and exercise training are able to activate the mitophagy pathway as it is a form of energetic stress (59, 63, 116). During exercise, energy demand outweighs the supply, causing the ATP/AMP ratio to decrease, activating AMPK, an established activator of mitophagy, while reducing the activity mTORC1, a known inhibitor of the process. Furthermore, ROS production increases with exercise, further activating AMPK as well as p38 MAPK, and sirtuin-1 (SIRT1) (4, 14, 81). Recent evidence has demonstrated that

PGC-1α not only has a role in exercise-induced mitochondrial biogenesis, but it is also implicated in mediating exercise-induced autophagy (117) suggesting a novel key player in this vital degradation mechanism. This further establishes a connection and interplay between the two processes mediating mitochondrial turnover and quality control.

3.0. TFEB

Autophagy, and more specifically, mitophagy, is a selective process able to discriminate between healthy and damaged organelles with the aid of receptors and signaling components. In order for the process to occur, there needs to be an effective cooperation of two specific organelles: the autophagosome and the lysosome. Recent work has identified a regulatory network of genes known as coordinated lysosomal enhancement and regulation (CLEAR) which controls lysosomal biogenesis and function (101). The master gene regulating this network is the basic helix loop helix (bHLH)-leucine zipper transcription factor TFEB. This protein is a part of the MiT/TFE transcription factor subfamily along with MITF, TFE3, and TFEC (94).

3.1. Role of TFEB

The activation and role of TFEB is extremely important for the regulation of lysosomal biogenesis and clearance, as well as autophagy and autophagy-lysosome fusion-related proteins. TFEB directly binds to CLEAR elements, thus promoting the expression of the entire network of genes that contains the CLEAR regulatory motif in their promoters (96). Therefore, it is not surprising that TFEB overexpression results in an increased number of lysosomes and lysosomal enzymes which in turn enhances lysosomal catabolic activity (96). In addition to regulating lysosomal biogenesis, TFEB has also been shown to coordinate the expression of genes involved in autophagosome

biogenesis and autophagosome-lysosome fusion, indicated by an increased clearance of lipid droplets and mitochondria with TFEB overexpression (66, 77, 104). Members of the CLEAR network that are directly targeted by TFEB include lysosomal hydrolases and accessory proteins, lysosomal membrane proteins, lysosomal acidification proteins and non-lysosomal proteins involved in lysosomal biogenesis and autophagy. Overall it is evident that TFEB is an essential mediator of the many steps involved in organelle clearance.

The role of TFEB has been evolutionary conserved. Work has demonstrated that overexpression of HLH-30, the worm TFEB orthologue, induces autophagy and lipid catabolism, indicating that this gene shares many of the essential roles that TFEB plays in mammals (53, 71). In contrast, loss of function mutations of this orthologue resulted in impaired expression of key enzymes required for proper fat catabolism and in impaired lipophagy (53, 90). This was conserved in mammals in which adenoviral overexpression of TFEB in mice allowed for protection against obesity and diabetes and caused the mice to utilize their fat more effectively (104). Many animal models have been used to elucidate a role for TFEB as a regulator of liver lipid metabolism, and in controlling energy balance in mouse skeletal muscle. In HeLa cells, TFEB overexpression was found to induce transcriptional activation of numerous lysosomal genes, resulting in a significant increase in the total number of lysosomes (96, 102), indicating a similar role for TFEB in human cells.

3.2. TARGETS OF TFEB

TFEB is ubiquitously expressed and plays an imperative role in the integrated biogenesis of two organelles involved in a tight partnership that promotes the degradation

of dysfunctional organelles such as the mitochondria. As previously mentioned, TFEB's role in autophagy was studied using overexpression models in HeLa cells. These studies showed a significantly increased number of autophagosomes, detected by immunofluorescence and immunoblotting of LC3. Similar results were shown in COS7 (monkey kidney fibroblast), as well as mouse embryonic fibroblasts (MEF) (102). Furthermore, mRNA levels of 11 genes involved in several steps of the autophagy pathway were significantly increased with TFEB overexpression in these cells. The expression of UVRAG, WIPI, LC3II, p62, VPS11, VPS18 and ATG9B was most significantly affected. Opposite results were shown with TFEB silencing (102).

The significance of TFEB as the master regulator of lysosomal biogenesis specifically was also characterized using TFEB overexpression studies. HeLa cells transfected with a plasmid containing TFEB cDNA displayed an increase in mRNA levels of 22 lysosomal genes, accompanied by augmented activation of lysosomal enzymes β-glucosidase, Cathepsin D, and β-glucuronidase (96). These results were duplicated in human embryonic kidney (HEK) 293 cells, which also exhibited an induction of lysosomal genes with TFEB overexpression (96). To further elucidate this role for TFEB, a microarray analysis was performed on HeLa cells after TFEB expression. These data showed an upregulation of 291 genes, most of which were lysosomal genes and genes related to lysosomal biogenesis and function (96). TFEB activation induced by starvation resulted in an increase of genes involved in ATPase pump formation, lipid metabolism, membrane proteins, fusion proteins, lysosomal membrane proteins, and autophagy proteins (96, 103, 104). Genes such as Cathepsin D, LAMP1, p62 where all shown to significantly increase with TFEB activation.

A combination of several genomic approaches and experiments has identified over 400 TFEB direct targets that represent essential components of the CLEAR network. These experiments found that TFEB regulates the transcription of at least five different degradation systems as well as target genes encoding the subunits of a vacuolar proton pump, which creates and maintains the lysosomal acidic environment (77). Furthermore, among TFEB direct targets are genes belonging to distinct families of pattern recognition molecules including membrane-anchored Toll-like receptors (TLRs), cytosolic Nod-like receptors (NLRs) and Rig-I-like receptors (RLRs). These genes are involved in innate immune detection of danger signals. In addition to autophagy signaling, TFEB is also involved in mitogen-activated protein (MAP) kinases and p53 signaling, both known to play key roles in cell differentiation and proliferation, as well as cell survival and apoptosis. Moreover, TFEB overexpression exerted beneficial effects on the regulation of lipid catabolism under high fat diet conditions. Under a normal diet mice overexpressing TFEB were leaner than their control counterparts. In addition, TFEB overexpression was able to rescue the development of the obese phenotype in mice fed a high fat diet. In contrast, the lipid content of muscles and body weight were both rescued by the effects of TFEB overexpression. The opposite was seen with a TFEB knockout model (104).

An interesting target of TFEB is PGC-1α, known as the master regulator of mitochondrial biogenesis. TEFB overexpression increased protein levels of PGC-1α, and activation of TFEB via starvation caused an increase in PGC-1α promoter activity. Several studies have demonstrated a correlation between the two master regulators. In 2013, Settembre et al (102) revealed that knocking out PGC-1α, causes an inhibition of the beneficial effects TFEB overexpression exerts on lipid catabolism. Other studies have

shown a decrease in TFEB content in PGC-1α KO mice (115). Recent work has investigated the role of GCN5-like protein 1 (GCN5L1) in mediating the interplay between the two proteins. GCN5L1 KO mice exhibit increased protein levels of TFEB and PGC-1α as well as their downstream targets. However, when either TFEB or PGC-1α was silenced in these KO mice, the expression of the protein was no longer increased (100). This indicates a coordinated regulation of the two proteins, mediated by GCN5L1.

3.3. ACTIVATION OF TFEB

Environmental stressors regulate the quality control of organelles such as mitochondria. Studies have demonstrated that fasting and conditions of nutrient deprivation such as caloric restriction are major stimuli for autophagy of these organelles. Therefore, it is not surprising that TFEB is regulated by environmental cues and is activated by starvation (66, 86). It is well documented that TFEB is mainly regulated though its phosphorylation status. Under basal conditions, TFEB is phosphorylated and sequestered in the cytosol where it remains inactive. However, dephosphorylation of TFEB causes its activation and subsequent translocation into the nucleus. Once translocated, TFEB can recognize the CLEAR motif and bind to the promoter regions of numerous autophagy and lysosome genes and induce their transcription. The upregulation of these genes stimulates the autophagy pathway and helps the cell return to homeostasis.

The transcriptional activity of TFEB is regulated by mTORC1. mTORC1 is a growth regulator and responds to amino acids arising from within the lysosomal lumen. When amino acids are released from the lysosome under high nutrient conditions they activate Rag GTPases. These Rag proteins interact with a complex known as Regulator. This complex binds to raptor on mTORC1 and promotes the relocalization of mTORC1

from the cytosol to the lysosomal membrane which contains Rheb, an activator of mTORC1 (54, 71, 86, 103, 127). TFEB is then recruited to the lysosome through an interaction with mTORC1, which phosphorylates TFEB on ser^{211}. Once phosphorylated, TFEB is detained in the cytosol by the chaperone 14-3-3 (86). During starvation conditions, TFEB is liberated from this chaperone and can translocate to the nucleus to stimulate the expression of autophagy-lysosomal genes (66, 71, 101). Inhibition of mTORC1 activity with various drugs such as PP242 or Torin 1, confirmed that mTORC1 had an inhibiting effect on the activation of TFEB (62, 126). TFEB can also be negatively regulated through ser^{142} phosphorylation by extracellular signal-regulated kinase (ERK) (86, 102). Not much is known about the mechanisms controlling ERK-mediated TFEB phosphorylation. However, studies have found an ERK pool on lysosomes which contains a machinery responsible for the recruitment of TFEB that is similar to that of mTORC1 (86).

The discovery that mTORC1 resides on the lysosome when controlling TFEB activity has demonstrated a vital role for the lysosome in regulating an adaptive response to environmental cues. This mechanism involves lysosome-to-nucleus signaling and post-translational modifications of the master regulator TFEB (65, 66, 103). Studies have found an additional pathway originating from the lysosome which controls TFEB sublocalization through its deposphorylation via calcium signaling. Calcineurin is a calcium-activated phosphatase that was found to dephosphorylate TFEB on ser^{211} and ser^{142}. Inhibition of calcineurin by cyclosporine A and FK506 was found to reduce TFEB translocation to the nucleus. Furthermore, *in vivo* studies revealed that transfection of mice with calcineurin promoted TFEB translocation, and exercise, a known activator of

calcineurin, had the same effect. During starvation and physical exercise calcineurin activity is locally induced near the lysosome by lysosomal calcium release through MCOLN1/mucolipin. Experiments conducted both *in vitro* and *in vivo* demonstrated that using Short hairpin (shRNA)-mediated inhibition of MCOLN1 significantly reduced TFEB translocation to the nucleus. In support of this, overexpression of MCOLN1 in HeLa cells significantly increased the shuttling of TFEB from the cytosol to the nucleus (65). Overall, it seems that two independent pathways mediated by lysosomal signaling mediate the regulation of TFEB. Environmental stimuli such as starvation and exercise cause a decreased rate of TFEB phosphorylation, through mTORC1 inhibition, and an induction of TFEB dephosphorylation by calcineurin (65, 66, 86, 103, 126).

3.3.1. TFEB AND EXERCISE

Little research has been done to investigate the activation of TFEB with exercise, however it is well documented that its activation is increased in low nutrient conditions and during increases in cytosolic calcium (66). During an acute bout of exercise an increase in calcium is known to occur, inducing a signaling pathway involved in mitochondrial biogenesis (10, 43, 61, 120, 121). Calcium also acts as an activator of calcineurin, which subsequently dephosphorylates TFEB and allows its translocation to the nucleus. Therefore, it is logical to speculate that exercise-mediated increased calcium levels can regulate TFEB activity (43, 66).

Recent studies have investigated this pathway by inhibiting calcineurin and subjecting mice to a bout of exercise. These studies shown that electroporation of calcineurin significantly induced TFEB nuclear translocation in WT mice. When WT mice were subjected to a bout of exercise, which is known to activate calcineurin, TFEB

translocation was reported as well. However, this effect was blunted when the calcineurin inhibitor CAIN was electroporated into the muscle. This suggests that exercise acts as a stimulus for the induction of TFEB activity. Autophagy is required during exercise in order to increase the turnover of damaged organelles. An increase in the expression of autophagy genes and proteins was demonstrated after an acute bout of exercise in heart and skeletal muscle (30, 117). Therefore, considering that TFEB is a master regulator of lysosomes and autophagy genes, it is not surprising that exercise plays a role in in mediating its activity.

RESEARCH OBJECTIVES

The objectives of my thesis were:

1. To determine if PGC-1α KO mice display reduced protein expression of downstream targets of TFEB, as well as antioxidant proteins;
2. To investigate the effect of exercise on TFEB promoter activity and whether this was dependent on the presence of PGC-1α;
3. To evaluate the effect of exercise on autophagy and lysosomal genes downstream of TFEB and whether this is dependent on the presence of PGC-1α;
4. To assess the effect of TFEB overexpression on its downstream targets and mitochondrial biogenesis proteins in skeletal muscle.

HYPOTHESES

We hypothesized that:

1. PGC-1α KO mice will display reduced protein expression of downstream targets of TFEB and antioxidant proteins;
2. TFEB promoter activity and its expression will increase with exercise, but this effect will be dependent on the presence of PGC-1α;
3. Exercise will increase TFEB nuclear translocation leading to increased downstream autophagy and lysosomal genes, however this will be dependent on PGC-1α;
4. TFEB overexpression will up-regulate gene expression of its downstream targets and increase protein levels of mitochondrial biogenesis markers in skeletal muscle.

REFERENCES

1. **Adamovich Y**, **Shlomai A**, **Tsvetkov P**, **Umansky KB**, **Reuven N**, **Estall JL**, **Spiegelman BM**, **Shaul Y**. The protein level of PGC-1α, a key metabolic regulator, is controlled by NADH-NQO1. *Mol Cell Biol* 33: 2603–2613, 2013.
2. **Adhihetty PJ**, **Ljubicic V**, **Menzies KJ**, **Hood DA**, **Peter J**, **Ljubicic V**, **Menzies KJ**, **Hood DA**. Differential susceptibility of subsarcolemmal and intermyofibrillar mitochondria to apoptotic stimuli. *Am J Physiol - Cell Physiol* 3: 994–1001, 2005.
3. **Adhihetty PJ**, **Uguccioni G**, **Leick L**, **Hidalgo J**, **Pilegaard H**, **Hood DA**. The role of PGC-1alpha on mitochondrial function and apoptotic susceptibility in muscle. *Am J Physiol Cell Physiol* 297: C217–C225, 2009.
4. **Akimoto T**, **Pohnert SC**, **Li P**, **Zhang M**, **Gumbs C**, **Rosenberg PB**, **Williams RS**, **Yan Z**. Exercise Stimulates Pgc-1α Transcription in Skeletal Muscle through Activation of the p38 MAPK Pathway. *J Biol Chem* 280: 19587–19593, 2005.
5. **Baar K**, **Wende AR**, **Jones TE**, **Marison M**, **Nolte LA**, **Chen MAY**, **Kelly DP**, **Holloszy JO**. Adaptations of skeletal muscle to exercise : rapid increase in the transcriptional coactivator PGC-1. *FASEB J* : 1879–1886, 2002.
6. **Barbieri E**, **Sestili P**. Reactive oxygen species in skeletal muscle signaling. *J Signal Transduct* 2012: 982794, 2012.
7. **Bartlett JD**, **Close GL**, **Drust B**, **Morton JP**. The emerging role of p53 in exercise metabolism. *Sport Med* 44: 303–309, 2014.
8. **Bartlett JD**, **Louhelainen J**, **Iqbal Z**, **Cochran AJ**, **Gibala MJ**, **Gregson W**, **Close GL**, **Drust B**, **Morton JP**. Reduced carbohydrate availability enhances exercise-induced p53 signaling in human skeletal muscle: implications for

mitochondrial biogenesis. *Am J Physiol Regul Integr Comp Physiol* 304: R450–R458, 2013.

9. **Bellot G**, **Garcia-Medina R**, **Gounon P**, **Chiche J**, **Roux D**, **Pouysségur J**, **Mazure NM**. Hypoxia-induced autophagy is mediated through hypoxia-inducible factor induction of BNIP3 and BNIP3L via their BH3 domains. *Mol Cell Biol* 29: 2570–81, 2009.

10. **Brookes PS**, **Yoon Y**, **Robotham JL**, **Anders MW**, **Sheu S**. Calcium , ATP , and ROS : a mitochondrial love-hate triangle. *Am J Physiol Cell Physiol* 287: 817–833, 2004.

11. **Calvo JA**, **Daniels TG**, **Wang X**, **Paul A**, **Lin J**, **Spiegelman BM**, **Stevenson SC**, **Rangwala SM**. Muscle-specific expression of PPARgamma coactivator-1alpha improves exercise performance and increases peak oxygen uptake. *J Appl Physiol* 104: 1304–1312, 2008.

12. **Calvo SE**, **Clauser KR**, **Mootha VK**. MitoCarta2.0: an updated inventory of mammalian mitochondrial proteins. *Nucleic Acids Res.* .

13. **Cannavino J**, **Brocca L**, **Sandri M**, **Bottinelli R**, **Pellegrino MA**. PGC1-α over-expression prevents metabolic alterations and soleus muscle atrophy in hindlimb unloaded mice. *J Physiol* 592: 4575–89, 2014.

14. **Cantó C**, **Gerhart-hines Z**, **Feige JN**, **Lagouge M**, **Milne JC**, **Elliott PJ**, **Puigserver P**, **Auwerx J**. AMPK regulates energy expenditure by modulating NAD + metabolism and SIRT1 activity. 458: 1056–1060, 2013.

15. **Carter HN**, **Chen CCW**, **Hood D a.** Mitochondria, Muscle Health, and Exercise with Advancing Age. *Physiology* 30: 208–223, 2015.

16. **Carter HN**, **Chen CCW**, **Hood DA**. Mitochondria, Muscle Health, and Exercise with Advancing Age. *Physiology* 30: 208–223, 2015.

17. **Chaban Y**, **Boekema EJ**, **Dudkina N V**. Structures of mitochondrial oxidative phosphorylation supercomplexes and mechanisms for their stabilisation ☆. *BBA - Bioenerg* 1837: 418–426, 2014.

18. **Chan K**, **Kan YW**. Nrf2 is essential for protection against acute pulmonary injury in mice. *Proc Natl Acad Sci U S A* 96: 12731–12736, 1999.

19. **Cogswell AM**, **Stevens RJ**, **Hood DA**. Properties of skeletal muscle mitochondria from subsarcolemmal and intermyofibrillar isolated regions. *Am J Physiol* 264: C383–389, 1993.

20. **Collu-Marchese M**, **Shuen M**, **Pauly M**, **Saleem A**, **Hood DA**. The regulation of mitochondrial transcription factor A (Tfam) expression during skeletal muscle cell differentiation. *Biosci Rep* 35: e00221, 2015.

21. **Drake JC**, **Wilson RJ**, **Yan Z**. Molecular mechanisms for mitochondrial adaptation to exercise training in skeletal muscle. *FASEB J* 30: 13–22, 2016.

22. **Erlich AT**, **Tryon LD**, **Crilly MJ**, **Memme JM**, **Moosavi ZSM**, **Oliveira AN**, **Beyfuss K**, **Hood DA**. Function of specialized regulatory proteins and signaling pathways in exercise-induced muscle mitochondrial biogenesis. *Integr Med Res* 5: 187–197, 2016.

23. **Eskelinen EL**. Roles of LAMP-1 and LAMP-2 in lysosome biogenesis and autophagy. *Mol Aspects Med* 27: 495–502, 2006.

24. **Fernandez-Marcos P**, **Auwerx J**. Regulation of PGC-1α , a nodal regulator of mitochondrial biogenesis. *Am J Clin Nutr* 93: 884–890, 2011.

25. **Fonslow BR**, **Stein BD**, **Webb KJ**, **Xu T**, **Choi J**, **Kyu S**, **Iii JRY**. Mitophagy: mechanisms, pathophysiological roles, and analysis. 10: 54–56, 2013.

26. **Frank M**, **Duvezin-Caubet S**, **Koob S**, **Occhipinti A**, **Jagasia R**, **Petcherski A**, **Ruonala MO**, **Priault M**, **Salin B**, **Reichert AS**. Mitophagy is triggered by mild oxidative stress in a mitochondrial fission dependent manner. *Biochim Biophys Acta - Mol Cell Res* 1823: 2297–2310, 2012.

27. **Geisler S**, **Holmström KM**, **Skujat D**, **Fiesel FC**, **Rothfuss OC**, **Kahle PJ**, **Springer W**. PINK1/Parkin-mediated mitophagy is dependent on VDAC1 and p62/SQSTM1. *Nat Cell Biol* 12: 119–131, 2010.

28. **Gordon JW**, **Rungi AA**, **Inagaki H**, **Hood DA**. Effects of contractile activity on mitochondrial transcription factor A expression in skeletal muscle. *J Appl Physiol* 90: 389–396, 2001.

29. **Handschin C**. Regulation of skeletal muscle cell plasticity by the peroxisome proliferator-activated receptor γ coactivator 1α. *J Recept Signal Transduct Res* 30: 376–384, 2010.

30. **He C**, **Bassik MC**, **Moresi V**, **Sun K**, **Wei Y**, **Zou Z**, **An Z**, **Loh J**, **Fisher J**, **Sun Q**, **Korsmeyer S**, **Packer M**, **May HI**, **Hill JA**, **Virgin HW**. Exercise-induced BCL2-regulated autophagy is required for muscle glucose homeostasis. *Nature* 481: 511–515, 2012.

31. **He C**, **Klionsky DJ**. Regulation Mechanisms and Signalling Pathways of Autophagy. *Annu Rev Genet* 43: 67, 2009.

32. **Hepple RT**. Mitochondrial involvement and impact in aging skeletal muscle. *Front Aging Neurosci* 6: 211, 2014.

33. **Heusch P**, **Canton M**, **Aker S**, **van de Sand A**, **Konietzka I**, **Rassaf T**, **Menazza S**, **Brodde O**, **Di Lisa F**, **Heusch G**, **Schulz R**. The contribution of reactive oxygen species and p38 mitogen-activated protein kinase to myofilament oxidation and progression of heart failure in rabbits. *Br J Pharmacol* 160: 1408–16, 2010.

34. **Hood DA**, **Irrcher I**, **Ljubicic V**, **Joseph A**. Coordination of metabolic plasticity in skeletal muscle. *J Exp Biol* 209: 2265–2275, 2006.

35. **Hood DA**, **Tryon LD**, **Vainshtein A**, **Memme J**, **Chen C**, **Pauly M**, **Crilly MJ**, **Carter H**. Exercise and the Regulation of Mitochondrial Turnover. *Prog Mol Biol Transl Sci* 135: 99–127, 2015.

36. **Hood DA**, **Uguccioni G**, **Vainshtein A**, **D'souza D**. Mechanisms of exercise-induced mitochondrial biogenesis in skeletal muscle: Implications for health and disease. *Compr Physiol* 1: 1119–1134, 2011.

37. **Horvath SE**, **Rampelt H**, **Oeljeklaus S**, **Warscheid B**, **Van Der Laan M**, **Pfanner N**. Role of membrane contact sites in protein import into mitochondria. *Protein Sci* 24: 277–297, 2015.

38. **Iqbal S**, **Ostojic O**, **Singh K**, **Joseph A-M**, **Hood D a**. Expression of mitochondrial fission and fusion regulatory proteins in skeletal muscle during chronic use and disuse. *Muscle Nerve* 48: 963–70, 2013.

39. **Irrcher I**, **Ljubicic V**, **Hood DA**. Interactions between ROS and AMP kinase activity in the regulation of PGC-1alpha transcription in skeletal muscle cells. *Am J Physiol Cell Physiol* 296: C116–23, 2009.

40. **Irrcher I**, **Ljubicic V**, **Kirwan AF**, **Hood DA**. AMP-Activated Protein Kinase-Regulated Activation of the PGC-1α Promoter in Skeletal Muscle Cells. *PLoS One*

3: e3614, 2008.

41. **Itoh K**, **Chiba T**, **Takahashi S**, **Ishii T**, **Igarashi K**, **Katoh Y**, **Oyake T**, **Hayashi N**, **Satoh K**, **Hatayama ØI**. An Nrf2 / Small Maf Heterodimer Mediates the Induction of Phase II Detoxifying Enzyme Genes through Antioxidant Response Elements. *Biochem Biophys Res Commun* 322: 313–322, 1997.

42. **Jäger S**, **Handschin C**, **St-Pierre J**, **Spiegelman BM**. AMP-activated protein kinase (AMPK) action in skeletal muscle via direct phosphorylation of PGC-1alpha. *Proc Natl Acad Sci U S A* 104: 12017–22, 2007.

43. **Jamart C**, **Naslain D**, **Gilson H**, **Francaux M**. Higher activation of autophagy in skeletal muscle of mice during endurance exercise in the fasted state. *Am J Physiol - Endocrinol Metab* 305: 964–974, 2013.

44. **Jensen RE**, **Dunn CD**. Protein import into and across the mitochondrial inner membrane: Role of the TIM23 and TIM22 translocons. *Biochim Biophys Acta - Mol Cell Res* 1592: 25–34, 2002.

45. **Jin SM**, **Youle RJ**. The accumulation of misfolded proteins in the mitochondrial matrix is sensed by PINK1 to induce PARK2/Parkin-mediated mitophagy of polarized mitochondria. *Autophagy* 9: 1750–1757, 2013.

46. **Joseph A**, **Hood DA**. Mitochondrion Plasticity of TOM complex assembly in skeletal muscle mitochondria in response to chronic contractile activity. *MITOCH* 12: 305–312, 2012.

47. **Joseph A-M**, **Ljubicic V**, **Adhihetty PJ**, **Hood DA**. Biogenesis of the mitochondrial Tom40 channel in skeletal muscle from aged animals and its adaptability to chronic contractile activity. *Am J Physiol Cell Physiol* 298: C1308–

14, 2010.

48. **Jung CH1, Ro SH, Cao J, Otto NM KD**. mTOR regulation of autophagy. *FEBS Lett* 48: 1–6, 2010.

49. **Kim Joungmok, Kundu Mondira, Viollet Benoit GK-L**. AMPK and mTOR regulate autophagy through direct phosphorylation of Ulk1. 48: 1–6, 2010.

50. **Kobayashi A**, **Kang M**, **Okawa H**, **Ohtsuji M**, **Zenke Y**, **Chiba T**, **Igarashi K**, **Yamamoto M**. Oxidative stress sensor Keap1 functions as an adaptor for Cul3-based E3 ligase to regulate proteasomal degradation of Nrf2. *Mol Cell Biol* 24: 7130–7139, 2004.

51. **Kobayashi M**, **Yamamoto M**. Nrf2-Keap1 regulation of cellular defense mechanisms against electrophiles and reactive oxygen species. *Adv Enzyme Regul* 46: 113–40, 2006.

52. **Kotiadis VN**, **Duchen MR**, **Osellame LD**. Mitochondrial quality control and communications with the nucleus are important in maintaining mitochondrial function and cell health ☆☆. *BBA - Gen Subj* 1840: 1254–1265, 2014.

53. **Lapierre LR**, **Filho CDDM**, **Mcquary PR**, **Chu C**, **Visvikis O**, **Chang JT**, **Gelino S**, **Ong B**, **Davis AE**. The TFEB orthologue HLH-30 regulates autophagy and modulates longevity in Caenorhabditis elegans. *Nat Commun 2013* 4: 1–17, 2013.

54. **Laplante M**, **David M**. mTOR signaling at a glance. *J Cell Sci* 122: 3589–3594, 2009.

55. **Lee J**, **Giordano S**, **Zhang J**. Autophagy, mitochondria and oxidative stress: cross-talk and redox signalling. *Biochem J* 441: 523–40, 2012.

56. **Lee JW**, **Park S**, **Takahashi Y**, **Wang HG**. The association of AMPK with ULK1 regulates autophagy. *PLoS One* 5: 1–9, 2010.

57. **Lee Y**, **Lee H-Y**, **Hanna R a.**, **Gustafsson a. B**. Mitochondrial autophagy by Bnip3 involves Drp1-mediated mitochondrial fission and recruitment of Parkin in cardiac myocytes. *AJP Hear Circ Physiol* 301: H1924–H1931, 2011.

58. **Leick L**, **Wojtaszewski J**, **Johansen S**, **Kiilerich K**, **Comes J**, **Hellsten Y**, **Hidalgo J**, **Pilegaard H**. PGC-1α is not mandatory for exercise-and training-induced adaptive gene responses in mouse skeletal muscle. *Am J Physiol Endocrinol Metab* 294: 463–474, 2008.

59. **Lira VA**, **Okutsu M**, **Zhang M**, **Greene NP**, **Laker RC**, **Breen DS**, **Hoehn KL**, **Yan Z**. Autophagy is required for exercise training-induced skeletal muscle adaptation and improvement of physical performance. *FASEB J* 27: 4184–4193, 2013.

60. **Ljubicic V**, **Joseph A-M**, **Saleem A**, **Uguccioni G**, **Collu-Marchese M**, **Lai RYJ**, **Nguyen LMD**, **Hood DA**. Transcriptional and post-transcriptional regulation of mitochondrial biogenesis in skeletal muscle: Effects of exercise and aging. *Biochim Biophys Acta - Gen Subj* 1800: 223–234, 2010.

61. **Marcil M**, **Bourduas K**, **Ascah A**, **Burelle Y**, **Bourduas K**, **Ascah A**. Exercise training induces respiratory substrate-specific decrease in Ca 2+ - induced permeability transition pore opening in heart mitochondria. *Am J Physiol - Hear Circ Physiol* 7: 1549–1557, 2006.

62. **Martina JA**, **Chen Y**, **Gucek M**, **Puertollano R**. MTORC1 functions as a transcriptional regulator of autophagy by preventing nuclear transport of TFEB. :

903–914, 2012.

63. **Masiero E**, **Agatea L**, **Mammucari C**, **Blaauw B**, **Loro E**, **Komatsu M**, **Metzger D**, **Reggiani C**, **Schiaffino S**, **Sandri M**. Autophagy Is Required to Maintain Muscle Mass. *Cell Metab* 10: 507–515, 2009.

64. **Matsuda N**, **Sato S**, **Shiba K**, **Okatsu K**, **Saisho K**, **Gautier CA**, **Sou YS**, **Saiki S**, **Kawajiri S**, **Sato F**, **Kimura M**, **Komatsu M**, **Hattori N**, **Tanaka K**. PINK1 stabilized by mitochondrial depolarization recruits Parkin to damaged mitochondria and activates latent Parkin for mitophagy. *J Cell Biol* 189: 211–221, 2010.

65. **Medina DL**, **Ballabio A**. Lysosomal calcium regulates autophagy. *Nature* 11: 970–971, 2015.

66. **Medina DL**, **Di Paola S**, **Peluso I**, **Armani A**, **De Stefani D**, **Venditti R**, **Montefusco S**, **Scotto-Rosato A**, **Prezioso C**, **Forrester A**, **Settembre C**, **Wang W**, **Gao Q**, **Xu H**, **Sandri M**, **Rizzuto R**, **De Matteis MA**, **Ballabio A**. Lysosomal calcium signalling regulates autophagy through calcineurin and TFEB. *Nat Cell Biol* 17: 288–299, 2015.

67. **Min K**, **Smuder AJ**, **Kwon O**, **Kavazis AN**, **Szeto HH**, **Powers SK**. Mitochondrial-targeted antioxidants protect skeletal muscle against immobilization-induced muscle atrophy. 32611: 1459–1466, 2011.

68. **Mitchell P**. COUPLING OF PHOSPHORYLATION TO ELECTRON AND HYDROGEN TRANSFER BY A CHEMI-OSMOTIC TYPE OF MECHANISM. 191: 144–148, 1961.

69. **Muller FL**, **Liu Y**, **Van Remmen H**. Complex III releases superoxide to both

sides of the inner mitochondrial membrane. *J Biol Chem* 279: 49064–73, 2004.

70. **Muller FL**, **Song W**, **Jang YC**, **Liu Y**, **Sabia M**, **Richardson A**, **Van Remmen H**. Denervation-induced skeletal muscle atrophy is associated with increased mitochondrial ROS production. *Am J Physiol Regul Integr Comp Physiol* 293: R1159–68, 2007.

71. **Napolitano G**, **Ballabio A**. TFEB AT A GLANCE. *J Cell Sci* 129: 2475–2481, 2016.

72. **Narendra DP**, **Jin SM**, **Tanaka A**, **Suen DF**, **Gautier CA**, **Shen J**, **Cookson MR**, **Youle RJ**. PINK1 is selectively stabilized on impaired mitochondria to activate Parkin. *PLoS Biol* 8, 2010.

73. **Nath S**, **Dancourt J**, **Shteyn V**, **Puente G**, **Wendy M**, **Nag S**, **Bewersdorf J**, **Yamamoto A**, **Antonny B**, **Thomas J**. Lipidation of the LC3/GABARAP family of autophagy proteins relies on a membrane-curvature-sensing domain in Atg3. 16: 415–424, 2014.

74. **Neill HMO**, **Maarbjerg SJ**, **Crane JD**, **Jeppesen J**, **Jørgensen SB**. AMP-activated protein kinase (AMPK) beta1beta2 muscle null mice reveal an essential role for AMPK in maintaining mitochondrial content and glucose uptake during exercise. *PNAS* 108: 16092–1609, 2011.

75. **Neupert W**, **Herrmann JM**. Translocation of proteins into mitochondria. *Annu Rev Biochem* 76: 723–749, 2007.

76. **Palmer JW**, **Tandler B**, **Hoppel C**. Biochemical Properties of Subsarcolemmal and Interfibrillar Mitochondria Isolaed from Rat Cardic Muscle. : 8731–8739, 1977.

77. **Palmieri M**, **Impey S**, **Kang H**, **Ronza A**, **Pelz C**, **Sardiello M**. Characterization of the CLEAR network reveals an integrated control of cellular clearance pathways. 20: 3852–3866, 2011.

78. **Pette DWG**. Myosin isoforms , muscle fiber types , and transitions. 50: 500–509, 2000.

79. **Piantadosi CA**, **Carraway MS**, **Babiker A**, **Suliman HB**. Heme oxygenase-1 regulates cardiac mitochondrial biogenesis via Nrf2-mediated transcriptional control of nuclear respiratory factor-1. *Circ Res* 103: 1232–1240, 2008.

80. **Pilegaard H**, **Saltin B**, **Neufer PD**. Exercise induces transient transcriptional activation of the PGC-1α gene in human skeletal muscle. *J Physiol* 546: 851–858, 2003.

81. **Pogozelski AR**, **Geng T**, **Li P**, **Yin X**, **Lira VA**, **Zhang M**, **Chi J**. p38 c Mitogen-Activated Protein Kinase Is a Key Regulator in Skeletal Muscle Metabolic Adaptation in Mice. 4, 2009.

82. **Powers SK**, **Ji LL**, **Kavazis AN**, **Jackson MJ**. Reactive Oxygen Species: Impact on Skeletal Muscle. *Compr Physiol* 1: 941–969, 2011.

83. **Powers SK**, **Kavazis AN**, **McClung JM**. Oxidative stress and disuse muscle atrophy. *J Appl Physiol* 102: 2389–97, 2007.

84. **Puigserver P**, **Rhee J**, **Lin J**, **Wu Z**, **Yoon JC**, **Zhang C**, **Krauss S**, **Mootha VK**, **Lowell BB**, **Spiegelman BM**. Cytokine Stimulation of Energy Expenditure through p38 MAP Kinase Activation of PPAR Coactivator-1. 8: 971–982, 2001.

85. **Quinlan CL**, **Treberg JR**, **Perevoshchikova I V**, **Orr AL**, **Martin D**. Native Rates of Superoxide Production from Multiple Sites in Isolated Mitochondria

Measured using Endogenous Reporters. 53: 1807–1817, 2013.

86. **Roczniak-ferguson A**, **Petit CS**, **Froehlich F**, **Qian S**, **Ky J**, **Angarola B**, **Walther TC**, **Ferguson SM**. The Transcription factor TFEB links mTORC1 signaling to Transcriptional Control of Lysosome Homeostasis. 5, 2012.

87. **Romanello V**, **Guadagnin E**, **Gomes L**, **Roder I**, **Sandri C**, **Petersen Y**, **Milan G**, **Masiero E**, **Del Piccolo P**, **Foretz M**, **Scorrano L**, **Rudolf R**, **Sandri M**. Mitochondrial fission and remodelling contributes to muscle atrophy. *EMBO J* 29: 1774–85, 2010.

88. **Roy RR**, **Monke SR**, **Allen DL**, **Edgerton VR**, **Edgerton VR**. Modulation of myonuclear number in functionally overloaded and exercised rat plantaris fibers. .

89. **Russell AP**, **Foletta VC**, **Snow RJ**, **Wadley GD**. Skeletal muscle mitochondria: A major player in exercise, health and disease. *Biochim Biophys Acta - Gen Subj* 1840: 1276–1284, 2014.

90. **Ruvkun EJOG**. MXL-3 and HLH-30 transcriptionally link lipolysis and autophagy to nutrient availability. *Nat Cell Biol* 15: 668–676, 2013.

91. **Safdar A**, **Little JP**, **Stokl AJ**, **Hettinga BP**, **Akhtar M**, **Tarnopolsky MA**. Exercise increases mitochondrial PGC-1alpha content and promotes nuclear-mitochondrial cross-talk to coordinate mitochondrial biogenesis. *J Biol Chem* 286: 10605–10617, 2011.

92. **Saleem A**, **Adhihetty PJ**, **Hood DA**. Role of p53 in mitochondrial biogenesis and apoptosis in skeletal muscle. *Physiol Genomics* 3: 58–66, 2009.

93. **Saleem A**, **Hood DA**. Acute exercise induces tumour suppressor protein p53 translocation to the mitochondria and promotes a p53-Tfam-mitochondrial DNA

complex in skeletal muscle. *J Physiol* 591: 3625–36, 2013.

94. **Salma N**, **Song JS**, **Arany Z**, **Fisher DE**. Transcription Factor Tfe3 Directly Regulates Pgc-1alpha in Muscle. *J Cell Physiol* 230: 2330–2336, 2015.

95. **Sandri M**. Autophagy in skeletal muscle. *FEBS Lett* 584: 1411–1416, 2010.

96. **Sardiello M**, **Palmieri M**, **Ronza A di**, **Medina DL**, **Valenza M**, **Gennarino, Vincenzo Alessandro Chiara Di Malta FD**, **Embrione V**, **Polishchuk RS**, **Banfi S**, **Parenti G**, **Cattaneo E**, **Andrea Ballabio1**. A Gene Network Regulating Lysosomal Biogenesis and Function. : 473–478, 2009.

97. **Scarpulla RC**. Transcriptional Paradigms in Mammalian Mitochondrial Biogenesis and Function. *Physiol Rev* 88: 611–638, 2008.

98. **Scarpulla RC**. metabolic stress. 1819: 1088–1097, 2013.

99. **Schiaffino S**, **Reggiani C**. FIBER TYPES IN MAMMALIAN SKELETAL MUSCLES. *Physiol Rev* 91: 1447–1531, 2011.

100. **Scott I**, **Webster BR**, **Chan CK**, **Okonkwo JU**, **Han K**, **Sack MN**. GCN5-like protein 1 (GCN5L1) controls mitochondrial content through coordinated regulation of mitochondrial biogenesis and mitophagy. *J Biol Chem* 289: 2864–2872, 2014.

101. **Settembre C**, **Ballabio A**. TFEB regulates autophagy: An integrated coordination of cellular degradation and recycling processes. 8627, 2016.

102. **Settembre C**, **Polito VA**, **Garcia M**, **Vetrini F**, **Erdin S**, **Erdin SU**, **Huynh T**, **Medina D**, **Colella P**, **Sardiello M**, **Rubinsztein DC**. TFEB Links Autophagy to Lysosomal Biogenesis. 332: 1429–1433, 2013.

103. **Settembre C**, **Zoncu R**, **Medina DL**, **Vetrini F**, **Erdin S**, **Erdin S**, **Huynh T**,

Ferron M, **Karsenty G**, **Vellard MC**, **Facchinetti V**. A lysosome-to-nucleus signalling mechanism senses and regulates the lysosome via mTOR and TFEB open. : 1095–1108, 2012.

104. **Settembre C1, De Cegli R, Mansueto G, Saha PK, Vetrini F, Visvikis O, Huynh T, Carissimo A, Palmer D, Klisch TJ, Wollenberg AC, Di Bernardo D, Chan L, Irazoqui JE BA**. TFEB controls cellular lipid metabolism through a starvation-induced autoregulatory loop. 230: 2330–2336, 2015.
105. **Song Y**, **Ding W**, **Xiao Y**, **Lu KJ**. The Progress of Mitophagy and Related Pathogenic Mechanisms of the Neurodegenerative Diseases and Tumor. 2015, 2015.
106. **St-Pierre J**, **Drori S**, **Uldry M**, **Silvaggi JM**, **Rhee J**, **J??ger S**, **Handschin C**, **Zheng K**, **Lin J**, **Yang W**, **Simon DK**, **Bachoo R**, **Spiegelman BM**. Suppression of reactive oxygen species and neurodegeneration by the PGC-1 transcriptional coactivators. *Cell* 127: 397–408, 2006.
107. **Takahashi M**, **Chesley a**, **Freyssenet D**, **Hood D a**. Contractile activity-induced adaptations in the mitochondrial protein import system. *Am J Physiol* 274: C1380–7, 1998.
108. **Takahashi M**, **Hood DA**. Protein Import into Subsarcolemmal and Intermyofibrillar Skeletal. 271: 27285–27291, 1996.
109. **Tanaka A**, **Cleland MM**, **Xu S**, **Narendra DP**, **Suen DF**, **Karbowski M**, **Youle RJ**. Proteasome and p97 mediate mitophagy and degradation of mitofusins induced by Parkin. *J Cell Biol* 191: 1367–1380, 2010.
110. **Tanida I**, **Ueno T**, **Kominami E**. LC3 conjugation system in mammalian

autophagy. *Int J Biochem Cell Biol* 36: 2503–2518, 2004.

111. **Tian W**, **Li W**, **Chen Y**, **Yan Z**, **Huang X**, **Zhuang H**, **Zhong W**, **Chen Y**, **Wu W**, **Lin C**, **Chen H**, **Hou X**, **Zhang L**, **Sui S**, **Zhao B**, **Hu Z**, **Li L**, **Feng D**. Phosphorylation of ULK1 by AMPK regulates translocation of ULK1 to mitochondria and mitophagy. *FEBS Lett* 589: 1847–1854, 2015.

112. **Tryon LD**, **Crilly MJ**, **Hood DA**. Effect of denervation on the regulation of mitochondrial transcription factor A expression in skeletal muscle. *Am J Physiol Cell Physiol* 309: C228–38, 2015.

113. **Tsunemi T**, **Ashe TD**, **Morrison BE**, **Soriano KR**, **Au J**, **Roque R a V**, **Lazarowski ER**, **Damian V a**, **Masliah E**. PGC-1α rescues Huntington's disease proteotoxicity by preventing oxidative stress and promoting TFEB function. 4, 2014.

114. **Uguccioni G**, **D'souza D**, **Hood DA**. Regulation of PPARγ Coactivator-1α Function and Expression in Muscle: Effect of Exercise. *PPAR Res* 2010: 1–7, 2010.

115. **Vainshtein A**, **Desjardins EM**, **Armani A**, **Sandri M**, **Hood DA**. PGC-1α modulates denervation-induced mitophagy in skeletal muscle. *Skelet Muscle* 5: 9, 2015.

116. **Vainshtein A**, **Hood DA**. The regulation of autophagy during exercise in skeletal muscle. *J Appl Physiol* 120: 664–673, 2016.

117. **Vainshtein A**, **Tryon LD**, **Pauly M**, **Hood DA**. Role of PGC-1α during acute exercise-induced autophagy and mitophagy in skeletal muscle. *Am J Physiol - Cell Physiol* 308: 710–719, 2015.

118. **Vincow ES**, **Merrihew G**, **Thomas RE**, **Shulman NJ**, **Beyer RP**, **MacCoss MJ**, **Pallanck LJ**. The PINK1-Parkin pathway promotes both mitophagy and selective respiratory chain turnover in vivo. *Proc Natl Acad Sci* 110: 6400–6405, 2013.

119. **Wei H**, **Liu L**, **Chen Q**. Selective removal of mitochondria via mitophagy: Distinct pathways for different mitochondrial stresses. *Biochim Biophys Acta - Mol Cell Res* 1853: 2784–2790, 2015.

120. **Wright DC**, **Geiger PC**, **Han DH**, **Jones TE**, **Holloszy JO**. Calcium induces increases in peroxisome proliferator-activated receptor gamma coactivator-1alpha and mitochondrial biogenesis by a pathway leading to p38 mitogen-activated protein kinase activation. *J Biol Chem* 282: 18793–9, 2007.

121. **Wu H**, **Olson EN**. Activation of the MEF2 transcription factor in skeletal muscles from myotonic mice. 109: 1327–1333, 2002.

122. **Wu W**, **Tian W**, **Hu Z**, **Chen G**, **Huang L**, **Li W**, **Zhang X**, **Xue P**, **Zhou C**, **Liu L**, **Zhu Y**, **Zhang X**, **Li L**, **Zhang L**, **Sui S**, **Zhao B**, **Feng D**. ULK1 translocates to mitochondria and phosphorylates FUNDC1 to regulate mitophagy. *EMBO Rep* 15: 566–575, 2014.

123. **Wu Z**, **Puigserver P**, **Andersson U**, **Zhang C**, **Adelmant G**, **Mootha V**, **Troy A**, **Cinti S**, **Lowell B**, **Scarpulla RC**, **Spiegelman BM**. Mechanisms controlling mitochondrial biogenesis and respiration through the thermogenic coactivator PGC-1. *Cell* 98: 115–124, 1999.

124. **Zhang J**, **Ney PA**. ROLE OF BNIP3 AND NIX IN CELL DEATH, AUTOPHAGY, AND MITO. 16: 939–946, 2010.

125. **Zhang Y**, **Uguccioni G**, **Ljubicic V**, **Irrcher I**, **Iqbal S**, **Singh K**, **Ding S**, **Hood**

DA. Multiple signaling pathways regulate contractile activity-mediated PGC-1 gene expression and activity in skeletal muscle cells. *Physiol Rep* 2: e12008–e12008, 2014.

126. **Zhou J**, **Tan S**, **Nicolas V**, **Bauvy C**, **Yang N**, **Zhang J**, **Xue Y**, **Codogno P**, **Shen H**. Activation of lysosomal function in the course of autophagy via mTORC1 suppression and autophagosome-lysosome fusion. 23: 508–523, 2013.

127. **Zonco R**, **Bar-Peled L**, **Efeyan A**, **Wang S**, **Sancak Y**, **Sabatini DM**. mTORC1 senses lysosomal amino acids through an inside-out mechanism that requires the Vacuolar H+ ATPase. 334: 678–683, 2011.

MANUSCRIPT

THE ROLE OF PGC-1α IN MEDIATING EXERCISE-INDUCED TFEB EXPRESSION AND ACTIVITY IN SKELETAL MUSCLE

Avigail T. Erlich[1], Kaitlyn Beyfuss[1] and David A. Hood[1,2]

SUMMARY

Skeletal muscle health is dependent on a functional mitochondrial network, controlled by opposing processes of mitochondrial biogenesis and mitophagy. The synthesis of new mitochondria is regulated by PGC-1α, whereas TFEB coordinates the transcription of lysosomal and autophagy-related genes. Exercise is a known activator of PGC-1α, and subsequent mitochondrial biogenesis. However, the expression and activation of TFEB in response to exercise has yet to be determined. Since biogenesis and mitophagy are closely linked, we investigated the relationship between PGC-1α and TFEB in maintaining mitochondrial health in response to acute treadmill exercise in WT and PGC-1α KO mice. TFEB protein levels were reduced by 30% in the KO mice compared to their WT counterparts, however no changes were observed in most TFEB downstream targets. In WT mice, exercise induced a 30-50% increase in mRNA levels of mitochondrial markers, a 50% decrease in the mRNAs encoding autophagy genes, as well as a 2.4-fold increase in TFEB translocation to the nucleus. TFEB transcription, assessed through the intramuscular electroporation of a TFEB promoter-reporter construct, was elevated 4-fold in response to exercise. These translocation and transcriptional responses were not observed in the KO mice. Our data suggest that acute exercise provokes immediate transcriptional signaling leading to increased biogenesis, decreased autophagy, and augmented TFEB activation, in a manner that is PGC-1α-dependent.

[1]Muscle Health Research Centre, School of Kinesiology and Health Science, York University, Toronto, Ontario,M3J 1P3, Canada.

[2]This work was supported by funding from the Natural Sciences and Engineering Research Council of Canada(NSERC) to D. A. Hood. D. A. Hood is also the holder of a Canada Research Chair in Cell Physiology.

INTRODUCTION

Mitochondrial content and function are essential for the maintenance of skeletal muscle health throughout the lifespan. Skeletal muscle comprises approximately 40% of body mass and is largely responsible for determining total metabolic rate (27). Muscle relies on mitochondria to play a central role in regulating muscle metabolism, as well as the control of energy-sensitive signaling pathways, reactive oxygen species production, and calcium homeostasis, (8, 28, 44). In response to the increased energy demands of exercise, muscle adapts remarkably well by remodeling and expanding the mitochondrial network. In contrast, a reduction in the quality and quantity of the mitochondrial pool has been implicated in a number of conditions affecting muscle metabolic health. In order to maintain an optimal pool of mitochondria, two competing, yet equally important quality control mechanisms are involved, termed mitochondrial biogenesis and mitochondrial specific autophagy, or mitophagy (35).

Mitochondrial biogenesis involves the proliferation of the mitochondrial network through the expansion of the existing organelle reticulum. Biogenesis is largely controlled by the peroxisome proliferator-activated receptor gamma coactivator 1-alpha (PGC-1α), a transcriptional coactivator which acts in the nucleus (1, 26). Increases in energy demand, such as that imposed by exercise, activate PGC-1α, thereby promoting the coordinated transcription of nuclear- and mtDNA-encoded genes to induce the synthesis of new mitochondria. As muscle adapts to exercise and the associated metabolic demands, there is an increase in PGC-1α expression, leading to augmented mitochondrial content and function.

Under steady state conditions, this expansion of the mitochondrial network is balanced by mitophagy, which mediates the degradation of dysfunctional mitochondria (6, 23, 35, 47). Hallmark indicators of dysfunctional mitochondria include reductions in membrane potential and an increase in reactive oxygen species production. This triggers mitochondrial detachment from the healthy reticulum via organelle fission, and the subsequent tagging of mitochondria for degradation (16, 21, 44, 47). Tagged mitochondria are then engulfed by double membrane vesicles known as autophagosomes, which travel on microtubule tracks to fuse with lysosomes for degradation (6, 12, 32, 46).

Mitophagy is thought to be regulated by transcription factor EB (TFEB), (22, 37) a protein that controls the expression of genes associated with lysosomes, autophagosome formation, cargo recognition, and autophagosome-lysosome fusion (22, 36, 37). Specifically, TFEB activates the transcription of the essential coordinated lysosomal expression and regulation (CLEAR) genes such as LC3, SQSTM1 and LAMP1. The nuclear localization and function of TFEB are regulated by its phosphorylation. Phosphorylation of TFEB on Ser^{142} and Ser^{211} by mTORC1 and ERK2 serves to retain TFEB inactive within the cytosol. Under conditions of cellular stress, TFEB is dephosphorylated by calcineurin, which itself is activated by elevations in cytosolic [Ca^{2+}] (21, 37, 45). Once dephosphorylated, TFEB translocates to the nucleus and promotes the transcription of lysosome and autophagy genes. Recent evidence suggest that mitophagy is activated following exercise (10, 17, 45). Since exercise is known to increase cytosolic Ca^{2+}, it is reasonable to speculate that TFEB may be activated under exercise conditions.

Mitochondrial biogenesis and mitophagy work hand-in-hand to conserve mitochondrial health in skeletal muscle. Since the two processes complement one another, we hypothesize that a coordination between TFEB and PGC-1α, the two master regulators of these pathways, could exists (35, 40). Recent evidence has found a role for PGC-1α in mediating exercise-induced mitophagy (46), yet little is known about the effect of exercise on TFEB in muscle, and whether there is a role for TFEB in exercise-induced mitochondrial biogenesis. Thus, the purposes of this study were to further elucidate the relationship between PGC-1α and TFEB, and to determine whether TFEB plays a role in exercise-induced mitochondrial biogenesis and mitophagy.

METHODS

***PGC WT and KO Animals*:** PGC-1α KO and wild-type (WT) mice were produced by crossing heterozygote mice. Ear clippings were obtained and DNA was extracted using the phenolchloroform-isoamyl alcohol method. Genotype was determined by the presence of either a KO- or WT-specific DNA fragment using traditional PCR analyses. The survival of PGC-1α KO animals was approximately half of the expected Mendelian ratio. Mice were housed in a 12:12-h light-to-dark cycle, fed normal rodent chow.

Plasmid DNA growth and isolation: The TFEB promoter containing 1.6 kb of sequence was sublconed into a PGL3 vector containing a firefly luciferase reporter. Ampicillin-resistance bacteria were transformed with this vector. Bacterial colonies were then amplified in order to isolate plasmid DNA using a Qiagin Plasmid Isolation Kit.

In vivo muscle transfection: In vivo experiments were carried out on 4-month-old PGC-1α WT and KO mice. Mice were anesthetized using gaseous isoflurane. The lower hindlimbs were shaved and sterilized prior to injection of a TFEB promoter-reporter construct. The gastrocnemius muscles from the distal portion of the leg were injected with 25 μg of the rTfeb-pGL3 and 1 μg of pRL-CMV using a short 29 gauge insulin syringe. Immediately after the injection, transcutaneous electrical pulses were applied using an electroporation system. The muscles were held on either side of the injection site by tweezerodes at the level of the skin, and a total of 10 pulses were delivered, with anode and cathode electrode orientation reversed with each pulse. The gastrocnemius of the left hindlimb was electrotransfected with an empty PGL3 vector, and the right with rTfeb-pGL3 vector. Following 7 days, animals were subjected to an exercise protocol.

Exercise protocol: PGC-1α WT and KO mice were acclimatized to the treadmill for two days prior to the exercise day. On the day of exercise, the mice ran on the treadmill with a fixed slope of 10%. Mice ran at 5m/min for 5 minutes followed by 10m/min for 10 minutes, 15m/min for 15 minutes and 20m/min for 20 minutes. The speed was then increased by 2m/min every 2 minutes until exhaustion was achieved. Exhaustion was defined as the inability of the animal to run on the treadmill for 10 seconds despite prodding. Immediately following exercise, animals were cervically dislocated prior to the removal of tissues. Following extraction, the quadriceps, and gastrocnemius muscles were weighed and immediately frozen at -80°C for further biochemical analysis. The tibialis anterior (TA) muscles were taken and used for nuclear and cytosolic fractionation.

TFEB overexpression: pAdEasy-TFEB virus and pAdEasy-GFP control virus (20 μl each) were thawed at 37°C. One gastrocnemius of PGC-1α heterozygous (HT) mice was injected with viral TFEB, with the contralateral leg serving as a control. The gastrocnemius muscle was extracted 8 weeks following injection, and frozen for further analysis.

Protein Extraction: Frozen tissues were pulverized into a powder and diluted 5X with extraction buffer containing phosphate and phosphatase inhibitors. Diluted samples were then rotated end-over-end at 4°C for 1 hour, followed by sonication 3 by 3 at 30% at max power. Following sonication, the samples were centrifuged at 4°C for 10 minutes at 16,000 g.

Protein Concentration: The Bradford protein assay was used to determine protein concentrations of samples. In order to standardize for concentrations, Bovine Serum Albumin (2mg/ml) was combined with double distilled water and Sakamoto extraction

buffer in tubes (29). Protein extracts were mixed with double distilled water and analyzed compared to the standard curve using a Bio-Tek Synergy HT micro plate reader.

Immunoblotting: Extracted protein samples (50-100ug) from quadriceps or gastrocnemius muscles, or from fractionated nucleus and cytosol samples, were separated using 10%- 15% sodium dodecyl sulfate polyacrylamide gel electrophoresis at 120 Volts for 90 minutes. Once the gel had run the desired duration, proteins were electroblotted onto a nitrocellulose membrane. After transfer, the membrane was stained with Ponceau Red, cut at the required molecular weights, and subsequently blocked in 5% milk for 1 hour in order to prevent any non-specific binding. Primary antibody targets (**Table 1)** were incubated at 4°C over night. The next day the blots were washed in wash buffer 3 x 5 minutes each, and subsequently incubated for one hour at room temperature with their specific secondary antibody before being washed again 3 x 5 minutes each. Detection of the bands was revealed using enhanced chemiluminescence. Films were scanned and analyzed using Image J Software.

Nuclear and Cytosolic Fractionation- NE-PER extraction reagents (Pierce, Thermo Scientific #38835) were used to obtain cytoplasmic and nuclear fractions using modifications of the manufacturer's recommendations and differential centrifugation.

Luciferase reporter assay: Muscle powders from WT and PGC-1α KO mice in either the control or the exercise group (30-50μg) were diluted sevenfold in passive lysis buffer. Homogenates were sonicated on ice and subsequently centrifuged at 16,000 g for 5 mins at 4° C. Following centrifugation, 20 μl of the supernate were used to assess pGL3 firefly luciferase activity. Values were corrected for electro transfection efficiency by the simultaneous assessment of pRL renilla luciferase activity.

Table 1: List of Antibodies Used

ANTIBODY	MANUFACTURER	REFERENCE #	LOT #
α-TUBULIN	Calbiochem (Millipore)	CP06	D00175772
Aciculin	In house		
Beclin1	Cell Signaling	3738S	2
Cathepsin D	Santa Cruz	SC6486	J1111
COXI	Abcam	AB14705	GR233531-3
COXIV	Abcam	AB14744	GR192963-3
GAPDH	Abcam	AB8245	GR232049-10
H2B	Cell Signaling	2934S	4
Keap1	Protein Tech Group	10503-2-AP	N/A
mnSOD	Upstate Solutions (Cell Signaling)	06-984	26654
mTOR (T)	Cell Signaling	2972S	9
mTOR (p)	Cell Signaling	2971S	18
Nrf2	Santa Cruz	SC722	C2013
NQO1	Abcam	AB34173	GR206757-1
LAMP1	Abcam	AB2470	GR268500-1
p53	In house		
p62	Sigma	P0067	055M4816V
p65	Santa Cruz	SC8008	F1814
PGC-1α	Millipore	AB3243	2757199
TFEB	MBS	MBS120432	319C2A-3
YY1	Santa Cruz	SC7341	L0208

RNA isolation and reverse transcription. Total RNA was isolated from frozen, whole muscle quadriceps powders as described previously (24). Briefly, Tissue powder (~70 mg) was added to TRIzol® reagent, homogenized, then mixed with chloroform. Samples were centrifuged at 4°C at 16,000 *g* for 15 min and the upper aqueous phase of the sample was transferred into a new tube along with isopropanol and left overnight at −20°C to precipitate. Samples were once again centrifuged at 4°C at 16,000 *g* for 10 min. The resultant supernate was discarded and the pellet resuspended in 30 µl of molecular grade sterile H_2O (Wisent Bio Products, Saint-Jean-Baptiste, QC). The concentration and purity of the RNA was measured using a Nano Drop 2000 Spectrophotometer. SuperScript® III reverse transcriptase (Invitrogen, Carlsbad, CA, USA) was used to reverse transcribe 1.5 µg of total RNA into cDNA.

Real-time PCR. Using sequences from GenBank, primers were designed with Primer 3 v. 0.4.0 software (Massachusetts Institute of Technology, Cambridge, MA) for genes of interest **(Table 2)**. Primer specificity was confirmed by OligoAnalyzer 3.1 (Integrated DNA Technologies, Toronto, ON, Canada). mRNA expression was measured with SYBR® Green chemistry (PerfeCTa SYBR® Green SuperMix; ROX, Quanta BioSciences, Gaithersburg, MD). Each well contained: SYBR® Green SuperMix, forward and reverse primers (20 µM), sterile water, and 10 ng of cDNA. The detection of all real-time PCR amplification took place in a 96-well plate using a StepOnePlus® Real-Time PCR System (Applied Biosystems, Foster City, CA). The final reaction volume of each well was 25 µl. Samples were run in duplicates to ensure accuracy. The PCR program consisted of an initial holding stage (95°C for 10 min), followed by 40 amplification cycles (60°C for 1 min, 95°C for 15 s), and was completed with a final

melting stage (95°C for 15 s, 60°C for 1 min, 95°C for 15 s). Nonspecific amplification and primer dimers were controlled for by the analysis of melt curves generated by the instrument for SYBR® Green analyses. Negative control wells contained water in place of cDNA.

Real-time qPCR quantification. First, the threshold cycle (CT) number of the endogenous reference gene was subtracted from the CT number of the target gene [ΔCT = CT(target) − CT(reference)]. Next, the ΔCT value of the control tissue was subtracted from the ΔCT value of the experimental tissue [ΔΔCT = ΔCT(experimental) − ΔCT(control)]. Results were reported as fold-changes using the ΔΔCT method, calculated as $2^{-\Delta\Delta CT}$. Primers detecting β-Actin along with glyceraldehyde-3 phosphate dehydrogenase (GAPDH) were chosen as endogenous reference genes.

Statistical Analyses: The data obtained are graphed using Graph Pad 4.0 software, and expressed as means of ± SE. The data are analyzed using a Student's t-Test. Statistical significance is accepted if $p<0.05$.

Table 2. List of primer oligonucleotide sequences used in real-time qPCR analysis for *Mus Muculus*

GENE	Forward Primer	Reverse Primer
β-actin	5`-TGTGACGTTGACATCCGTAA -3`	5`-GCTAGGAGCCAGAGCAGTAA-3`
Beclin1	5`-AGGCTGAGGCGGAGAGATT-3`	5`-TCCACACTCTTGAGTTCGTCAT-3`
Catsd	5`-TTTGCCAATGCTGTCGTACT-3`	5`-AGCGAGTGTGACTATGTGTGAG-3`
Coxi	5`-CTAGCCGCAGGCATTACTAT-3`	5`-TGCCCAAAGAATCAGAACA-3`
Coxiv	5`-CTCCAACGAATGGAAGACAG-3`	5`-TGACAACCTTCTTAGGGAAC-3`
EGR1	5`-GCCCTTCCAGTGTCGAATCT-3`	5`-GGCAAACTTCCTCCCACAAAT-3`
Gapdh	5`-AACACTGAGCATCTCCCTCA-3`	5`-GTGGGTGCAGCGAACTTTAT-3`
Hspa (Hsp70)	5`-TGGCTATTACTGCGGGTTCT-3`	5`-CATCTGCTCCACCTCCTCT-3`
Lamp1	5`-CTAGTGGGAGTTGCGGTATCA-3`	5`-AGGGCATCAGGAAGAGTCATAT-3`
Lamp2	5`-GCTGAACAACAGCCAAATTA-3`	5`-CTGAGCCATTAGCCAAATACAT-3`
Ppargc1a (PGC-1α)	5`-TTCCACCAAGAGCAAGTAT-3`	5`-CGCTGTCCCATGAGGTATT-3`
Sqstm1 (p62)	5`-TGTGGTGGGAACTCGCTATAA-3`	5`-CAGCGGCTATGAGAGAAGCTAT-3`
Tfam	5`-GAAGGGAATGGGAAAGGTAGA-3`	5`-AACAGGACATGGAAAGCAGAT-3`
TFEB	5`-AGCTCCAACCCGAGAAAGAGTTTG-3`	5`-CGTTCAGGTGGCTGCTAGAC-3`

RESULTS

PGC-1α KO animals exhibit reduced body weight and endurance capacity. The phenotypic characteristics of the PGC-1α knockout (KO) mice have been described previously (1, 46). In our study, deletion of PGC-1α resulted in a 30% reduction in body mass (Fig. 1A). To examine the involvement of PGC-1α in exercise-mediated TFEB activation, 3 month old PGC-1α KO and wild type (WT) mice were subjected to acute, incremental, exhaustive treadmill running. PGC-1α KO resulted in decreased endurance capacity, represented by a 45% ($p < 0.05$) reduction in distance to exhaustion (Fig. 1B), and a 50% higher levels of lactate following exercise compared to WT littermates (Fig. 1C).

Gene expression of early response genes and mitochondrial markers increase immediately following exercise. To examine the effectiveness of our exercise protocol in altering gene expression, we measured the mRNA levels of the early response gene Egr-1, as well as that of PGC-1α and mitochondrial markers. Exercise increased Egr-1 expression in WT and KO mice by 18-fold and 12-fold respectively ($p < 0.05$) (Fig. 2A). PGC-1α mRNA levels also showed a trend to increase in WT mice immediately following the acute exercise (Fig. 2B). Under basal, non-exercise conditions, levels of COXI mRNAs, the mitochondrially-encoded subunit of complex IV of the ETC, were reduced by 47% in KO mice compared to WT counterparts, as expected. In both the WT mice and KO, COX mRNA levels were elevated by 33-38% ($p < 0.05$) following exercise, however levels in KO mice were significantly lower than in the WT animals (Fig. 2C). In contrast to our expectations, Tfam mRNA levels were 2-fold higher in the KO mice compared to WT animals basally. However, exercise increased Tfam mRNA

Fig. 1

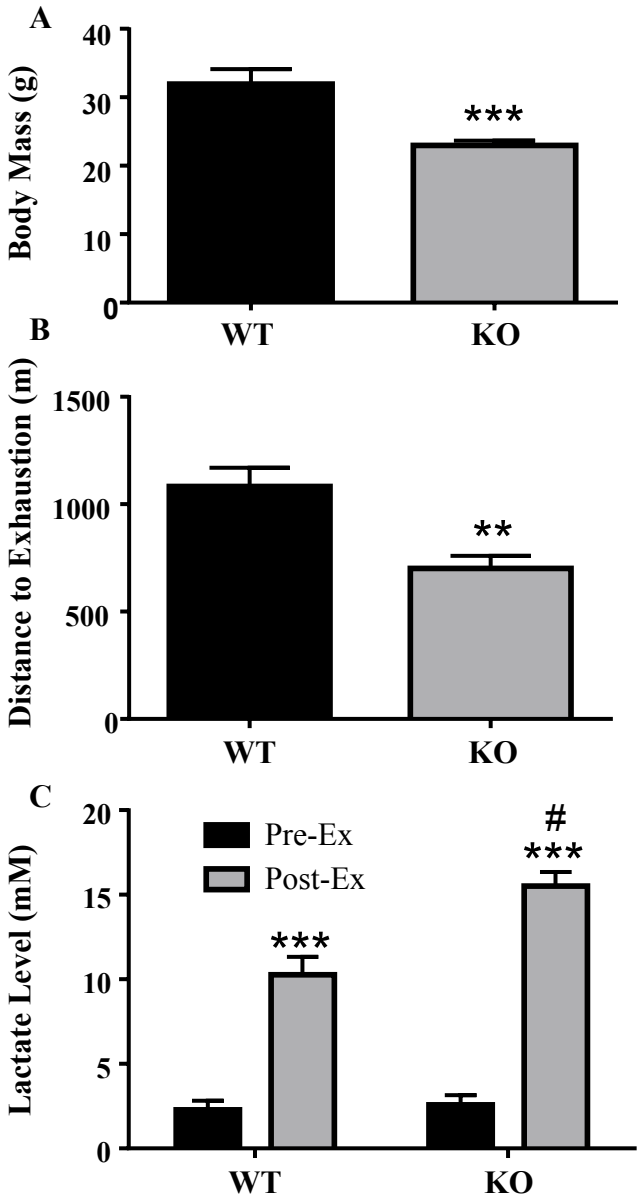

Figure 1: Animal characteristics and response to exercise. A) Body mass differences between WT and PGC-1α KO animals (n=18). **P*<0.001 WT vs KO, Student's t-test. WT and PGC-1α KO animals were subjected to an exhaustive bout of exercise. Running and performance were measured by recording **B)** Distance to exhaustion (n=9) ***P*<0.01 WT vs KO, Student's t-test, and **C)** Lactate production was also measured before and after exercise (n=9). ****P*<0.001 WT vs KO post-exercise; #P<0.0001 Pre-exercise vs Post-exercise; 2-way ANOVA. Data are means of ± SEM.

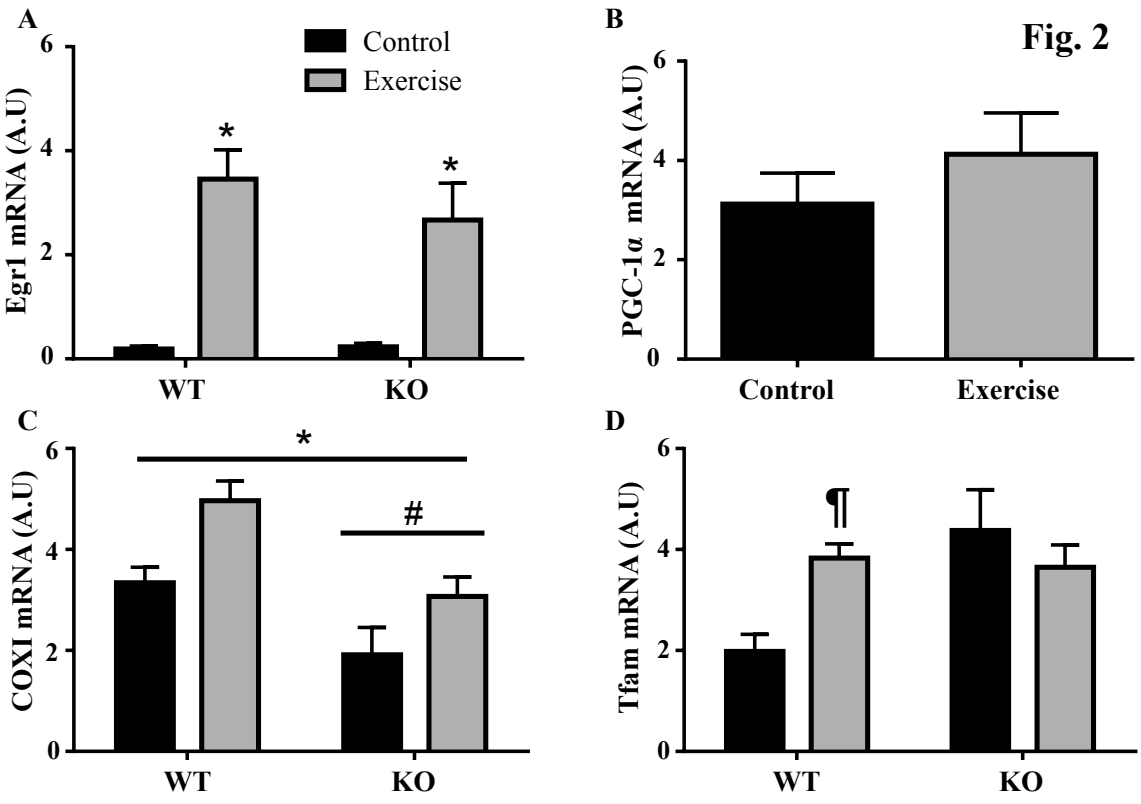

Figure 2: Gene expression of early response genes and mitochondrial markers. mRNA levels of early response genes and mitochondrial markers. **A)** Egr-1, **B)** PGC-1α (WT vs KO) **C)** COX1, and **D)** Tfam in WT and PGC-1α KO mice before and after an acute bout of exercise. *Gapdh and Actb* were used as housekeeping genes (n=6-7). **P*<0.05; 2-way ANOVA produced a main effect of exercise. #*P*<0.05; 2-way ANOVA produced a main effect of genotype; ¶*P*<0.05; 2-way ANOVA produced interaction effect indicating increase with exercise only in WT animals. Data are means ± SEM.

levels by 2-fold ($p < 0.05$) in the WT mice, but did not produce any alterations in the PGC-1α KO mice (Fig. 2D).

TFEB localization to the nucleus following an acute bout of exercise is dependent on the presence of PGC-1α. To evaluate the localization of TFEB, the TA muscles of PGC-1α KO and WT mice were separated into nuclear and cytosolic fractions. TFEB nuclear localization did not differ significantly between WT and KO animals in resting muscle. However, exercise induced the translocation of TFEB to the nucleus, which increased 4-fold from 3% to 12% of total TFEB ($p < 0.05$) following an acute bout of exercise. This response was not observed in the KO mice (Fig. 3A, B). TFEB phosphorylation by mTORC serves to sequester it in the cytosol and render it inactive. Basal mTORC phosphorylation on Ser^{2448} did not differ between WT and KO animals. While exercise did not increase $mTORC^{s2448}$ phosphorylation in the WT mice, a 1.6-fold increase ($p < 0.05$) was evident following an acute bout of exercise in KO animals (Fig. 3C).

TFEB transcription is increased with an acute bout of exercise. To determine whether TFEB transcription was increased following an acute bout of exercise, and whether this was dependent on PGC-1α, we used a TFEB promoter-reporter assay. TFEB promoter activity did not differ between WT and PGC-1α KO animals basally. In the WT mice, promoter activity was increased 2.4-fold ($p < 0.05$) following exercise. This response was completely attenuated in KO animals (Fig. 4A). We then used immunoblotting of nuclear and cytosolic samples to investigate the levels of potentially important nuclear transcription factors with binding sites located on the TFEB promoter. Nuclear protein levels of YY1 and p65 did not differ basally between genotypes. However, YY1 and p65

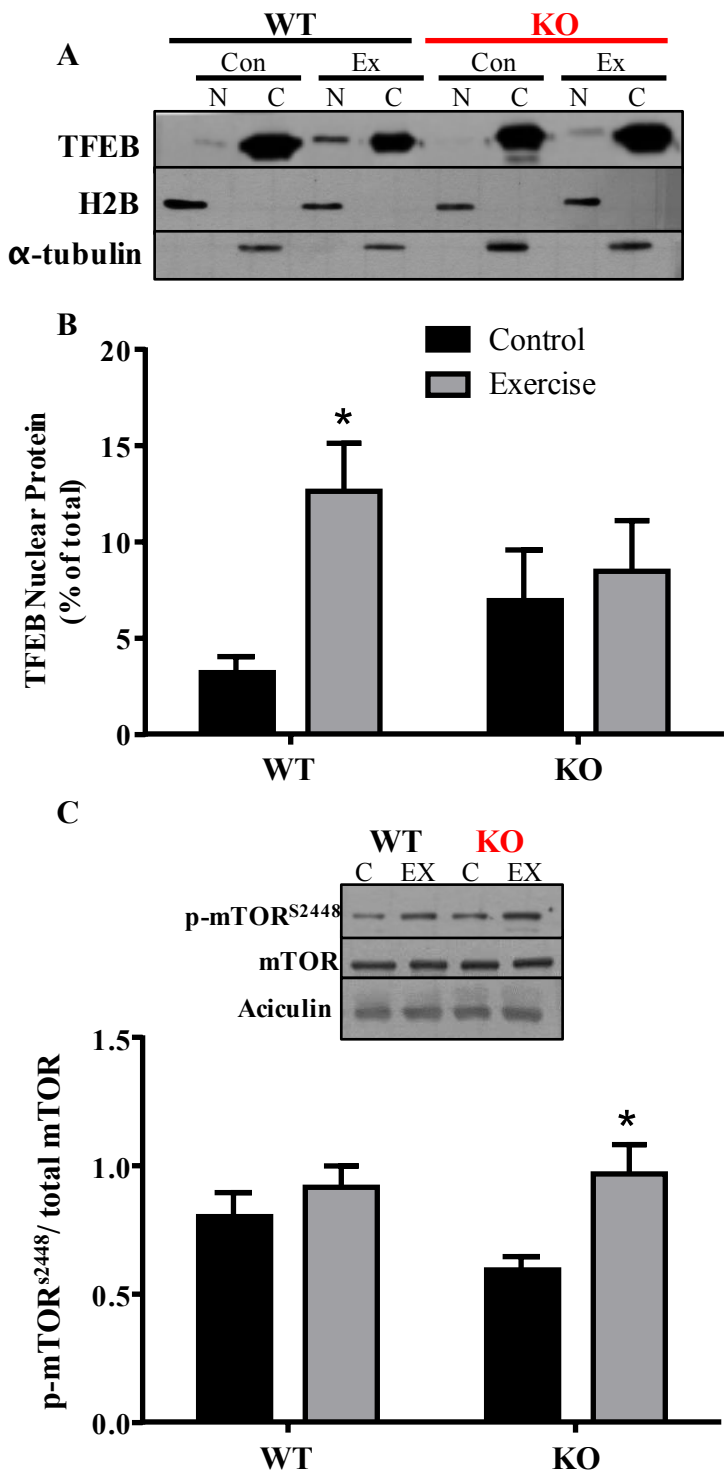
A
WT
KO
Con
Ex
Con
Ex
N C N C N C N C
TFEB
H2B
α-tubulin
B
Control
Exercise
TFEB Nuclear Protein (% of total)
20
15
10
5
0
*
WT
KO
C
WT
KO
C EX C EX
p-mTOR^{S2448}
mTOR
Aciculin
p-mTOR^{S2448}/ total mTOR
1.5
1.0
0.5
0.0
*
WT
KO

Fig. 3

Figure 3: TFEB localization and activation. A) TFEB translocation into the nucleus was measured in WT and PGC-1α KO mice following an acute bout of exercise. **B)** TFEB nuclear content as a % of total. H2B and α-tubulin were used as nuclear and cytosolic purity controls (n=7-9). **P*<0.05, WT control vs WT exercise; 2-way ANOVA. Data are means ± SEM. mTORC activation was measured by **C)** Ser^{2448} phosphorylation. Aciculin was used as a loading control (n=7-9). **P*<0.05, KO control vs KO exercise; 2-way ANOVA. Data are means ± SEM.

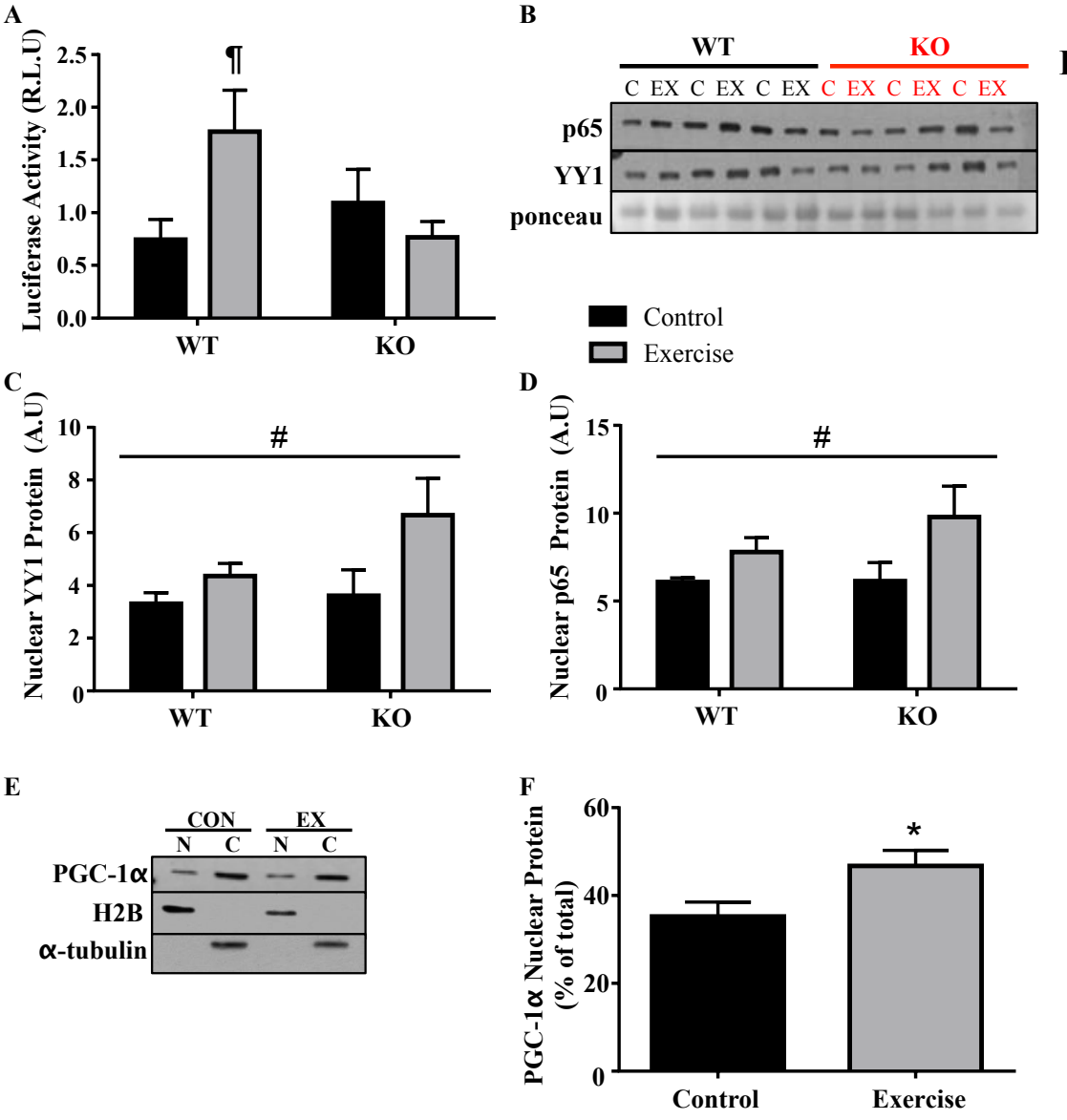

Fig. 4

Figure 4: TFEB transcription with exercise. TFEB transcription was analyzed in WT and PGC-1α KO mice following an acute bout of exercise **A)** TFEB promoter-reporter assay (n=7-9). ¶P<0.05, Interaction effect indicating increase with exercise only in WT animals; 2-way ANOVA. **B)** Immunoblotting of transcription factors p65 and YY1 in nuclear fractions. Quantifications of **C)** YY1 and **D)** p65. Ponceau was used as a loading control (n=7-9). #P<0.05, 2-way ANOVA produced a main effect of exercise. PGC-1α translocation to the nucleus following exercise was measured in WT mice. **E-F)** PGC-1α nuclear content as a % of total. H2B and α-tubulin were used as nuclear and cytosolic purity controls (n=7-9). *P<0.05, WT control vs WT exercise; Student's t-test. Data are means ± SEM.

nuclear levels increased by 20 and 30% respectively ($p < 0.05$) with exercise in the WT mice. These significant increases were moderately greater (40-50% ($p < 0.05$) in the PGC-1α KO mice (Fig. 4B-D). As expected, exercise also provoked an increase in PGC-1α translocation to the nucleus following exercise (Fig 4E). Nuclear PGC-1α content increased from 35% of total before exercise, to 47% ($p < 0.05$) following exercise in WT mice (Fig. 4F).

TFEB protein is reduced in PGC-1α KO animals. TFEB protein content was reduced by 30% in KO mice compared to their WT counterparts (Fig. 5A-B). Similarly, the TFEB family member Tfe3 was also reduced by 50% in KO animals (Fig. 5A, C). To further examine the relationship between TFEB and PGC-1α, downstream targets of TFEB were measured in WT and PGC-1α KO mice (Fig. 5D). While Cathepsin D and p62 expression did not differ significantly between genotypes, there was a surprising 1.3-fold increase ($p < 0.05$) in the autophagy marker Beclin1 protein, and a trend for an increase in protein levels of Lamp1, a lysosomal marker, in the KO mice (Fig. 5D-F).

mRNA expression of TFEB downstream targets change with exercise, but do not differ between genotypes. To examine the effect of exercise on TFEB and its downstream mRNA targets, as well as the role of PGC-1α, we measured mRNA expression in WT and PGC-1α KO mice. Under basal conditions, there were no differences between the levels of **A)** TFEB, **B)** p62, **C)** Lamp1, **D)** Cathepsin D, and **E)** Beclin1 mRNAs between WT and PGC-1α KO mice. Acute exercise also had no effect on Tfeb and p62 mRNAs (Fig 6A, B). However, mRNAs encoding the lysosomal markers Lamp1 and Cathepsin D as well as

Fig. 5

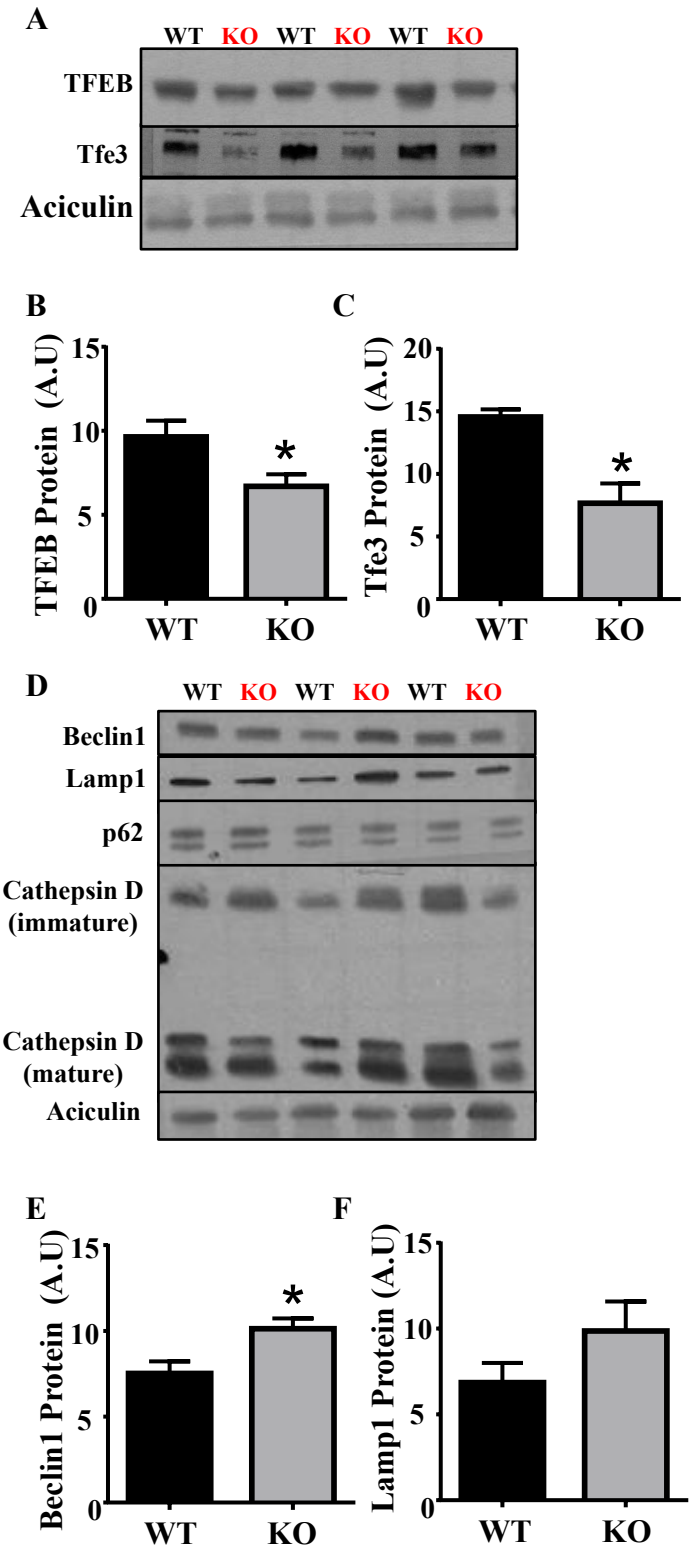
A
WT KO WT KO WT KO
TFEB
Tfe3
Aciculin
B
TFEB Protein (A.U)
15
10
5
0
*
WT
KO
C
Tfe3 Protein (A.U)
20
15
10
5
0
*
WT
KO
D
WT KO WT KO WT KO
Beclin1
Lamp1
p62
Cathepsin D (immature)
Cathepsin D (mature)
Aciculin
E
Beclin1 Protein (A.U)
15
10
5
0
*
WT
KO
F
Lamp1 Protein (A.U)
15
10
5
0
WT
KO

Figure 5: Protein expression of TFEB and downstream targets in WT and PGC-1α KO mice. A-C) Western blots and quantification of TFEB and its family member Tfe3 in WT and PGC-1α KO mice. Aciculin was used as a loading control. **D)** Western blots of TFEB downstream targets in WT and PGC-1α KO mice. Aciculin was used as a loading control. **E-F)** Quantification of **E)** Beclin1 and **F)** Lamp1. (n=7-9). **P*<0.05 WT vs KO, Student's t-test. Data are means of ± SEM.

Fig. 6

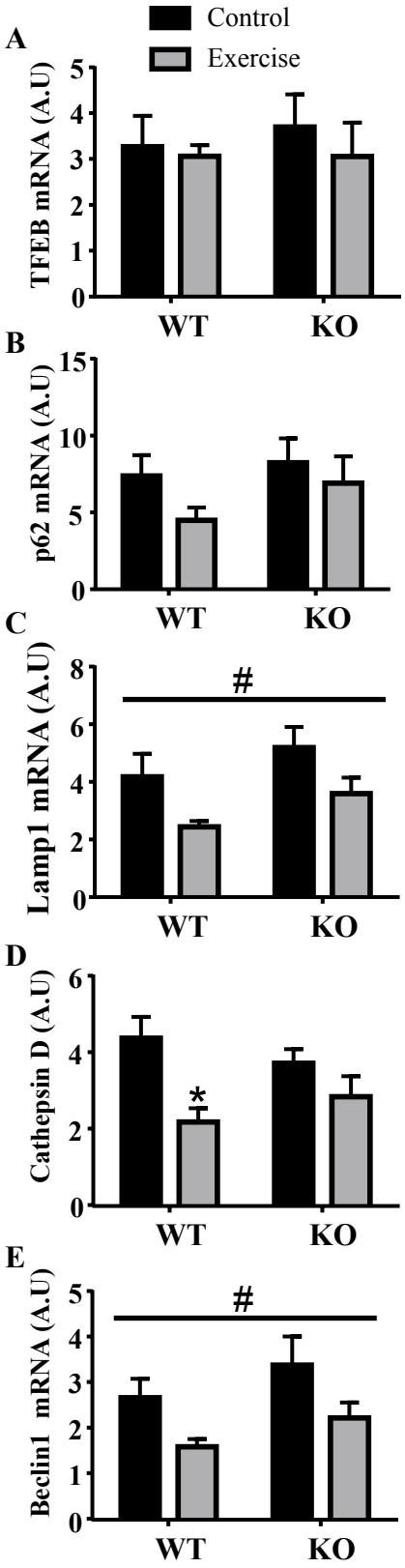
Control
Exercise
A
TFEB mRNA (A.U)
0
1
2
3
4
5
WT
KO
B
p62 mRNA (A.U)
0
5
10
15
WT
KO
C
Lamp1 mRNA (A.U)
#
0
2
4
6
8
WT
KO
D
Cathepsin D (A.U)
*
0
2
4
6
WT
KO
E
Beclin1 mRNA (A.U)
#
0
1
2
3
4
5
WT
KO

Figure 6: Gene expression of Tfeb and its downstream targets. mRNA levels of **A)** Tfeb and its downstream targets **B)** p62 **C)** Lamp1, **D)** Cathepsin D and **E)** Beclin1 in WT and PGC-1α KO mice before and after an acute bout of exercise. *Gapdh and Actb* were used as housekeeping genes (n=6-7). #$P<0.05$; 2-way ANOVA produced a main effect of exercise; *$P<0.05$; WT control vs WT exercise; 2-way ANOVA. Data are means ± SEM.

the autophagy marker Beclin1, were significantly reduced following exercise by 30-50 % ($p < 0.05$) in both WT and KO mice, (Fig. 6C-E).

TFEB overexpression PGC-1α mitochondrial marker content in muscle. In order to further study the relationship between TFEB and mitochondrial biogenesis and autophagy, TFEB was overexpressed using direct injection of adenovirus into skeletal muscles. TFEB levels were augmented by approximately 2-fold in the quadriceps and gastrocnemius of two mice, compared to their contralateral control leg (Fig 7A). Overexpression of TFEB did not result in any changes in p62 and Beclin1 protein. However, levels of the downstream target Cathepsin D were decreased TFEB overexpression. As expected, mTORC phosphorylation on ser^{2448} also tended to decrease with TFEB overexpression, indicating a possible reduction in mTORC activation and a subsequent dephosphorylation of TFEB. The mitochondrial biogenesis regulator PGC-1α did not display any changes, but COXIV, a target of PGC-1α, was markedly reduced in response to TFEB overexpression (Fig. 7).

Fig. 7

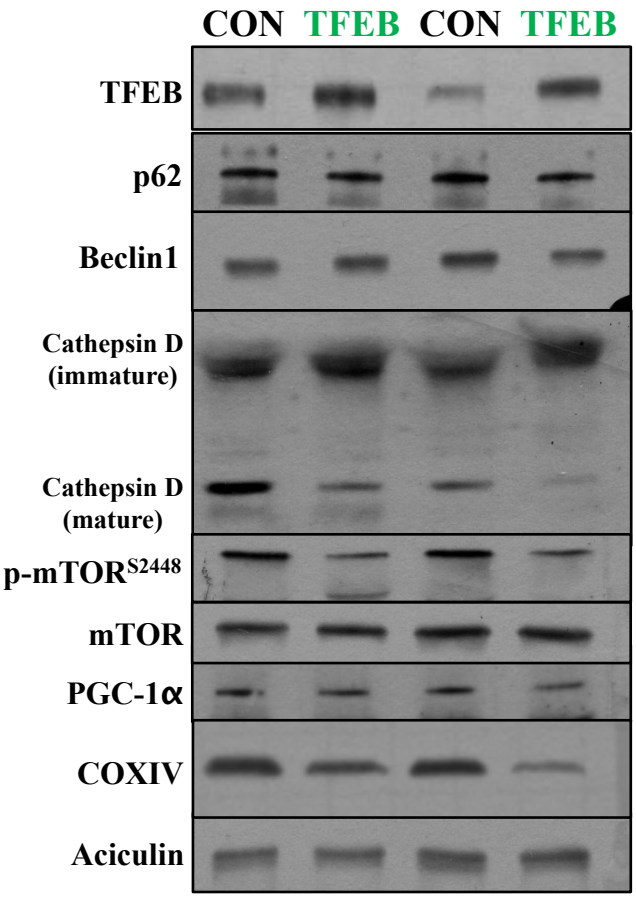

Figure 7: The effect of TFEB overexpression on autophagy and mitochondrial biogenesis markers. Western blots of TFEB downstream targets and mitochondrial biogenesis markers with virally-mediated TFEB overexpression.

DISCUSSION

A healthy mitochondrial pool is essential for cellular homeostasis. This requires a coordination of the processes of mitochondrial biogenesis and mitochondrial-specific autophagy, or mitophagy (10, 14, 28). Mitochondrial biogenesis occurs in response to environmental stressors such as exercise, and involves the expansion of the mitochondrial network to augment mitochondrial content and quality (4, 5, 11, 43). This process is controlled by PGC-1α, a transcriptional coactivator coordinating the expression of nuclear genes encoding mitochondrial proteins (NUGEMPS) (1, 9, 34). Under steady state conditions, the synthesis of new mitochondria is accompanied by the degradation of dysfunctional organelles through the process of mitophagy. Mitophagy is coordinated by TFEB, (37, 38, 41), which transcribes lysosomal genes, along with other autophagy-related genes involved in autophagosome formation and cargo recognition (21, 37). Recent evidence has demonstrated an interplay between PGC-1α and TFEB, and suggests a much broader function for these proteins than their designated roles would suggest (35, 46). The objective of this work was to study the relationship between biogenesis and mitophagy by examining the crosstalk between these proteins and investigating their dual activation in response to exercise in skeletal muscle.

The role of PGC-1α in the regulation of mitochondrial content and function in skeletal muscle is well established. This has been demonstrated by reduced COX activity, and mitochondrial respiration in muscles of PGC-1α KO mice compared to their WT littermates (1). Our data suggest that these deficits are accompanied by elevated lactate levels following exercise, and reduced endurance capacity, represented by decreases in distance run to exhaustion in KO animals. Our exercise protocol was also successful in

inducing changes in gene expression as it elevated the mRNA levels of early response genes and mitochondrial markers as previously demonstrated (30, 46). Exercise and/or contractile activity have also been shown to be effective activators of PGC-1α promoter activity following electrical stimulation in cell culture models, as well as after an acute bout of exercise in mice (2, 30, 31, 50), further supporting the initiation of mitochondrial biogenesis with a single bout of exercise. Recent work has also discovered an emerging role for PGC-1α in mitophagy and lysosomal biogenesis following exercise, strengthening the coactivator's significance in the regulation of mitochondrial turnover (35, 44). PGC-1α KO mice also displayed reductions in TFEB protein levels and other autophagy genes in skeletal muscle, indicating a direct relationship between the two proteins (35, 44), as well as the potential involvement of TFEB in both autophagy and mitochondrial biogenesis.

The activation of TFEB in response to energy deprivation in cell culture models has been well characterized (22, 37–39). Previous work in our laboratory has shown the translocation of TFEB into the nucleus, as well as increased TFEB promoter activity with starvation. However, little is known about the activation of TFEB with an increase in energy expenditure, such as that provided with exercise. A recent study by Medina et al (21) found a calcineurin-dependent translocation of TFEB into the nucleus following exercise, leading to the induction of lysosomal and autophagy genes. We have also demonstrated increased TFEB nuclear translocation and activation after 2 and 5 hours of acute contractile activity in C2C12 cells (Brownlee et al, unpublished observations). This was accompanied by increases in TFEB promoter activity and mRNA expression. In the current study, we examined the dependence of TFEB activation during exercise on the

presence of PGC-1α in WT and PGC-1α KO mice. TFEB translocation to the nucleus was increased in the exercised mice compared to control, but this response was not evident in the KO mice, indicating a PGC-1α-mediated translocation of TFEB with exercise. This impaired translocation may have been facilitated, in part, by the exercise-induced increase in the Ser^{2448} phosphorylation of mTORC in KO animals. As a downstream target of mTORC, TFEB may be retained in the cytosol and inactive by mTORC-mediated TFEB phosphorylation (13, 20, 38). The increased TFEB translocation to the nucleus in the WT animals suggests a possible role for Calcineurin-mediated TFEB dephosphorylation. Exercise is known to cause increases in cytoplasmic [Ca^{2+}], along with the subsequent activation of Calcineurin (3, 18, 49). Further investigations of calcineurin activation with exercise will help us better understand TFEB dephosphorylation and translocation.

We also sought to examine whether TFEB transcription was increased with exercise *in vivo* by using a TFEB promoter-reporter assay. Indeed, TFEB transcription was increased by 2-3-fold in the WT mice following exercise, however this response did not occur in the PGC-1α KO mice. In contracting myotubes, the 1600 bp TFEB promoter used in the current study also exhibited an increase in activity (Brownlee et al, unpublished observations). This increase was not evident with the transfection of the TFEB 1200 bp construct. These data suggests that the 400 bp segment, which distinguishes the two promoter-reporter constructs, is responsible for the differences in response to contractile activity. Examination of this 400bp segment revealed a high concentration of putative transcription factors binding sites for YY1, PPARα, GATA-1, Sp1, p53, myogenin and NF-κB. Therefore, we performed fractionation assays on the

tibialis anterior (TA) muscles of control and exercise mice and examined the nuclear content of YY1, p65, and the coactivator PGC-1α. The nuclear content of both p65 and YY1 was increased with exercise in the WT mice, and this increase was moderately higher in the PGC-1α KO mice. Since TFEB transcription was not elevated by exercise in the KO animals, this suggests that neither p65 nor YY1 play a large role in determining TFEB transcription during exercise. However, PGC-1α translocation was increased following exercise in WT mice, and its absence is the likely reason for the impaired transcription in KO animals. Further investigation of these binding sites using DNA binding ChIP assays will be necessary to fully define the factors mediating TFEB transcription with exercise.

In order to investigate the relationship between PGC-1α and TFEB on a protein level, we measured TFEB and its related family member Tfe3 in the KO mice. We discovered reductions in both TFEB and Tfe3, demonstrating a role for PGC-1α in mediating their expression. However, we did not discover any differences in the protein content of TFEB downstream targets such as p62, Cathepsin D, or Lamp1. Interestingly, the levels of Beclin1, a downstream target of TFEB, were elevated in the KO mice, suggesting that PGC-1α normally suppresses Beclin1. Previous work has found increases in the anti-apoptotic protein Bcl2 in muscle of PGC-1α KO mice (1). It is well established that Bcl2 forms a complex with Beclin-1 which inhibits the induction of autophagy (7, 19, 25, 42). Therefore, we speculate that this parallel rise in both Beclin1 and Bcl-2 may serve to neutralize an increase in autophagic flux in the absence of PGC-1α. Interestingly, mRNA levels of Beclin1 did not differ between genotypes, however exercise significantly reduced Beclin1 mRNA levels in both WT and PGC-1α KO mice.

Exercise also reduced mRNA levels of p62 and Cathepsin D in both genotypes, in a manner that is the direct opposite to the effect of exercise on NUGEMPS. Thus, our data suggest that acute exercise initiates transcriptional activity that represents an increased drive for mitochondrial biogenesis, alongside a parallel reduction in autophagy gene expression, indicating a decline in the signaling towards this catabolic process immediately after an acute bout of exercise.

Our attempt to use an adenoviral transduction system to overexpress TFEB in muscle met with limited success in our initial studies. Our purpose was to further assess the relationship between TFEB and PGC-1α and to investigate TFEB's role in mitochondrial biogenesis. In two animals, we successfully achieved a 2-fold induction of TFEB above empty vector control levels. In examining the downstream targets of TFEB, we found that p62, Lamp1, and Beclin-1 protein levels were unaffected by TFEB overexpression, however Cathepsin D levels displayed a trend for a decrease. Studies have shown increased Cathepsin D mRNA levels with TFEB overexpression in Hela cells, and increases in Cathepsin D protein in the brain (33, 36, 48), however little work has examined protein levels of TFEB downstream targets in skeletal muscle. In 2013, Spampanato et al studied TFEB overexpression in Pompe disease using a new muscle cell culture system, and in mouse models of the disease (41). They reported increased exocytosis of autophagolysosomes with TFEB overexpression. Therefore, decreases in Cathepsin D protein levels could be due to increased exocytosis of lysosomes and their contents, rather than an effect of TFEB on Cathepsin D synthesis. Surprisingly, TFEB overexpression also appeared to cause a decrease in mTORC Ser^{2448} phosphorylation, indicating reduced mTORC activity. mTORC is involved in many processes in the cell

other than autophagy, such as protein and lipid synthesis, as well as mitochondrial metabolism and biogenesis (15). Thus, this consequence of TFEB overexpression requires further analyses. Previous work in our lab has demonstrated increased mRNA levels of mitochondrial biogenesis markers COXIV and PGC-1α in response to TFEB overexpression in C2C12 cells. In this limited sample size, our findings demonstrate a potential reduction in COXIV protein levels, indicating a potential mismatch in the mRNA to protein ratio. This could be due to a TFEB-induced elevation in mRNA stability, or an increased rate of mitophagy occurring due to chronic TFEB overexpression, thereby degrading mitochondrial proteins.

Taken together, our data elucidate a direct role for PGC-1α in mediating the exercise-induced increases in TFEB expression and activation. We have also demonstrated that exercise causes an induction in TFEB transcription and activity, similar to that of PGC-1α, further strengthening the crosstalk between the two proteins and processes they regulate. More research is required to elaborate on the many roles that TFEB has, and to establish the importance of TFEB in contributing to the induction not only of mitophagy, but of mitochondrial biogenesis as well.

REFERENCES

1. **Adhihetty PJ**, **Uguccioni G**, **Leick L**, **Hidalgo J**, **Pilegaard H**, **Hood DA**. The role of PGC-1alpha on mitochondrial function and apoptotic susceptibility in muscle. *Am J Physiol Cell Physiol* 297: C217–C225, 2009.
2. **Akimoto T**, **Pohnert SC**, **Li P**, **Zhang M**, **Gumbs C**, **Rosenberg PB**, **Williams RS**, **Yan Z**. Exercise Stimulates Pgc-1α Transcription in Skeletal Muscle through Activation of the p38 MAPK Pathway. *J Biol Chem* 280: 19587–19593, 2005.
3. **Brookes PS**, **Yoon Y**, **Robotham JL**, **Anders MW**, **Sheu S**. Calcium , ATP , and ROS : a mitochondrial love-hate triangle. *Am J Physiol Cell Physiol* 287: 817–833, 2004.
4. **Collu-Marchese M**, **Shuen M**, **Pauly M**, **Saleem A**, **Hood DA**. The regulation of mitochondrial transcription factor A (Tfam) expression during skeletal muscle cell differentiation. *Biosci Rep* 35: e00221, 2015.
5. **Fernandez-Marcos P**, **Auwerx J**. Regulation of PGC-1α , a nodal regulator of mitochondrial biogenesis. *Am J Clin Nutr* 93: 884–890, 2011.
6. **Fonslow BR**, **Stein BD**, **Webb KJ**, **Xu T**, **Choi J**, **Kyu S**, **Iii JRY**. Mitophagy: mechanisms, pathophysiological roles, and analysis. 10: 54–56, 2013.
7. **He C**, **Bassik MC**, **Moresi V**, **Sun K**, **Wei Y**, **Zou Z**, **An Z**, **Loh J**, **Fisher J**, **Sun Q**, **Korsmeyer S**, **Packer M**, **May HI**, **Hill JA**, **Virgin HW**. Exercise-induced BCL2-regulated autophagy is required for muscle glucose homeostasis. *Nature* 481: 511–515, 2012.
8. **Hepple RT**. Mitochondrial involvement and impact in aging skeletal muscle. *Front Aging Neurosci* 6: 211, 2014.

9. **Hood DA**, **Irrcher I**, **Ljubicic V**, **Joseph A**. Coordination of metabolic plasticity in skeletal muscle. *J Exp Biol* 209: 2265–2275, 2006.

10. **Hood DA**, **Tryon LD**, **Vainshtein A**, **Memme J**, **Chen C**, **Pauly M**, **Crilly MJ**, **Carter H**. Exercise and the Regulation of Mitochondrial Turnover. *Prog Mol Biol Transl Sci* 135: 99–127, 2015.

11. **Hood DA**, **Uguccioni G**, **Vainshtein A**, **D'souza D**. Mechanisms of exercise-induced mitochondrial biogenesis in skeletal muscle: Implications for health and disease. *Compr Physiol* 1: 1119–1134, 2011.

12. **Ivankovic D**, **Chau K-Y**, **Schapira AHV**, **Gegg ME**. Mitochondrial and lysosomal biogenesis are activated following PINK1/parkin-mediated mitophagy. *J Neurochem* 136: 388–402, 2016.

13. **Jung CH1, Ro SH, Cao J, Otto NM KD**. mTORC regulation of autophagy. *FEBS Lett* 48: 1–6, 2010.

14. **Kotiadis VN**, **Duchen MR**, **Osellame LD**. Mitochondrial quality control and communications with the nucleus are important in maintaining mitochondrial function and cell health ☆☆. *BBA - Gen Subj* 1840: 1254–1265, 2014.

15. **Laplante M**, **David M**. mTORC signaling at a glance. *J Cell Sci* 122: 3589–3594, 2009.

16. **Lee J**, **Giordano S**, **Zhang J**. Autophagy, mitochondria and oxidative stress: cross-talk and redox signalling. *Biochem J* 441: 523–40, 2012.

17. **Lira VA**, **Okutsu M**, **Zhang M**, **Greene NP**, **Laker RC**, **Breen DS**, **Hoehn KL**, **Yan Z**. Autophagy is required for exercise training-induced skeletal muscle adaptation and improvement of physical performance. *FASEB J* 27: 4184–4193,

2013.

18. **Marcil M**, **Bourduas K**, **Ascah A**, **Burelle Y**, **Bourduas K**, **Ascah A**. Exercise training induces respiratory substrate-specific decrease in Ca 2+ - induced permeability transition pore opening in heart mitochondria. *Am J Physiol - Hear Circ Physiol* 7: 1549–1557, 2006.

19. **Marquez RT**, **Xu L**. Bcl-2 : Beclin 1 complex : multiple , mechanisms regulating autophagy / apoptosis toggle switch. 2: 214–221, 2012.

20. **Martina JA**, **Chen Y**, **Gucek M**, **Puertollano R**. MTORCC1 functions as a transcriptional regulator of autophagy by preventing nuclear transport of TFEB. : 903–914, 2012.

21. **Medina DL**, **Di Paola S**, **Peluso I**, **Armani A**, **De Stefani D**, **Venditti R**, **Montefusco S**, **Scotto-Rosato A**, **Prezioso C**, **Forrester A**, **Settembre C**, **Wang W**, **Gao Q**, **Xu H**, **Sandri M**, **Rizzuto R**, **De Matteis MA**, **Ballabio A**. Lysosomal calcium signalling regulates autophagy through calcineurin and TFEB. *Nat Cell Biol* 17: 288–299, 2015.

22. **Medina DL**, **Paola S Di**, **Peluso I**, **Armani A**, **Stefani D De**, **Venditti R**, **Montefusco S**, **Scotto-rosato A**, **Prezioso C**, **Forrester A**, **Settembre C**, **Wang W**, **Gao Q**, **Xu H**, **Sandri M**, **Rizzuto R**, **Matteis MA De**. Lysosomal calcium signalling regulates autophagy through calcineurin and TFEB. 17, 2015.

23. **Narendra DP**, **Jin SM**, **Tanaka A**, **Suen DF**, **Gautier CA**, **Shen J**, **Cookson MR**, **Youle RJ**. PINK1 is selectively stabilized on impaired mitochondria to activate Parkin. *PLoS Biol* 8, 2010.

24. **Ostojic O**, **O'Leary MFN**, **Singh K**, **Menzies KJ**, **Vainshtein A**, **Hood DA**. The

effects of chronic muscle use and disuse on cardiolipin metabolism. *J Appl Physiol* 114: 444–52, 2013.

25. **Pattingre S**, **Tassa A**, **Qu X**, **Garuti R**, **Liang XH**, **Mizushima N**, **Packer M**, **Schneider MD**, **Levine B**. Bcl-2 antiapoptotic proteins inhibit Beclin 1-dependent autophagy. *Cell* 122: 927–39, 2005.

26. **Pilegaard H**, **Saltin B**, **Neufer PD**. Exercise induces transient transcriptional activation of the PGC-1α gene in human skeletal muscle. *J Physiol* 546: 851–858, 2003.

27. **Russell AP**, **Foletta VC**, **Snow RJ**, **Wadley GD**. Skeletal muscle mitochondria: a major player in exercise, health and disease. *Biochim Biophys Acta* 1840: 1276–84, 2014.

28. **Russell AP**, **Foletta VC**, **Snow RJ**, **Wadley GD**. Skeletal muscle mitochondria: A major player in exercise, health and disease. *Biochim Biophys Acta - Gen Subj* 1840: 1276–1284, 2014.

29. **Sakamoto K**, **Hirshman MF**, **Aschenbach WG**, **Goodyear LJ**. Contraction Regulation of Akt in Rat Skeletal Muscle *. 277: 11910–11917, 2002.

30. **Saleem A**, **Carter HN**, **Hood DA**. p53 is necessary for the adaptive changes in the cellular milieu subsequent to an acute bout of endurance exercise. *Am J Physiol Cell Physiol* 306: C241–9, 2014.

31. **Saleem A**, **Hood DA**. Acute exercise induces tumour suppressor protein p53 translocation to the mitochondria and promotes a p53-Tfam-mitochondrial DNA complex in skeletal muscle. *J Physiol* 591: 3625–36, 2013.

32. **Sandri M**. Autophagy in skeletal muscle. *FEBS Lett* 584: 1411–1416, 2010.

33. **Sardiello M**, **Palmieri M**, **Ronza A di**, **Medina DL**, **Valenza M**, **Gennarino, Vincenzo Alessandro Chiara Di Malta FD**, **Embrione V**, **Polishchuk RS**, **Banfi S**, **Parenti G**, **Cattaneo E**, **Andrea Ballabio1**. A Gene Network Regulating Lysosomal Biogenesis and Function. : 473–478, 2009.

34. **Scarpulla RC**. Nuclear control of respiratory chain expression by nuclearrRespiratory factors and PGC 1 related coactivator. *Ann N Y Acad Sci* 1147: 321–334, 2008.

35. **Scott I**, **Webster BR**, **Chan CK**, **Okonkwo JU**, **Han K**, **Sack MN**. GCN5-like protein 1 (GCN5L1) controls mitochondrial content through coordinated regulation of mitochondrial biogenesis and mitophagy. *J Biol Chem* 289: 2864–2872, 2014.

36. **Settembre C**, **Ballabio A**. TFEB regulates autophagy: An integrated coordination of cellular degradation and recycling processes. 8627, 2016.

37. **Settembre C**, **Polito VA**, **Garcia M**, **Vetrini F**, **Erdin S**, **Erdin SU**, **Huynh T**, **Medina D**, **Colella P**, **Sardiello M**, **Rubinsztein DC**. TFEB Links Autophagy to Lysosomal Biogenesis. 332: 1429–1433, 2013.

38. **Settembre C**, **Zoncu R**, **Medina DL**, **Vetrini F**, **Erdin S**, **Erdin S**, **Huynh T**, **Ferron M**, **Karsenty G**, **Vellard MC**, **Facchinetti V**. A lysosome-to-nucleus signalling mechanism senses and regulates the lysosome via mTORC and TFEB open. : 1095–1108, 2012.

39. **Settembre C1, De Cegli R, Mansueto G, Saha PK, Vetrini F, Visvikis O, Huynh T, Carissimo A, Palmer D, Klisch TJ, Wollenberg AC, Di Bernardo D, Chan L, Irazoqui JE BA**. TFEB controls cellular lipid metabolism through a

starvation-induced autoregulatory loop. 230: 2330–2336, 2015.

40. **Siddiqui A**, **Bhaumik D**, **Chinta SJ**, **Rane A**, **Rajagopalan S**, **Lieu CA**, **Lithgow GJ**, **Andersen JK**. Mitochondrial Quality Control via the PGC1α-TFEB Signaling Pathway Is Compromised by Parkin Q311X Mutation But Independently Restored by Rapamycin. *J Neurosci* 35: 12833–12844, 2015.

41. **Spampanato C**, **Feeney E**, **Li L**, **Cardone M**, **Lim J**, **Annunziata F**, **Zare H**, **Polishchuk R**, **Puertollano R**, **Parenti G**, **Ballabio A**, **Raben N**. Transcription factor EB (TFEB) is a new therapeutic target for Pompe disease. (2013). doi: 10.1002/emmm.201202176.

42. **Sun Q**, **Gao W**, **Loughran P**, **Shapiro R**, **Fan J**, **Billiar TR**, **Scott MJ**. Caspase 1 Activation Is Protective against Hepatocyte Cell Death by Up-regulating Beclin 1 Protein and Mitochondrial Autophagy in the Setting of Redox Stress . 288: 15947–15958, 2013.

43. **Uguccioni G**, **Hood D a**. The importance of PGC-1α in contractile activity-induced mitochondrial adaptations. *Am J Physiol Endocrinol Metab* 300: E361–E371, 2011.

44. **Vainshtein A**, **Desjardins EM**, **Armani A**, **Sandri M**, **Hood DA**. PGC-1α modulates denervation-induced mitophagy in skeletal muscle. *Skelet Muscle* 5: 9, 2015.

45. **Vainshtein A**, **Hood DA**. The regulation of autophagy during exercise in skeletal muscle. *J Appl Physiol* 120: 664–673, 2016.

46. **Vainshtein A**, **Tryon LD**, **Pauly M**, **Hood DA**. Role of PGC-1α during acute exercise-induced autophagy and mitophagy in skeletal muscle. *Am J Physiol - Cell*

Physiol 308: 710–719, 2015.

47. **Vincow ES**, **Merrihew G**, **Thomas RE**, **Shulman NJ**, **Beyer RP**, **MacCoss MJ**, **Pallanck LJ**. The PINK1-Parkin pathway promotes both mitophagy and selective respiratory chain turnover in vivo. *Proc Natl Acad Sci* 110: 6400–6405, 2013.

48. **Wang H**, **Wang R**, **Carrera I**, **Xu S**, **Neurobiology S**, **Pines T**, **Studies M**, **Lucie P Saint**. TFEB Overexpression in the P301S Model of Tauopathy Mitigates Increased PHF1 Levels and Lipofuscin Puncta and Rescues Memory. 3, 2016.

49. **Wright DC**, **Geiger PC**, **Han DH**, **Jones TE**, **Holloszy JO**. Calcium induces increases in peroxisome proliferator-activated receptor gamma coactivator-1alpha and mitochondrial biogenesis by a pathway leading to p38 mitogen-activated protein kinase activation. *J Biol Chem* 282: 18793–9, 2007.

50. **Zhang Y**, **Uguccioni G**, **Ljubicic V**, **Irrcher I**, **Iqbal S**, **Singh K**, **Ding S**, **Hood DA**. Multiple signaling pathways regulate contractile activity-mediated PGC-1 gene expression and activity in skeletal muscle cells. *Physiol Rep* 2: e12008–e12008, 2014.

FUTURE WORK

Given the present findings, future research should focus on the following:

SHORT TERM:

- Exploring the role of [Ca^{2+}] and calcineurin in TFEB dephosphorylation with the utilization of a calcineurin activation kit;
- Examining the effect of TFEB overexpression on mRNA levels of its downstream targets and mitochondrial biogenesis markers;
- Elucidating the effect of TFEB overexpression on TFEB translocation to the nucleus;
- Investigating binding sites on the TFEB promoter by performing ChiP assays in order to fully define the factors mediating TFEB transcription with exercise.

LONG TERM:

- Continue to inject adenoviral TFEB and increase the sample size of TFEB overexpression animals to investigate mitochondrial and lysosomal changes in muscle;
- Isolate lysosomes in order to examine mTORC localization and Ca^{2+} release to better understand mitophagy induction with exercise;
- Add an exercise + recovery group to the exercise study to further analyze mitophagy signaling and transcription in WT and PGC-1α KO mice;
- Develop TFEB transgenic mice to further elucidate the role of TFEB in mitochondrial biogenesis.

APPENDIX A: DATA AND STATISTICAL ANALYSIS

Table 1A: Body mass of WT and KO animals

Body Mass (g)		
N	**WT**	**KO**
1	30.6	25.9
2	21.2	20.1
3	23.1	20.2
4	44.8	28
5	45.7	25.5
6	25.4	26.4
7	31.5	20.7
8	48.7	19.9
9	29.1	23.5
10	19.5	20.5
11	42.2	24.4
12	26.5	26
13	42.1	23.1
14	26.4	19.3
15	24.5	24.8
16	22.3	18.7
17	38	23.1
18	32.9	
AVG	**31.92**	**22.95**
SEM	**2.27**	**0.69**

Unpaired t test	
P value	0.0006
P value summary	***
Significantly different? (P < 0.05)	Yes

Table 1B: Endurance exercise capacity test - lactate production (WT vs KO; Pre-Ex vs Post-Ex)

Lactate (nM)				
N	**WT pre-EX**	**WT post-EX**	**KO pre-Ex**	**KO post-Ex**
1	1.5	8.9	2.3	18.1
2	2.6	12.2	2.4	11.8
3	1.4	7.4	2.9	15.5
4	2.7	17.1	3.4	16.7
5	2.5	10.4	2.4	17.4
6	2.2	8.8	2.8	13.4
7	2	6.2	1.9	17.4
8	3	9.7	3.3	12
9	2.6	11.6	1.8	17.3
AVG	**2.28**	**10.09**	**2.68**	**15.29**
SEM	**0.19**	**1.12**	**0.17**	**0.85**

2-WAY ANOVA			
Source of Variation	P value	P value summary	Significant?
Interaction	0.001	**	Yes
Genotype	0.0003	***	Yes
Exercise	< 0.0001	****	Yes

POST-HOC TEST				
Tukey	Mean Diff.	q-value	P-value	Summary
WT:PRE-EX vs. WT:POST-EX	-7.978	11.64	P<0.05	****
WT:PRE-EX vs. KO:PRE-EX	-0.3	0.4377	P>0.05	ns
WT:PRE-EX vs. KO:POST-EX	-13.23	19.31	P<0.05	****
WT:POST-EX vs. KO:PRE-EX	7.678	11.2	P<0.05	****
WT:POST-EX vs. KO:POST-EX	-5.256	7.668	P<0.05	****
KO:PRE-EX vs. KO:POST-EX	-12.93	18.87	P<0.05	****

Table 1C: Endurance exercise capacity test - Distance to Exhaustion (WT vs KO)

Distance to exhaustion		
N	**WT**	**KO**
1	930	750
2	1142	792
3	1086	550
4	590	550
5	1200	792
6	1386	884
7	1452	350
8	980	884
9	980	750
AVG	**1082.89**	**700.222**
SEM	**86.0253**	**59.761**

Unpaired t test	
P value	0.0021
P value summary	**
Significantly different? (P < 0.05)	Yes

Table 2A: mRNA expression of PGC-1α (CON vs EX)

PGC-1α mRNA		
N	**CON**	**EX**
1	19.78514	8.510172
2	28.53412	
3	11.38533	21.83355
4	16.1676	31.94833
5	9.119626	8.229695
6		24.23482
7	8.697449	29.07577
AVG	**15.61**	**20.64**
SEM	**3.12**	**4.14**

Unpaired t test	
P value	0.3556
P value summary	ns
Significantly different? (P < 0.05)	No

Table 2B: mRNA expression of EGR1 (WT vs KO; CON vs EX)

EGR1 mRNA				
N	**WT CON**	**WT EX**	**KO CON**	**KO EX**
1	2.139566298	49.85712558	0.285113479	49.99921
2	2.269663096	112.5461016	1.338244924	45.98128
3	2.025877293	116.0291377	9.237119116	41.52738
4	7.079833449	42.62523676	4.234388181	60.89267
5	12.85249782	63.61546231	5.085176865	167.9118
6	1.897141626	81.1906352	12.42590404	26.30458
7	4.641261071	139.3334302	7.624364369	74.00675
AVG	**4.70**	**86.46**	**5.75**	**66.66**
SEM	**1.54**	**13.94**	**1.64**	**17.80**

2-WAY ANOVA			
Source of Variation	P value	P value summary	Significant?
Interaction	0.3681	ns	No
Genotype	0.4173	ns	No
Exercise	< 0.0001	****	Yes

POST-HOC TEST				
Tukey	Mean Diff.	q-value	P-value	Summary
WT:Control vs. WT:Exercise	-81.76	7.197	P<0.05	***
WT:Control vs. KO:Control	-1.046	0.09211	P>0.05	ns
WT:Control vs. KO:Exercise	-61.96	5.455	P<0.05	**
WT:Exercise vs. KO:Control	80.71	7.105	P<0.05	***
WT:Exercise vs. KO:Exercise	19.8	1.743	P>0.05	ns
KO:Control vs. KO:Exercise	-60.91	5.362	P<0.05	**

Table 2C: mRNA expression of COXI (WT vs KO; CON vs EX)

COX1 mRNA				
N	**WT CON**	**WT EX**	**KO CON**	**KO EX**
1	17928.4854	25008.87	5053.245	16633.8
2	10764.05098	23307.55	6618.918	14638.9
3	17398.04079	25925.13	6975.05	20452.8
4	34652.44707	38093.97	40221.39	16840.51
5	40017.95583	61801.8	18029.46	32989.05
6	17326.22353	19046.98	20110.7	8420.253
7	20008.97791	30900.9	9014.732	16494.52
AVG	**22585.17**	**32012.17**	**15146.21**	**18067.12**
SEM	**4000.43**	**5467.67**	**4732.54**	**2841.87**

2-WAY ANOVA			
Source of Variation	P value	P value summary	Significant?
Interaction	0.5759	ns	No
Genotype	0.001	**	Yes
Exercise	0.0041	**	Yes

POST-HOC TEST				
Tukey	Mean Diff.	q-value	P-value	Summary
WT:Control vs. WT:Exercise	-8153	3.913	P>0.05	ns
WT:Control vs. KO:Control	7131	3.423	P>0.05	ns
WT:Control vs. KO:Exercise	1357	0.6514	P>0.05	ns
WT:Exercise vs. KO:Control	15283	7.336	P<0.05	***
WT:Exercise vs. KO:Exercise	9510	4.565	P<0.05	*
KO:Control vs. KO:Exercise	-5774	2.771	P>0.05	ns

Table 2D: mRNA expression of Tfam (WT vs KO; CON vs EX)

Tfam mRNA				
N	**WT CON**	**WT EX**	**KO CON**	**KO EX**
1	2.728228	3.581833942		2.850414
2	1.293121	3.547128967	1.421876	3.053972
3	2.517968	3.269825098	2.894583	2.639926
4	1.051792		4.099311	
5		3.855993871	5.838172	4.445744
6	2.300932	4.90280846	6.669174	3.498161
7			5.34484	5.403624
AVG	**1.98**	**3.83**	**4.38**	**3.65**
SEM	**0.31**	**0.28**	**0.80**	**0.44**

2-WAY ANOVA			
Source of Variation	P value	P value summary	Significant?
Interaction	0.0288	*	Yes
Genotype	0.0563	ns	No
Exercise	0.3147	ns	No

POST-HOC TEST				
Tukey	Mean Diff.	q-value	P-value	Summary
WT:Control vs. WT:Exercise	-1.853	3.266	P>0.05	ns
WT:Control vs. KO:Control	-2.4	4.417	P<0.05	*
WT:Control vs. KO:Exercise	-1.67	3.075	P>0.05	ns
WT:Exercise vs. KO:Control	-0.5465	1.006	P>0.05	ns
WT:Exercise vs. KO:Exercise	0.1829	0.3367	P>0.05	ns
KO:Control vs. KO:Exercise	0.7294	1.408	P>0.05	ns

Table 3A: TFEB nuclear protein (% of total) – WT vs KO; CON vs EX

TFEB NUC CONTENT %				
N	**WT CON**	**WT EX**	**KO CON**	**KO EX**
1	5.95	18.75		15.52
2		13.50	10.68	
3	6.26	6.61	4.24	16.04
4	2.07	16.76	20.68	15.67
5		23.80		3.69
6	1.25		1.74	
7	1.07	4.06	2.03	2.86
8	2.74	12.81	2.21	1.73
9	3.12	4.27	6.78	3.80
AVG	**3.21**	**12.57**	**6.91**	**8.47**
SEM	**0.80**	**2.71**	**2.60**	**2.58**

2-WAY ANOVA			
Source of Variation	P value	P value summary	Significant?
Interaction	0.1015	ns	No
Genotype	0.9314	ns	No
Exercise	0.0252	*	Yes

POST-HOC TEST				
Tukey	Mean Diff.	q-value	P-value	Summary
WT:Control vs. WT:Exercise	-9.363	4.149	P<0.05	*
WT:Control vs. KO:Control	-3.7	1.588	P>0.05	ns
WT:Control vs. KO:Exercise	-5.264	2.258	P>0.05	ns
WT:Exercise vs. KO:Control	5.663	2.509	P>0.05	ns
WT:Exercise vs. KO:Exercise	4.099	1.817	P>0.05	ns
KO:Control vs. KO:Exercise	-1.564	0.6708	P>0.05	ns

Table 3B: p-mTOR^{s2448}/ total mTOR (WT vs KO; CON vs EX)

p-mTOR^{s2448}/ total mTOR				
N	**WT CON**	**WT EX**	**KO CON**	**KO EX**
1	1.157902	1.235692	0.327542	0.774845
2	0.844667		0.692741	
3	0.809889	0.893417	0.464679	0.821302
4	0.7000122	0.979403	0.788455	0.794774
5	0.9949668		0.744054	1.075174
6	0.9192349	1.03887		1.352448
7	1.027671	0.622434	0.576448	0.524145
8	0.3515786	0.584104	0.541237	
9	0.3786054	1.041128	0.603921	1.415164
AVG	**0.80**	**0.91**	**0.59**	**0.97**
SEM	**0.09**	**0.09**	**0.05**	**0.12**

2-WAY ANOVA			
Source of Variation	P value	P value summary	Significant?
Interaction	0.174	ns	No
Genotype	0.4112	ns	No
Exercise	0.0134	*	Yes

POST-HOC TEST				
Tukey	Mean Diff.	q-value	P-value	Summary
WT:Control vs. WT:Exercise	-0.1153	1.266	P>0.05	ns
WT:Control vs. KO:Control	0.2059	2.345	P>0.05	ns
WT:Control vs. KO:Exercise	-0.1671	1.836	P>0.05	ns
WT:Exercise vs. KO:Control	0.3212	3.435	P>0.05	ns
WT:Exercise vs. KO:Exercise	-0.05183	0.5367	P>0.05	ns
KO:Control vs. KO:Exercise	-0.373	3.989	P<0.05	*

Table 4A: TFEB promoter activity-Luciferase reporter assay (WT vs KO; CON vs EX)

TFEB promoter activity				
N	**WT CON**	**WT EX**	**KO CON**	**KO EX**
1		1.716369	1.6825	1.52047
2		3.981057	2.5295	0.99023
3	0.371325	1.16568	0.58869	
4	0.7132671	1.156073	0.406	0.69616
5		0.9742066		0.14805
6	0.3952042	1.990165	3.20482	0.29054
7	1.657868			0.9296
8	0.6606687		0.15457	0.73586
9	0.6670193	1.404834	0.76976	0.81637
AVG	**0.74**	**1.77**	**1.33**	**0.77**
SEM	**0.19**	**0.42**	**0.44**	**0.14**

2-WAY ANOVA			
Source of Variation	P value	P value summary	Significant?
Interaction	0.0242	*	Yes
Genotype	0.2546	ns	No
Exercise	0.2254	ns	No

POST-HOC TEST				
Tukey	Mean Diff.	q-value	P-value	Summary
WT:Control vs. WT:Exercise	-1.026	3.526	P>0.05	ns
WT:Control vs. KO:Control	-0.3481	1.197	P>0.05	ns
WT:Control vs. KO:Exercise	-0.02168	0.0768	P>0.05	ns
WT:Exercise vs. KO:Control	0.6775	2.424	P>0.05	ns
WT:Exercise vs. KO:Exercise	1.004	3.71	P>0.05	ns
KO:Control vs. KO:Exercise	0.3264	1.206	P>0.05	ns

Table 4B: YY1 Protein -Nuclear (WT vs KO; CON vs EX)

YY1-Nuclear Protein Expression				
N	**WT CON**	**WT EX**	**KO CON**	**KO EX**
1	34.13409968	55.39126569		96.01246504
2	27.17791235	49.70707471	63.2595153	119.7192446
3	22.08030856	41.62628709		26.6097325
4	23.12942719	47.17267551	18.90366271	32.25035712
5	29.65511199	28.57256224	24.82450603	90.86177036
6	45.03047855	57.31479683	37.42481338	68.14632777
7	50.7297463	25.6066695		33.23213552
AVG	**33.13**	**43.63**	**36.10**	**66.69**
SEM	**4.15**	**4.71**	**8.80**	**13.95**

2-WAY ANOVA			
Source of Variation	P value	P value summary	Significant?
Interaction	0.2983	ns	No
Genotype	0.1816	ns	No
Exercise	0.0407	*	Yes

POST-HOC TEST				
Tukey	Mean Diff.	q-value	P-value	Summary
WT:Control vs. WT:Exercise	-10.49	1.214	P>0.05	ns
WT:Control vs. KO:Control	-2.969	0.2929	P>0.05	ns
WT:Control vs. KO:Exercise	-33.56	3.882	P>0.05	ns
WT:Exercise vs. KO:Control	7.524	0.7423	P>0.05	ns
WT:Exercise vs. KO:Exercise	-23.06	2.668	P>0.05	ns
KO:Control vs. KO:Exercise	-30.59	3.017	P>0.05	ns

Table 4C: p65 Protein -Nuclear (WT vs KO; CON vs EX)

p65-Nuclear Protein Expression				
N	**WT CON**	**WT EX**	**KO CON**	**KO EX**
1	56.38086404	84.67584362		
2	68.79814029	87.39149163	124.85488	162.6137
3	63.41709793	84.08643174	95.637775	86.19347
4	65.7303618	97.95185159	54.694494	94.71703
5	55.19036681		73.441581	
6		31.77362305	45.843151	28.33087
7	52.72743939	72.37089167	37.804945	90.72799
8	63.77851879	40.95770532		54.96508
AVG	**60.86**	**71.32**	**72.05**	**86.26**
SEM	**2.29**	**9.51**	**13.55**	**17.12**

2-WAY ANOVA			
Source of Variation	P value	P value summary	Significant?
Interaction	0.3435	ns	No
Genotype	0.314	ns	No
Exercise	0.0146	*	Yes

POST-HOC TEST				
Tukey	Mean Diff.	q-value	P-value	Summary
WT:Control vs. WT:Exercise	-17.05	1.836	P>0.05	ns
WT:Control vs. KO:Control	-0.624	0.06386	P>0.05	ns
WT:Control vs. KO:Exercise	-36.98	3.785	P>0.05	ns
WT:Exercise vs. KO:Control	16.42	1.625	P>0.05	ns
WT:Exercise vs. KO:Exercise	-19.94	1.973	P>0.05	ns
KO:Control vs. KO:Exercise	-36.36	3.445	P>0.05	ns

Table 4D: PGC-1α nuclear protein (% of total) – WT vs KO; CON vs EX

PGC-1α NUC CONTENT %		
N	**CON**	**EX**
1	46.04316	41.12775
2		55.73234
3	32.86166	
4	38.19807	39.11822
5	24.49555	
6	28.56993	
7	41.83674	39.93956
8	45.39293	44.90271
9		59.45982
AVG	**36.77**	**46.71**
SEM	**3.17**	**3.57**

Unpaired t test	
P value	0.039
P value summary	*
Significantly different? (P < 0.05)	Yes

Table 5A: TFEB Protein - WT vs KO (whole muscle)

TFEB Protein		
N	**WT**	**KO**
1	6.29988	
2	12.2201	8.69244
3	8.307921	3.47442
4	14.4639	7.38446
5	8.40486	3.67846
6		8.80001
7	8.38502	6.92037
8	8.13737	7.42738
9	10.9757	7.16422
AVG	**9.65**	**6.69**
SEM	**0.94**	**0.72**

Unpaired t test	
P value	0.0261
P value summary	*
Significantly different? (P < 0.05)	Yes

Table 5B: Tfe3 Protein - WT vs KO (whole muscle)

Tfe3 Protein		
N	**WT**	**KO**
1	13.19251	4.54019
2	16.78008	8.131931
3	15.29915	11.48529
4		
5	13.77586	6.161952
6	12.99027	2.898399
7	8.13737	7.42738
8	10.9757	7.16422
AVG	**13.02**	**6.83**
SEM	**1.00**	**0.97**

Unpaired t test	
P value	0.0023
P value summary	**
Significantly different? (P < 0.05)	Yes

Table 5C: Beclin1 Protein - WT vs KO (whole muscle)

Beclin1 Protein		
N	**WT**	**KO**
1		
2	7.01276	9.05803
3	6.57364	8.11204
4	6.76078	10.636
5	11.5543	
6	6.33364	12.1204
7	8.19699	9.40041
8	6.17817	12.3177
9		9.25538
AVG	**7.52**	**10.27**
SEM	**0.72**	**0.65**

Unpaired t test	
P value	0.0168
P value summary	*
Significantly different? (P < 0.05)	Yes

Table 5D: Lamp1 Protein - WT vs KO (whole muscle)

Lamp1		
N	**WT**	**KO**
1	7.36879	13.0705
2	5.84132	10.2615
3	9.28359	
4	1.88746	
5	11.469	6.33328
6		16.6769
7	5.61569	4.78691
8	3.58973	12.6572
9	9.70886	5.2055
AVG	**6.44**	**10.63**
SEM	**1.24**	**1.68**

Unpaired t test	
P value	0.1601
P value summary	ns
Significantly different? (P < 0.05)	No

Table 6A: mRNA expression of Lamp1 (WT vs KO; CON vs EX)

Lamp1 mRNA				
N	**WT CON**	**WT EX**	**KO CON**	**KO EX**
1	57.85830983	31.79273103	54.25056672	56.81344
2		20.08928097	24.4882799	19.88722
3	31.21554029	30.1328032	70.58540287	48.47141
4	23.27056001	20.17571837	29.98425695	22.07317
5	22.13135114	20.24485496	56.14929454	20.83267
6	41.73536023			
7	80.95402368	21.34462912	74.65520638	43.25677
8	34.98237642	27.40698562	53.31883527	39.8079
AVG	**35.24**	**24.49**	**47.09**	**33.62**
SEM	**5.62**	**2.25**	**7.29**	**6.67**

2-WAY ANOVA			
Source of Variation	P value	P value summary	Significant?
Interaction	0.9203	ns	No
Genotype	0.0905	ns	No
Exercise	0.0119	*	Yes

POST-HOC TEST				
Tukey	Mean Diff.	q-value	P-value	Summary
WT:Control vs. WT:Exercise	17.28	2.821	P>0.05	ns
WT:Control vs. KO:Control	-10.18	1.663	P>0.05	ns
WT:Control vs. KO:Exercise	5.858	0.9564	P>0.05	ns
WT:Exercise vs. KO:Control	-27.46	4.484	P<0.05	*
WT:Exercise vs. KO:Exercise	-11.42	1.865	P>0.05	ns
KO:Control vs. KO:Exercise	16.04	2.619	P>0.05	ns

Table 6B: mRNA expression of Cathepsin D (WT vs KO; CON vs EX)

Cathepsin D mRNA				
N	**WT CON**	**WT EX**	**KO CON**	**KO EX**
1	579.0969764	427.4275293	530.5697042	570.0315
2	220.4950376	200.8928097	244.882799	198.8722
3		155.3890489	327.4809691	199.3189
4	313.4731173	222.8931243	327.2267075	173.4922
5	368.2289122	193.951148	464.09799	209.909
6	439.4146738	144.1579526		
7	604.2373042		384.5689124	367.5243
8	550.9566953	194.2230771	337.773443	282.8808
AVG	**370.32**	**240.11**	**378.85**	**270.32**
SEM	**57.43**	**40.63**	**43.73**	**63.53**

2-WAY ANOVA			
Source of Variation	P value	P value summary	Significant?
Interaction	0.1667	ns	No
Genotype	0.9954	ns	No
Exercise	0.0028	**	Yes

POST-HOC TEST				
Tukey	Mean Diff.	q-value	P-value	Summary
WT:Control vs. WT:Exercise	219.6	4.752	P<0.05	*
WT:Control vs. KO:Control	65.61	1.42	P>0.05	ns
WT:Control vs. KO:Exercise	153.4	3.32	P>0.05	ns
WT:Exercise vs. KO:Control	-154	3.332	P>0.05	ns
WT:Exercise vs. KO:Exercise	-66.16	1.432	P>0.05	ns
KO:Control vs. KO:Exercise	87.8	1.9	P>0.05	ns

Table 6C: mRNA expression of Beclin1 (WT vs KO; CON vs EX)

Beclin1 mRNA				
N	**WT CON**	**WT EX**	**KO CON**	**KO EX**
1	14.33739739	15.26130869	14.69320599	13.17938
2		15.31138315	29.17093212	19.9482
3	23.16930247	21.2136593	35.92310846	21.52386
4	12.47841164	14.32834919	47.68037884	14.87333
5	29.23775419	7.848036415		
6	39.4171		21.21445863	18.4965
7	28.85720873	18.20753918	35.72635155	28.80073
AVG	**16.66**	**16.53**	**31.87**	**17.38**
SEM	**2.33**	**1.29**	**5.62**	**1.63**

2-WAY ANOVA			
Source of Variation	P value	P value summary	Significant?
Interaction	0.9256	ns	No
Genotype	0.1444	ns	No
Exercise	0.019	*	Yes

POST-HOC TEST				
Tukey	Mean Diff.	q-value	P-value	Summary
WT:Control vs. WT:Exercise	10.76	2.376	P>0.05	ns
WT:Control vs. KO:Control	-7.139	1.628	P>0.05	ns
WT:Control vs. KO:Exercise	4.464	0.9854	P>0.05	ns
WT:Exercise vs. KO:Control	-17.9	4.081	P<0.05	*
WT:Exercise vs. KO:Exercise	-6.298	1.39	P>0.05	ns
KO:Control vs. KO:Exercise	11.6	2.645	P>0.05	ns

Table 6D: mRNA expression of TFEB (WT vs KO; CON vs EX)

Tfeb mRNA				
N	**WT CON**	**WT EX**	**KO CON**	**KO EX**
1	50.51283575	38.60927787	41.70953598	40.43186018
2	22.67216515	37.09042156	3.894115452	29.37650664
3	28.24238652	27.64029808	10.86897606	17.51639572
4	37.49541272	27.94728466	38.21085431	28.90822397
5	19.57758941	17.23358289	54.94607915	17.28683159
6	59.30073757	32.0053569	41.21669334	77.47601755
7	0.187487802	27.9129069	63.25404536	13.54959052
8	43.54632907	36.25951123	41.63875106	19.90272975
AVG	**34.73**	**32.82**	**23.67**	**29.06**
SEM	**4.30**	**2.06**	**6.74**	**3.31**

2-WAY ANOVA			
Source of Variation	P value	P value summary	Significant?
Interaction	0.7332	ns	No
Genotype	0.7369	ns	No
Exercise	0.5016	ns	No

POST-HOC TEST				
Tukey	Mean Diff.	q-value	P-value	Summary
WT:Control vs. WT:Exercise	2.105	0.3365	P>0.05	ns
WT:Control vs. KO:Control	-4.276	0.6836	P>0.05	ns
WT:Control vs. KO:Exercise	2.136	0.3415	P>0.05	ns
WT:Exercise vs. KO:Control	-6.38	1.02	P>0.05	ns
WT:Exercise vs. KO:Exercise	0.03131	0.005006	P>0.05	ns
KO:Control vs. KO:Exercise	6.411	1.025	P>0.05	ns

Table 6E: mRNA expression of p62 (WT vs KO; CON vs EX)

p62 mRNA				
N	**WT CON**	**WT EX**	**KO CON**	**KO EX**
1	1362.343679	427.5185186	1304.475259	1600.45
2	400.0105963	334.840952	440.6249636	426.9933
3	316.504243	307.294271	656.821078	495.817
4	515.9435831	407.2057294	800.6663771	407.9152
5	579.30143	274.7777858	759.2080506	351.8782
6	1262.140198	1000.914963	1628.671646	1256.613
7	736.469868	365.9444183	246.7743909	194.5778
8	719.045347	478.714451	751.4363326	788.2569
AVG	**648.70**	**369.21**	**800.65**	**732.79**
SEM	**170.67**	**20.27**	**129.77**	**204.94**

2-WAY ANOVA			
Source of Variation	P value	P value summary	Significant?
Interaction	0.5928	ns	No
Genotype	0.2579	ns	No
Exercise	0.15	ns	No

POST-HOC TEST				
Tukey	Mean Diff.	q-value	P-value	Summary
WT:Control vs. WT:Exercise	286.8	2.021	P>0.05	ns
WT:Control vs. KO:Control	-87.11	0.6138	P>0.05	ns
WT:Control vs. KO:Exercise	46.16	0.3252	P>0.05	ns
WT:Exercise vs. KO:Control	-373.9	2.635	P>0.05	ns
WT:Exercise vs. KO:Exercise	-240.7	1.696	P>0.05	ns
KO:Control vs. KO:Exercise	133.3	0.9391	P>0.05	ns

Table 6F: mRNA expression of Lamp2 (WT vs KO; CON vs EX)

Lamp2 mRNA				
N	**WT CON**	**WT EX**	**KO CON**	**KO EX**
1	32.42276931	12.16184917	59.50856671	24.16701
2	27.57336032	34.95302217	30.92424868	25.95197
3	26.3698471	27.31329225	32.4783596	41.85638
4	12.97501654	14.59722864	51.44932567	17.34472
5	45.3639677	18.92208137	24.50159097	62.26164
6	45.24794069	30.6731312	30.15594935	24.34456
AVG	**28.79**	**24.81**	**40.97**	**30.66**
SEM	**1.31**	**4.74**	**6.56**	**3.98**

2-WAY ANOVA			
Source of Variation	P value	P value summary	Significant?
Interaction	0.7825	ns	No
Genotype	0.1549	ns	No
Exercise	0.21	ns	No

POST-HOC TEST				
Tukey	Mean Diff.	q-value	P-value	Summary
WT:Control vs. WT:Exercise	8.555	1.575	P>0.05	ns
WT:Control vs. KO:Control	-6.511	1.199	P>0.05	ns
WT:Control vs. KO:Exercise	-0.9956	0.1833	P>0.05	ns
WT:Exercise vs. KO:Control	-15.07	2.773	P>0.05	ns
WT:Exercise vs. KO:Exercise	-9.551	1.758	P>0.05	ns
KO:Control vs. KO:Exercise	5.515	1.015	P>0.05	ns

APPENDIX B: SUPPLEMENTARY AND ADDITIONAL DATA
(STATISTIC TABLES NOT SHOWN)

Fig. S1

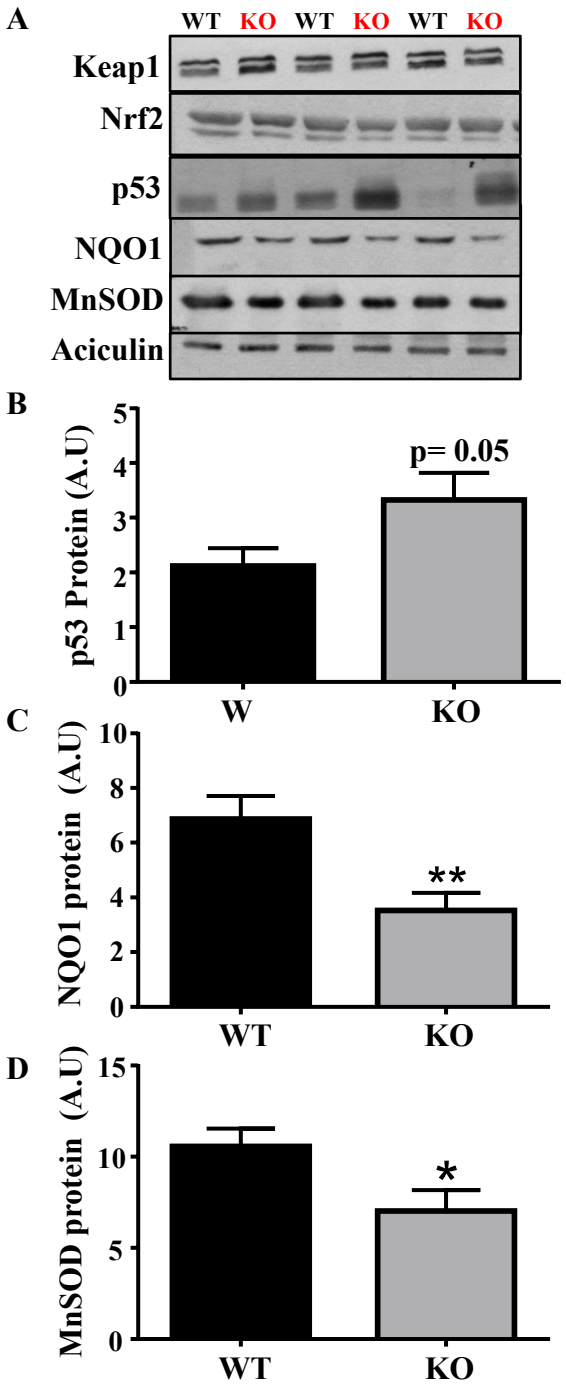

Figure S1. Nrf2-Keap1 antioxidant pathway in WT and PGC-1α KO mice. **A)** Western blots of Keap1, Nrf2, p53, NQO1, MnSOD. Quantifications of **B)** p53, C)NQO1, and **D)** MnSOD. Aciculin was used as a loading control (n=6-8). *P<0.05, **P<0.001. (WT vs PGC-1α KO). Data are means ± SEM.

Fig. S2

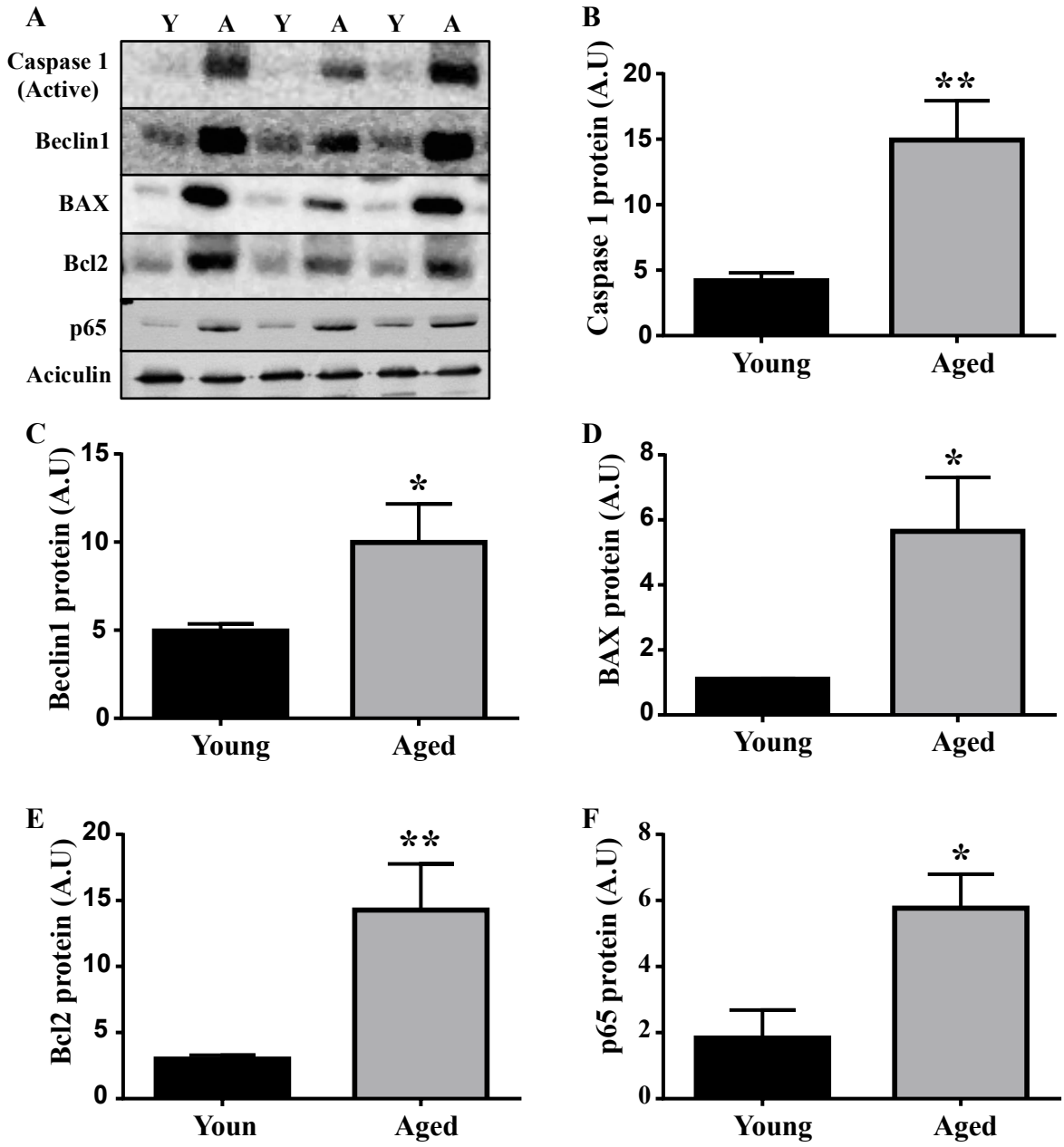

Figure S2. Inflammation, apoptotic, and autophagy markers in response to aging. **A)** Western blots of Caspase1, Beclin1, BAX, Bcl2, p65. Quantifications of **B)** Caspase 1, **C)** Beclin1, **D)** BAX, **F)** Bcl2, and **G)**p65. Aciculin was used as a loading control (n=6-8). *P<0.05, **P<0.001. (Young vs Aged).Data are means ± SEM.

Fig. S3

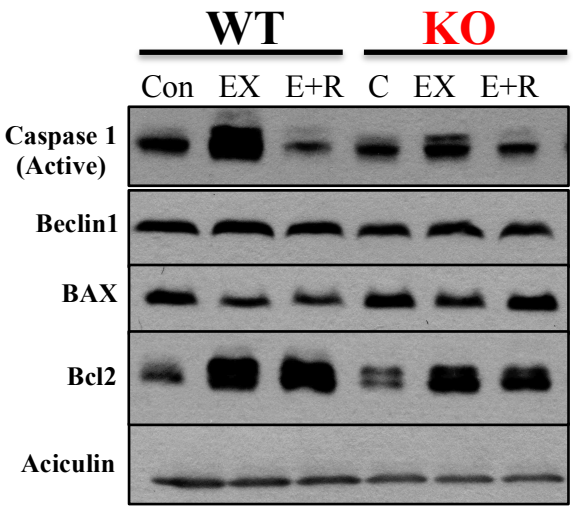

Figure S3. Inflammation, apoptotic, and autophagy markers in. WT and PGC-1α KO mice. Western blots of Caspase1, Beclin1, and Bcl2 in control, exercise, and exercise and recovery groups in WT and PGC-1α KO mice. Aciculin was used as a loading control.

APPENDIX C: LABORATORY METHODS AND PROTOCOLS

E-Coli transformation with Plasmid DNA

1. Thaw frozen bacterial cells (-80^{o}C) quickly with finger tips and keep it on ice just before you are ready to proceed
2. Slowly add DNA (1 – 2µl) or ligation mixture (~10ml) to cells with gently stirring
3. Incubate on ice for 30 minutes
4. *If the transformation is done with pure DNA,* ***you could*** *directly plate cells onto the pre-warm LB + appropriate antibiotics plate (pre-warm @ 37^{o}C for at least 1 hour) and incubate overnight @ 37^{o}C*
5. Heat shock cells @ 42^{o}C for 45 seconds
6. Put cells on ice for 2 minutes
7. Add appropriate amount of SOC medium (DNA:SOC → 1 : 80) and inoculate @ 37^{o}C (250 rpm) for 1 hour
8. Spin cells @ 5000xg, 30 seconds, room temperature and remove most of the supernatant (leave ~50ml to resuspend cells for platting)
9. Resuspend cells gently and plate them on the pre-warm LB + appropriate antibiotics plate (pre-warm @ 37^{o}C for at least 1 hour) and incubate overnight @ 37^{o}C

DNA injection and electroporation into muscle hindlimb muscles

References:

Wolff JA, Malone RW, Williams P, Chong W, Ascadi G, Jani A, Felgner PL. Direct gene transfer into mouse muscle *in vivo*. *Science* 247(4949 Pt 1):1465-8, 1990.
Wolff JA, Williams P, Ascadi G, Jiao S, Jani A, Chong W. Conditions affecting direct gene transfer into rodent muscle *in vivo*. *Biotechniques* 11(4): 474-85, 1991.
Davis HL, Whalen RG, Demeneix BA. Direct gene transfer into skeletal muscle *in vivo*: factors affecting efficiency of transfer and stability of expression. *Hum Gen Ther* 4(2):151-9, 1993.

Materials:
29 gauge insulin syringe, ½" needle (Ultrafine, Becton Dickson)
Forceps (sterile)
Plasmid DNA: 50µg plasmid of interest + 1µg of pRL-CMV plasmid (use spectrophotometer to determine DNA concentration)
ECM 830 Electroporation system (BTX)
0.7cm tweezertrodes (BTX)

DNA preparation:
DNA is prepared using the alkaline lysis plasmid DNA preparation to produce plasmids inserted with the promoter of interest upstream of the luciferase gene, which can be used to both *in vivo* and *in vitro* transfections. DNA is stored in stab cultures, in glycerol at -80°C for long-term storage. Follow the manufacturer's instructions to isolate DNA from these stores, using a MaxiPrep isolation kit (Sigma-Aldrich, GenElute HP Plasmid Maxiprep kit). Transfection efficiency is determined through the co-transfection of the pRL-CMV (renilla luciferase) plasmid, as it is assumed that the cells transfected with the plasmids containing the promoter of interest have also been transfected with the pRL-CMV plasmid.

Sample calculation:

[TFEB + pGL3] = 3.13µg/µl (arbitrary concentration)
∴ 40µg [TFEB + pGL3] = 40/3.13
=**12.78µl of plasmid DNA**

[pGL3 empty vector] = 2.18µg/µl (arbitrary concentration)
∴ 40µg [TFEB + pGL3] = 40/2.18
=**18.35µl of plasmid DNA**

[pRL-CMV]=1.00µg/µl (measured by spectrophotometry, and solution is kept at this concentration)
∴ 1µg of [pRL-CMV] = 1/1 = **1µl of plasmid DNA**

Volume up to 20µl (3 units on the syringe) with 0.9% sterile saline.
12.78ul of plasmid DNA [TFEB+pGL3] + 1µl of plasmid DNA [pRL-CMV] +6.22µl sterile saline = 30µl to be injected into muscle

*NOTE: to fill syringes, fill a 1.5ml sterile Eppendorf with a solution of all plasmid DNA and sterile saline sufficient for all injections to be performed in a single day. Insert the needle into the Eppendorf, and slowly withdraw fluid from the Eppendorf, ensure that **no air bubbles** are

present in the syringe. Do not store syringes in the fridge after filling, but rather use them immediately.

Injection procedure:

1. Animals are anesthetized using isoflurane.
2. Set the appropriate parameters on the electroporator (100 V/cm, 20ms pulse duration, 200ms interval, 4 pulses, unipolarity).
3. The lower part of the limb in shaved, providing a clear view of the outline of the tibialis anterior muscle.
4. The injection site is sterilized by applying iodine (Providine solution) and subsequently ethanol to the shaved area.
5. The animal is turned slightly on its side to provide clear access to the injection site at the gastrocnemius muscle.
6. Take a prefilled syringe (containing 40µg of plasmid DNA of the gene of interest, 1µg of plasmid DNA of the control plasmid in a 40µl solution with 0.9% sterile saline) and perform the injection into the muscle. Take time to perform the injection (up to 30 seconds per injection), and maintain a very small angle between the muscle and the syringe. Do not insert the needle of the syringe more than 1-3mm into the muscle, and ensure injection takes places into the belly of the muscle.
7. Remove the needle from the muscle very slowly (take 10-15 seconds to do so). If the injection has been successfully completed, no leak from the site of injection will be visible to the eye.
8. Adjust the width of the tweezertrodes according to the size of the muscle. Tweezertrodes are positioned over the skin, and on either side of the muscle in a direction parallel to the muscle fiber orientation. Pulse the muscle, and observe contraction of the muscle. Repeat this if no contraction is observed. Switch the polarity by reversing the orientation of the electrodes and pulse the muscle again.
9. Repeat steps 6-9 on the contralateral hindlimb,
10. Remove the isoflurane anesthetic, and allow the animal to recover for 7 days without any further handling. Do not massage or put any pressure on the injected muscle, as this has been shown to markedly reduce expression of the reporter gene (Davis HL et al, *Hum Gen Ther*). Antibiotic water should be given to the animal during recovery.
11. Perform exercise protocol 7 days following injection, and remove the Gastrocnemius muscle for analysis of promoter activity using a luciferase assay.

Whole muscle tissue preparation for luciferase assay

1. Add 1ml of 5X passive lysis buffer (PLB) into 4ml sterile water to dilute 5-fold. Add 100µl of this now diluted 1X PLB into 1.5ml eppendorfs.
2. Pound the tibialis anterior muscle tissue at the temperature of liquid nitrogen into a fine powder using a mortar and pestle. Weigh 30-50mg of this powdered tissue into the 1.5ml eppendorfs already containing 100µl of 1X PLB.
3. Dilute this 7-fold in more 1X PLB.
4. Mix samples by flicking the eppendorfs briefly, and sonicate samples 3 X 10 seconds on ice.
5. Centrifuge at max speed on a tabletop centrifuge for 5 minutes at 4°C.
6. Retain supernates and transfer them to new 1.5ml eppendorfs. Use these supernates for a luciferase assay on the same day.

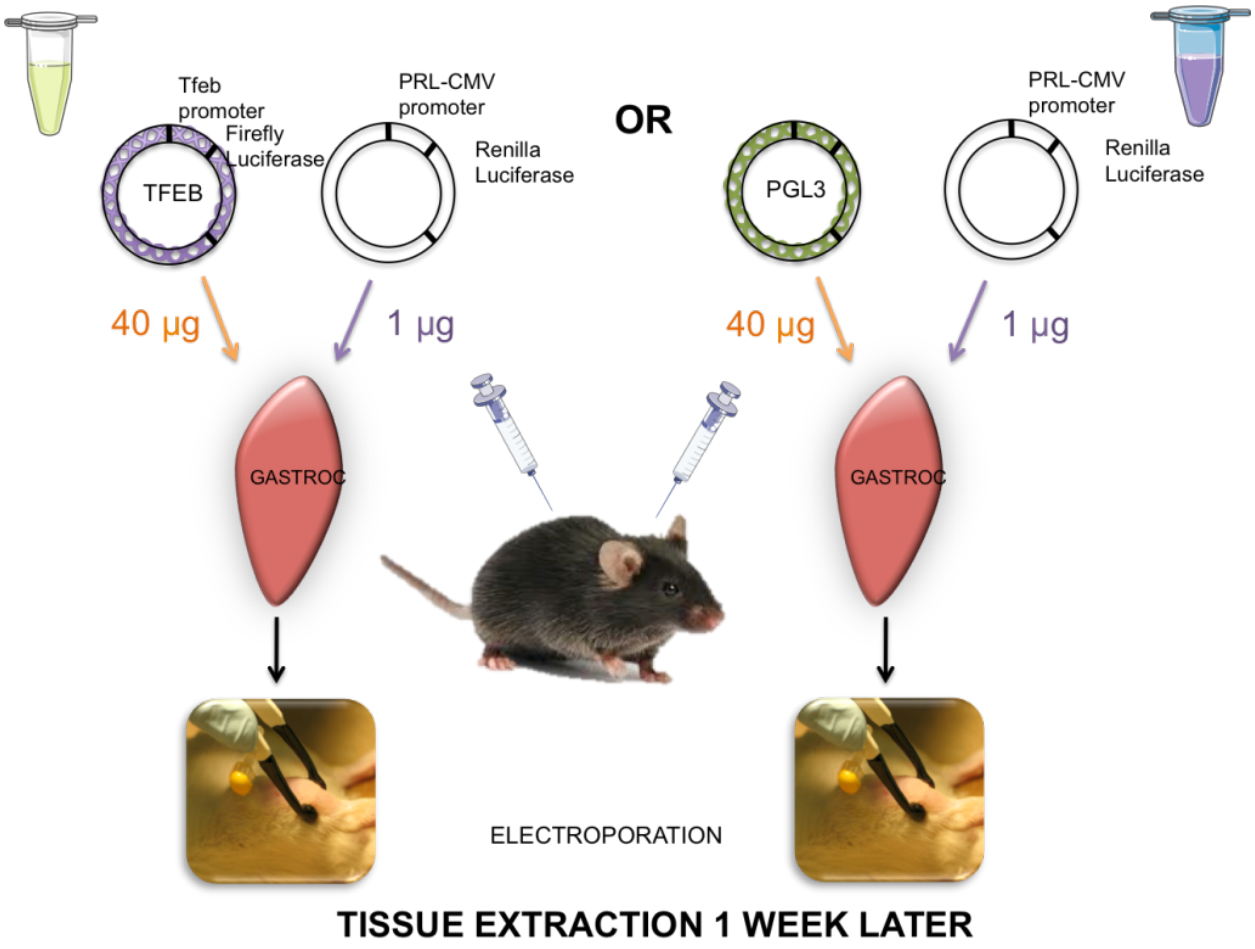

Figure 1. Illustration for in vivo muscle transfection. (See methods for details)

Mouse Muscle Tissue Preparation for Luciferase Assay

1. Pulverize muscle tissue at the temperature of liquid nitrogen. Store in vials in liquid nitrogen until use in assay.
2. Add 1ml 5xPassive Lysis Buffer (PLB) into 4ml sterile ddH_2O to dilute 5-fold (in a 13ml Falcon tube). Vortex briefly to mix. Add 100ul of this 1xPLB into 1.5ml eppendorfs.
3. Weigh 30-50mg of powdered muscle tissue into each eppendorf already containing 100ul of 1x PLB.
4. Dilute 7-fold in 1x PLB
5. Sonicate each sample 3x10 seconds at 4°C (or in holder on ice).
6. Centrifuge samples at 4°C at maximum speed for 5 minutes.
7. Retain supernates and transfer to a new, pre-chilled 1.5ml eppendorf for use in the luciferase assay the same day.

Luciferase Assay

Before beginning the luciferase assay, retrieve required supplies from the -80C freezer and allow time for them to thaw. An extra ice box is required to set the solutions down while the assay is in progress.

Materials Required: Stop and Glo Substrate
Stop and Glo Buffer
Luciferase Assay Substrate
Luciferase Assay Buffer II

Preparation of Solutions

- **Stop and Glo Substrate** needs to be spun down to collect the whole volume, which is then pipetted (in its entirety) into the **Stop and Glo Buffer** vial to prepare a **Stop and Glo Buffer Solution**. Mix simply by twirling.
- Add entire vial of **Luciferase Assay Buffer II** into the **Luciferase Assay Substrate** vial (by pouring) to prepare a **Luciferase Assay Solution**. Mix again by twirling.

Machine Set-Up

1. Turn ON Luminometer machine → OTHERS → OPERATION FUNCTION → REAGENT → OTHERS → WASH → INJ1 → ENTER →insert new tube → START → EXIT WHEN CLEAR
2. INJ2 →, ENTER → START → EXIT WHEN CLEAR → EXIT (X2) TO MAIN SCREEN
3. OTHERS → OPERATION FUNCTION → REAGENT → OTHERS → MANUAL UNLOAD → INJ1 → Keep pushing button until bubbles are visible in the water container, after which the lid is removed, Injector 1 is wiped and inserted into the Luciferase solution (**Luciferase Assay Substrate Solution**)
    i. INJ2 → Again, keep pushing button until bubbles are visible, wipe down and put Injector 2 into the **Stop and Glo Buffer Solution**
    ii. Both the **Luciferase Assay Solution** and **Stop and Glo Buffer Solution** are kept on ice while assay is being performed
4. EXIT

5. OTHERS → OPERATION FUNCTION → REAGENT → PRIME → INJECT 1 → START → INJECT 2 → EXIT
6. MEASURE → PROTOCOLS → 6 → ENTER → YES → ADD COMMENT (if required)
7. Simply add 20ul of supernate from prepared sample to bottom of 5ml Rohre tube (measure each sample twice – two separate tubes) → START
8. Once assay is complete, repeat steps 1 and 2 to clean the injectors with water. Place tubes in the garbage, and turn machine off. Supernates can be stored at -80°C; return prepared solutions (caps covered in parafilm to keep closed) to -80°C as well.

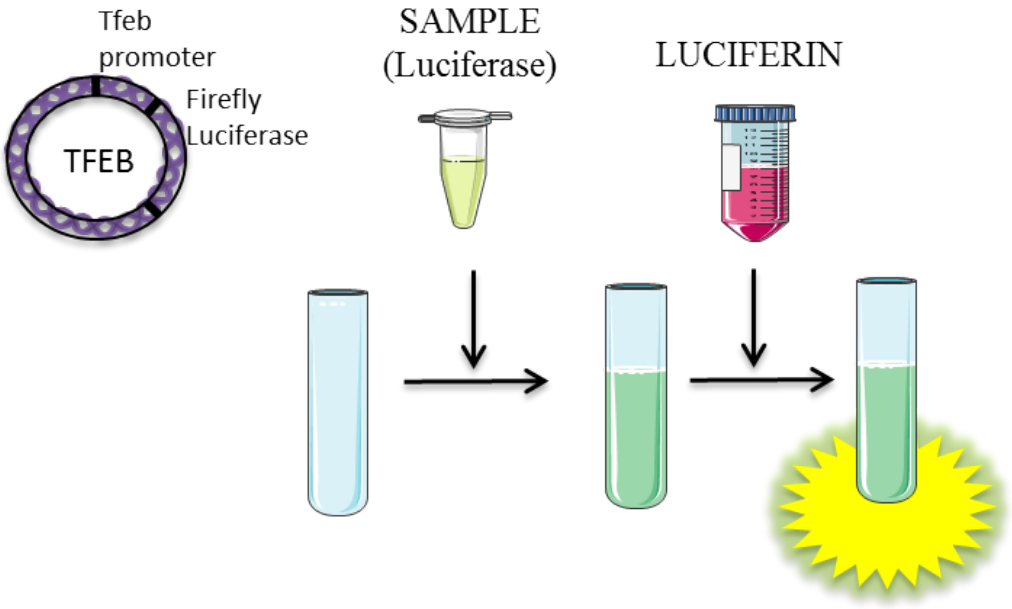

Figure 3. Illustration for luciferase assay protocol. (See methods for details)

RNA Isolation

Procedure:
Day 1

1. Homogenize tissues (100 mg, frozen and powdered) in 1 ml TRIzol reagent in a sterile 13 ml Sarstedt tube (approximately 3 x 10 seconds @ 30% power);
   Note: The homogenizer must be sterilized in 0.1M NaOH and rinsed in sterile water prior to use. Rinse homogenizer in sterile water between samples.

2. Transfer homogenized solution to a sterile 1.5ml Eppendorf, and let stand for 5 min at room temperature;

3. Add 400µ chloroform and shake vigorously for 15 sec, let stand for 2-3 min at room temperature;

4. Spin at 16100 *g* for 15 min at 4°C;

5. Transfer aqueous phase to a new sterile 1.5ml Eppendorf;

6. Add 500µl isopropanol, shake vigorously for 15 seconds and place in -20°C freezer to allow for RNA precipitation overnight,

Day 2

7. Allow RNA to thaw for 10 min at room temperature;

8. Spin at 16000 *g* for 10 min at 4°C;

9. Remove supernatant and add 700µl 75% ethanol, washing and resuspending the RNA pellet;

10. Spin again at 16,000 *g* for 10 min at 4°C;

11. Remove supernatant, and allow for pellet to air-dry for 40-45 minutes (or until all ethanol has evaporated);

12. Dissolve pellet in 30-40µl sterile distilled water and measure absorbance at 260 nm and 280 nm to determine RNA purity and concentration.

Reverse Transcription

First-strand cDNA synthesis is performed following the manufacturer's recommendations that are outlined below:

Reagents:
Total RNA (isolated as described above)
Oligo$(dT)_{20}$
10 mM each dATP, dTTP, dCTP, dGTP (diluted in sterile DEPC treated water)
Sterile DEPC treated ddH_20
RNAse OUT
0.1M Dithiothreitol (DTT)
5X First-strand Buffer
SuperScript III RT

Procedure:

1. Add following components to a nuclease/ RNA-free 500 µl eppendorf:

Oligo$(dT)_{20}$	1µl
1.5 µg of RNA	x µl
dNTP mix	1 µl
Sterile ddH_20	to 20 µl

2. Employ a thermal cycler to heat mixture to 65°C for 5 minutes. Collect the contents with a quick spin in a tabletop microcentrifuge and then add:

5X First-strand buffer	4 µl
0.1 M DTT	2 µl
RNAse OUT	1 µl
SuperScript III Reverse Transcriptase	1 µl

3. Using a thermal cycler, incubate at 55°C for 50 minutes, and then inactivate the reaction by heating at 70°C for 15 minutes.

4. cDNA is ready for use in PCR amplification.

Oligonucleotide Primer Design

Websites required:

- Pubmed Nucleotide Search
- Primer3 Primer Design Program – http://bioinfo.ut.ee/primer3/
- BLAST – http://www.ncbi.nlm.nih.gov/tools/primer-blast/
- IDT website – http://www.idtdna.com/calc/analyzer

1. Know the gene of interest.
2. Use the Pubmed.com nucleotide search and choose the most complete cDNA or mRNA version of the gene.
3. Copy the sequence and insert it into the Primer3 program.
4. Remove numbers from the copied sequence because the program will treat them as nucleotides.
5. In the text box for **Product Size Ranges,** input 100-150.
6. In the text box for **Number to Return,** input 10 (or whatever you want).
7. Under the heading **General Primer Picking Conditions** go to **Primer Size** and enter 10-20-22 from min to max.
8. For **Primer Tm** enter 58-60-62 from min to max.
9. For **Max Tm Difference** enter 2.
10. For **Primer GC%** enter 40-50-60 from min to max.
11. For **Max Self Complementary** enter 6.
12. For **Max Ploy-X** enter 3.
13. Under the heading **Objective Function Penalty Weights for Primer** go to **End Stability** and enter 9.
14. Click on the "Pick Primers" button.
15. Examine the primers on the list. 3' end of primer must not end with a G or C. No more than three G or C in last five nucleotides at 3' end.
16. Check specificity using BLAST.
17. Calculate the ΔG to estimate secondary structures that can form. Go to the IDT website.
18. Enter each oligo one at a time and press "Analyze". ΔG must be greater than or equal to -9 to continue.
19. Continue down the list selecting **Hairpin, Self-Dimer, Hetero-Dimer, Tm Mismatch.** Check ΔG for each one.

Polymerase Chain Reaction (qPCR)

1) 2 ug of RNA is converted to 2 ug of cDNA (STOCK cDNA)
2) We dilute STOCK cDNA to 1:30 (2 µL STOCK cDNA added to 58 uL nuclease-free ddH_2O)
3) We add 4 µL of diluted cDNA, thus loading 10 µg cDNA per well
4) For SYBR Green analyses, primers were optimized, diluted and mixed with PerfeCTa SYBR® Green SuperMix, ROX Master Mix and nuclease-free ddH_2O
5) Total reaction volumes were always 25 µL
6) Samples must be duplicated to ensure accuracy.
7) Use negative wells to monitor contamination, using nuclease-free ddH_2O in place of cDNA.
8) Check for nonspecific amplification and primer dimers by analyzing melt curves

Gel Electrophoresis-SDS PAGE (Protein BIORAD System)

Reagents:

1. Acrylamide/Bis-Acrylamide, 30% Solution 37.5:1 (BioShop 10.502)
    a. Store at 4°C
2. Under Tris Buffer
    a. 1M Tris-HCl, pH 8.8 (60.5g/500ml)
    b. Store at 4°C
3. Over Tris Buffer
    a. 1M Tris-HCl, pH 6.8 (12.1g/100ml)
    b. Bromophenol Blue (for colour)
    c. Store at 4°C
4. Ammonium Persulfate (APS)
    a. 10% (w/v) APS in ddH_20 (1g/10ml)
    b. Stored at 4°C
5. Sodium Dodecyl Sulfate (SDS)
    a. 10% (w/v) in ddH_20 (1g/10ml)
    b. Store at room temperature
6. TEMED (Sigma T-9281)
7. Electrophoresis Buffer, pH 8.3 (10L)
    a. 25mM Tris 30.34g, 192mM Glycine 144g, 0.1% SDS 10g
    b. Volume to 10L with ddH_20
    c. Store at room temperature
8. 6X SDS
    a. Warm 100% glycerol in water bath at 65°C for 30 minutes
    b. Combine 1.2g SDS, 0.06g Bromophenol Blue, 3mls of 1M Tris, pH 6.8 and 1ml of ddH_20 and stir at 4°C for 5 minutes
    c. Add 3mls of 100% glycerol, stir and aliquot mixture.
    d. Store at -20°C
    e. Add 5% (v/v) ß-mercaptoethanol (Sigma M6250) to 6X SDS <u>just prior</u> to use
9. *tetra*-Amyl alcohol ReagentPlus, 99% (Sigma 152463)

Procedure:

1. **Prepare electrophoresis rack:**
    a. Clean glass plates thoroughly with soap followed by 95% ethanol then ddH_20.
    b. Dry carefully with a kimwipe.
    c. Assemble glass plates as shown below:
    d. Check the seal by adding a small volume of ddH_20 then pour off and let dry.
2. **Prepare separating gels:**
    a. Mini Protean 3 Bio-Rad System volumes:

	8%	10%	12%	15%	18%
Acrylamide	2.7 ml	3.3 ml	4.0 ml	5.0 ml	6.0 ml
ddH_20	4.1 ml	3.5 ml	2.8 ml	1.8 ml	0.8 ml
Under Tris	3.0 ml	3.0 ml	3.0 ml	3.0 ml	3.0 ml
SDS	100µl	100µl	100µl	100µl	100µl
APS	100µl	100µl	100µl	100µl	100µl
TEMED	10µl	10µl	10µl	10µl	10µl

b. Mix the contents of the separating gel without adding APS or TEMED. Stir.
c. Add APS and TEMED. Stir.
d. Slowly pour the entire volume of the solution into the space between the two plates while keeping plates tilted to prevent bubble formation.
e. Add *tert*-Amyl alcohol to coat top surface of gel solution.
f. Allow 30 minutes for gel polymerization.
g. Remove *tert*-Amyl alcohol by pouring it off and remove any remainder with a kimwipe. Rinse with ddH_20.

3. Prepare stacking gel:

a. For a single mini gel use the following volumes:

Acrylamide	500 µl
Over Tris	625 µl
ddH_20	3.75 ml
SDS	50 µl
APS	50 µl
TEMED	7.5 µl

b. Mix the contents of the stacking gel without adding APS or TEMED. Stir.
c. Add APS and TEMED. Stir.
d. Using a Pasteur pipette slowly add the entire volume from the beaker in between the plates.
e. Add comb for desired number of wells.
f. Allow 30 minutes for gel polymerization.

4. **Prepare samples:**
    a. Turn on the block heater to 95ºC.
    b. Pipette required volume of sample into new eppendorf with same amount of lysis buffer and 5 µl of sample dye. Keep samples on ice until all samples are prepared (use pipette plan).
    c. Briefly spin each sample to bring volume to the bottom of the eppendorf.
    d. Incubate each sample at 95 ºC for 5 minutes in the heating block to denature the proteins.
    e. Briefly spin again to return volume to the bottom of the eppendorf.

5. **Assemble Mini-PROTEAN gel caster system:**
    a. See images below
    b. If you are only running one gel a plastic rectangular pseudo plate must be clamped on the other side of the caster.
    c. Fill with electrophoresis buffer between the plates and outside of the plates in the chamber.
    d. Slowly remove the comb using both hands (one on each side) by pulling the comb straight upwards.
    e. Fix any wells that are deformed using a small spatula.
    f. Clean out the wells using a syringe filled with electrophoresis buffer.
    g. Withdraw the entire volume of the sample using a Hamilton syringe. Inject volume slowly into the bottom of the well.

6. **Gel electrophoresis**
    a. Immediately after all samples are loaded place the lid on the gel chamber.
    b. Place positive and negative plugs into the power supply and turn on power supply.
    c. Set power supply to 120V. Gel will run for ~2 hours depending on percent gel made.
    d. When the bromophenol blue has run off the bottom of the gel (or when gel has separated the desire amount) turn off the power supply. Remove plugs from power supply and remove lid.
    e. Prepare for electrotransfer of proteins from the gel to nitrocellulose membrane.

Western Blotting-Transfer and Immunodetection:

Reagents:

1. Transfer Buffer
    a. 0.025M Tris-HCl pH 8.3 12.14g
    b. 0.15M Glycine 45.05g
    c. 20% Methanol 800ml
    d. make up to 4L with ddH_20
    e. store at 4°C
2. Ponceau S stain
    a. 0.1% (w/v) Ponceau S
    b. 0.5% (v/v) Acetic Acid
    c. Store at room temperature
3. Wash Buffer
    a. Tris-HCl pH 7.5 12g
    b. NaCl 58.5g
    c. 0.1% Tween 10ml
    d. Store at room temperature
4. Blocking Solution
    a. 5% (w/v) skim milk power in wash buffer OR
    b. 5% (w/v) BSA in wash buffer
5. Enhanced Chemiluminescence Fluid (ECL; Santa Cruz sc-2048)
6. Film/Developer/Fixer

Procedure:

1. **Transfer Procedure**
    a. Remove electrophoresis plates from chamber and separate the plates.
    b. Cut away unnecessary parts of the gel using a spatula and measure remaining gel size.
    c. Using a paper cutter cut 6 pieces of Whatman paper per gel to the same size as the gel. Wearing gloves cut nitrocellulose membrane (GE Healthcare RPN303D) to the dimensions of the gel.
    d. Assemble Whatman paper, nitrocellulose memebrane and gel as shown above:
    e. Close the cassette and place in the transfer chamber with the black side of the cassette facing the back side of the chamber.
    f. Place ice pack in the chamber.
    g. Place lid on the chamber and connect the leads to the power supply.
    h. Turn on the power supply and run at 120V for 2 hours. This can vary depending on the size of the protein of interest.

2. **Removal of transfer membrane:**
    a. Turn off the power supply and disconnect leads from the power supply then remove the lid from the chamber.
    b. Remove the cassette from the chamber.
    c. With gloves on, remove the Whatman paper and gel and place the nitrocellulose membrane in a plastic dish.
    d. Add Ponceau S stain on the membrane and gently swirl.
    e. Drain off the remaining Ponceau S and save for reuse.
    f. Rinse the membrane with ddH_20 to reduce the red background. Wrap membrane in saran wrap and scan image.
    g. Cut the membrane while protein bands are still visible at the desired molecular weight.
    h. Rotate membrane at room temperature in wash buffer until remaining Ponceau S has been removed.
    i. Incubate membrane for 1 hour with rotation in blocking solution.
    j. Incubate membrane with desired antibody diluted in blocking solution overnight at 4ºC. Membrane is placed face up into the solution on a glass plate covered in parafilm. To maintain a moist environment overnight, wet a small kimwipe and form it into a ball and place in each corner of the dish. Cover the dish with saran wrap.

3. **Immunodetection**
    a. Wash the blots in wash buffer with gentle rotation for 5 minutes 3X.
    b. Incubate the blots for 1 hour in room temperature with the appropriate secondary antibody diluted in blocking solution.
    c. Membrane is placed face up in solution on a glass plate covered with parafilm. Place moist kimwipes in each corner of the dish and cover the dish with saran wrap.
    d. Following the incubation, wash the membrane 3X for 5 minutes with wash buffer.

4. **Enhanced Chemiluminescence Detection**
    a. Mix ECL fluids “A” and “B” in a 1:1 ratio in a disposable Rohr tube.
    b. Place blots on saran wrap face up and apply ECL solution for 2 minutes.
    c. Dab off excess ECL on a kimwipe and place blots face down on a fresh piece of saran wrap and wrap tightly.
    d. Expose blot to film (time will vary depending on protein and antibody).
    e. Place film into developer (time will vary).
    f. Once image appears place film into fixer for 2 minutes. Wash with fresh water when complete.

OTHER CONTRIBUTIONS TO LITERATURE

PEER-REVIEWED PUBLICATIONS

1. **Erlich AT**, Tryon LD, Crilly, MJ, Memme JM, Moosavi, ZM, Oliveira AN, Beyfuss K, Hood DA. (2016). Function of specialized regulatory proteins and signaling pathways in exercise-induced muscle mitochondrial biogenesis. *Integrative Medicine Research,* 5(3), 187–197.
2. Crilly MJ, Tryon LD, **Erlich AT**, Hood DA. (2016). The role of Nrf2 in skeletal muscle contractile and mitochondrial function. *Journal of Applied Physiology,* 121(3), 730-740.

PUBLISHED ABSTRACTS AND CONFERENCE PROCEEDINGS

1. Carter HN, Zarrin-khat D, Kim Y, **Erlich AT**, Hood DA. Mitophagy flux with aging and chronic exercise in skeletal muscle. *Integrative Biology of Exercise 2016.* Phoenix, AZ. November 2016- Poster presentation.
2. **Erlich AT**, Beyfuss K, Hood DA. Regulation of TFEB transcriptional activity and translocation during exercise by PGC-1α. *Proceedings of the 7th Annual Muscle Health Awareness Day*. Toronto, ON. May 2016 – Poster presentation.
3. **Erlich AT**, Vainshtein A, Hood, DA. The Correlation between TFEB and PGC-1α in Skeletal Muscle. *Experimental Biology 2016.* San Diedo, CA. April 2016 – Poster presentation.
4. **Erlich AT**, Vainshtein A, Hood DA. Levels of inflammatory proteins in muscle under aging and PGC-1α KO conditions. *Canadian Society for Exercise Physiology conference 2015.* Hamilton, ON. October 2015 – Poster presentation.
5. **Erlich AT,** Vainshtein A, Hood DA. Effect of Aging, PGC-1α, and exercise on levels of inflammatory proteins in muscle. *Proceedings of the 6th Annual Muscle Health Awareness Day.* Toronto, ON. May 2015- poster presentation.

ORAL PRESENTATIONS

1. **Erlich AT, Hood DA**. The relationship between TFEB and PGC-1α in skeletal muscle. *KAHS Graduate Seminar 2016.* York University, Toronto, ON. March 2016 – Oral presentation.